Applications of N,N'-Disubstituted-1,8-Diaminonaphthalene as a Scaffold to Support Group 13 Compounds, Carbenes and Pd(II) carbene Complexes

Sojung Lee

Thesis submitted to the
Faculty of Graduate and Postdoctoral Studies
in partial fulfillment of the requirements for the degree of

Master of Science
in
Chemistry

University of Ottawa

Candidate
Sojung Lee

Supervisor
Darrin S. Richeson

Acknowledgements

First of all, I would like to thank my supervisor Dr. Darrin Richeson for being an amazing supervisor for over two years in every single moment. He has always showed us passion and enthusiasm for research and inspired me to advance significantly. He always considers us as a family and tries to understand how international students feel, which makes me enjoy working in the lab so much. Moreover, he does not mind helping the students and giving advices for every challenge we have had. Without his guideline, nothing could be possible.

I also appreciate him to give me an opportunity to join such a great lab. Everyone I have worked with in the lab was amazing and gave me priceless memories in Canada. I sincerely appreciate all of them for being such a nice group and great friends. Especially, I would like to express my gratitude to Dr. Gyan for his great support for everything and his patience to teach me. His contribution was significantly helpful for this thesis. I would love to express my gratitude to Dr. Tito Scaiano and Dr. Yu to afford scholarships. Thanks to these scholarships, I could focus on my study more and it was significantly helpful.

I also sincerely appreciate Hanbin for being a fantastic supporter in every single moment together. With his support and help, I could be always positive and motivated to make a progress. Moreover, I could get over any challenges I have had during the study with him. Finally, I would like to thank my family to give me support all the time and encourage me to try what I would like to do. I always miss them so much and thank them to give me this great opportunity to study chemistry in University of Ottawa. I would like to give all glory to my parents.

1
Abstract

This work is mainly concentrated on the development of new versatile ligand based on N,N'-disubstituted-1,8-diaminonaphthalene (1,8-DAN) for main group chemistry. Therefore, our initial efforts were made on the design of new ligand scaffold by using 1,8-DAN. Following that, new ligand family supported by 1,8-DAN was applied as ligands to main group elements (B, Al, In, Ga, and C). Furthermore, six-membered ring carbenes which are derived from the reaction between N,N'-disubstituted-1,8-diaminonaphthalene and carbon are also investigated. In addition, the stable carbenes were implied as a new ligand system for palladium, leading to the formation of metal ligand complexes. Therefore, the synthesis and reactivity of these complexes are also reported.

Chapter I gives an explanation on the basic concepts in terms of the ligand designs and reports the reasons why N,N'-disubstituted-1,8-diaminonaphthalene has been chosen as the framework of for these ligands.

Chapter II presents the approach to synthesize ligands depending on the substitution. Regarding this, three methods were successfully used: reductive amination, application of acyl halide followed by reduction, and copper catalyzed C-N coupling reactions.

Chapter III describes the reactions between the N,N'-disubstituted-1,8-diaminonaphthalene and main group elements B, Al, Ga, and In in 13 group. In this chapter, a variety of mononuclear and dinuclear complexes are investigated and fully characterized. Furthermore, some computational studies are also reported for the comparison with experimental results.

Chapter IV deals with new ligand family, carbene, which is derived from N,N'-disubstituted-1,8-diaminonaphthalene. Therefore, not only fundamental concepts for the NHC (N-heterocyclic carbene) are discussed but also synthetic pathways are introduced. Moreover, interesting features of free carbene are presented as well.

Chapter V reports the potential of this new carbene ligand family as ligands for transition metal compound, especially, Pd(II) compounds. Several different pathways for synthesizing the desired metal carbene complexes are presented.

Contents

IV Carbene Chemistry

V Pd Complexes of Perimidine-Based Carbenes

List of Common Abbreviations

1. Chemicals and Ligand

Acac	Acetylacetonate
Ar	Aromatic group
Bn	Benzyl
Cp*	Pentamethylcyclopentadienyl, C_5Me_5
1,8-DAN	1,8-diaminonaphthalene, 1,8-$(NH_2)_2C_{10}H_6$
iPr	Isopropyl
L	Ligand
Me	Methyl
Nacnac	β-diketiminate
NHC	N-heterocyclic carbene
Np	Neopentyl
OAc	Acetate
Ph	Phenyl
py	Pyridine
R	Alkyl or aryl
THF	Tetrahydrofuran
X	Halogen

2. Miscellaneous

Å	Angstrom unit 10^{-10}m
°	Degree
Hz	Hertz
NMR	Nuclear magnetic resonance
PPM	Parts per million

List of Figures

Figure 4.5 X-ray structure of **4.6 (**Only one of the independent molecules is shown and the counter anion Br^- and hydrogen atoms have been omitted for clarity)

Figure 4.6 X-ray structure of **4.13** (Only one of the independent molecules is shown and hydrogen atoms have been omitted for clarity)

Figure 5.1 X-ray structure of **5.3** (Thermal ellipsoids are shown for only selected atoms and hydrogen atoms have been omitted for clarity & The second part of the molecule (with primes') is symmetrically dependent by inversion center (1-x,1-y,2-z))

Figure 5.2 X-ray structure of **5.4** (Thermal ellipsoids are shown for only selected atoms and hydrogen atoms and a crystallized THF molecule have been omitted for clarity & The second part of the molecule (with primes') is symmetrically dependent by inversion center (1-x,1-y,1-z))

Figure 5.3 X-ray structure of **5.5 (**Only one molecule of the asymmetric unit is shown and thermal ellipsoids are shown for only selected atoms & Hydrogen atoms have been omitted for clarity)

Figure 5.4 X-ray structure of **5.6 (**Thermal ellipsoids are shown for only selected atoms and hydrogen atoms have been omitted for clarity)

Figure 5.5 X-ray structure of **5.8 (**Thermal ellipsoids are shown for only selected atoms and hydrogen atoms have been omitted for clarity & The 3-chloropyridine solvate, Cl2 and Br1 have been omitted, only Br2 and Cl1 are shown (0.688(3) and 0.525(3) occupancies)

List of Tables

Chapter I
Introduction

I. Introduction

One of the key motivating forces behind the synthesis and characterization of metal complexes is their use in stoichiometric and catalytic applications. Such compounds have wide applications in various fields of chemistry, affording faster and easier routes for certain chemical reactions. In this regard, electronic and steric properties of metal based complexes affect the reaction significantly. Therefore, both effects should be monitored in order to control chemical reactions. With regards to this, the ligand design also needs to be considered since ligand properties affect not only the stability of metal complexes but also the reactivity of them.

It is well-known that there is a rich family of ligands that are useful and distinct for the range of metal systems. Simple examples that are often used to highlight the role of ligand electronic and steric features are carbon monoxide (CO) and acetylacetonate (acac). Firstly, since

CO has strong σ donation as well as π accepting ability from the metal center, it has been used widely especially with late transition metals. These exceptional properties of CO as a neutral ligand enable the synthesis of a tremendous variety of metal ligand complexes. For another example, acetylacetonate (acac) in **Chart 1.1** has been utilized as a ligand for a significant number of metal centers due to the stability from the conjugated framework with delocalized charge. Additionally, this species displays different bonding modes such as monodentate and bidentate since charge can be delocalized. Therefore, the acac ligand can form strong bonding with various metals throughout the periodic table. However, one of disadvantages of acac ligand is the limitation of control for both electronic and steric properties. This is because of lack of substituents at donating oxygen atoms.

Chart 1.1

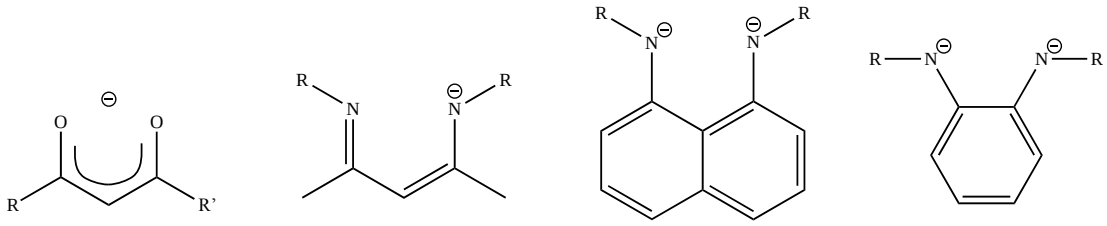

Acetylacetonate β-diketiminate R_2DAN^{2-} $(R_3Si)_2DAB^{2-}$

An interesting example of employing both electronic and steric modification of a ligand frame is provided by the ligand β-diketiminate (**Chart 1.1**), which is also called nacnac. This ligand is derived from the idea of the acac ligand. The advantage of acac ligand, delocalization of charge, is kept for nacnac ligand but instead of oxygen, nitrogen atoms are used as donating groups which provides a means to modulate both electronic and steric properties by controlling the substituents. Furthermore, nitrogen is more basic than oxygen, leading stronger electron donor ligand. Consequently, the nacnac ligand continues to play an important role as a

supporting ligand due to their strong metal binding at the same time control of steric demands and donation properties by altering substituents at nitrogen atoms. In fact, nacnac ligand have been used as catalyst with group 4 elements in olefin polymerization reaction.[1] In addition, Mo and W(IV) complexes supported by nacnac ligand was already developed and characterized.[2]

Cleary, the nature of the ligand donor sites and the steric features of a ligand are important and provide a motivation for the development of arrays of new ligand system. When it comes to the design of ligands, donation properties, structure, stability, and reactivity of coordination compounds should be considered. As stated, these factors can be manipulated by modification not only ligand framework but also ligand substituents. Accordingly, we came up with new framework of dianionic ligands that are reminiscent of the β-diketiminate scaffold in terms of geometry and frontier orbital topology. This idea led to the development of a new ligand system with the N,N'-disubstituted-1,8-diaminonaphthalene (R_2-DAN^{2-}) scaffold (**Chart 1.1**). R_2-DAN^{2-} has unique properties that make this ligand more attractive relative to β-diketiminate. one of the most significant features is that delocalized π electrons in R_2-DAN^{2-} can lead to the robust ligand which is comparable to β-diketiminate.

Furthermore, our efforts to investigate R_2-DAN^{2-} have also been motivated from the application of aromatic diamido ligands N,N'-bis(trialkylsilyl)-o-diamidobenzene ($(R_3Si)_2DAB^{2-}$) (**Chart 1.1**). Especially, $(R_3Si)_2DAB^{2-}$ ligand has been used as ligands in order to prepare high–valent group 4[3], Ta[4,5], Mo, and W[6,7,8,9] complexes. In terms of structure, $(R_3Si)_2DAB^{2-}$ also possesses the dianionic charge and aromatic scaffold as analogous to that of R_2-DAN^{2-}. Nonetheless, the diamidobenzene and the diamidonaphthalene reveal significantly different

topologies, affecting the reactivity of the respective metal complexes substantially. Among the unique properties of $(R_3Si)_2DAB^{2-}$, a distortion of ligand system when forming metal ligand complexes is the most different feature compared to R_2-DAN^{2-}. This character can lead to the presence of an additional π electron donation from the lone pair of nitrogen atoms to an empty d orbital of metal center, affording more stable metal complexes.[10] As consequence, these characters motivated us to investigate unique properties of R_2-DAN^{2-} as a ligand system. Additionally, since substituents at nitrogen atoms can affect the steric environment as well as electronic features of the coordinated metal by changing electron density on nitrogen atoms, donor properties of the ligand can be modified by exchanging substituents. Regarding this, we also decided to modify steric demands and electronic properties by applying different substituents.

II. 1,8-Diaminonaphthalene as a Ligand

Chart 1.2

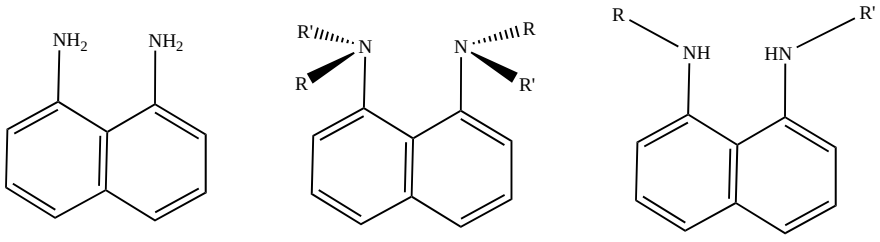

A **B** **C**

The 1,8-diaminonaphthalene framework has three simplified versions, which are unsubstituted, monosubstituted, and disubstituted as shown in **Chart 1.2**. First of all, unsubstituted diamine 1,8-$NH_2(C_{10}H_6)$ **A** can be used as a ligand and there are various papers on the formation of diaminonaphthalene bridged diiridium complexes[11,12], a bridged trimetallic

magnesium cage[13], chelated ruthenium[14] and platinum complexes[15], bridged dinuclear rhodium complexes[16], ligated osmium carbonyl clusters[17], and some chelated boron complexes[18,19,20,21]. Moreover, three coordinated boron complexes supported by unsubstituted diamine **A** ligand have been reported as well. However, there have not been any boron complexes with **A** fully characterized yet. Additionally, since there are still reactive N-H groups, the stability of these complexes is not guaranteed. Another weakness of **A** is a lack of control for steric and electronic properties due to the lack of nitrogen substituents.

At the other end of substitution patterns is the fully tetrasubstituted derivatives **B**. For example, N,N,N'N'-tetramethyl-1,8-DAN has extraordinary basicity and shows a unique ability to accept protons. Accordingly, N,N,N'N'-tetramethyl-1,8-DAN is often called "proton sponge". By implying these features, N,N,N'N'-tetramethyl-1,8-DAN has been used as a neutral chelating ligand for various metal systems such as Mn(II) [22] and Cu(II) [23]. Interestingly, boron also activates the compound, leading to the formation of cationic salts by displacement of one anionic ligands (hydride or halide) [24,25,26]. In spite of these interesting features, the use of **B** is limited due to the lack the anionic charge of this ligand framework.

Accordingly, as consequence of some limitations of **A** and **B** described above, we chose to focus on the design and development of new ligand systems based on the N,N'-disubstituted-diaminonaphthalene scaffold **C** in **Chart 1.2**. Since it has a substituent at each nitrogen atoms, modifications of ligand properties are easily accessible depending on the need. Another attractive feature is an ability to form the dianionic charges so that stronger electron donation is possible. Moreover, the coordinated element would be placed in a six-membered heterocyclic ring with

the extended aromatic system from the naphthalene backbone, possessing 14 π electrons. Therefore, we expected that N,N'-disubstituted-diaminonaphthalene (**C**) could play an important role. The bis(trimethylsilyl)derivative (R, R' = $SiMe_3$), was first reported as a ligand for a Sn(II) compound in the mid-seventies.[27] At that time very few examples were introduced in the field of this particular class of dianionic ligands. The ancillary dianionic ligands began to receive attention only very recently.

Given the range of substituents that could be applied to N,N'-disubstitued-1,8-diaminonaphthalene family of ligands, a shorthand notation for identifying these species is useful. With this is mind, I have chosen to use the notation "R,R'-DAN", with R and R' denoting the two N-bonded substituents, as an abbreviated name for these ligands For instance, N,N'-diisopropyl-1,8-daminonaphthalene and N-benzyl, N'- isopropyl-1,8-daminonaphthalene will be abbreviated as ($^{i}Pr)_2$-DAN and (Bn)(^{i}Pr)-DAN respectively. ^{i}Pr, Np, and Bn stand for isopropyl group, neopentyl, and benzyl group respectively.

As mentioned, the trialkylsilyl substituted diaminonaphthalene framework was the first reported application of these ligands and this substitution pattern remains the dominantly reported species in the literature. However, our group initiated an exploration of the design of new R,R'-DAN possessing alkyl and aryl groups at nitrogen and began to investigate the reactivity in terms of coordination chemistry with main group elements and transition metals. Initially our group started transition metal chemistry with R,R'-DAN using high oxidation state metal centers for two reasons. First, higher valent metal centers can obtain stronger donation from dianionic ligand system and can support a dianionic ligand along with other anionic ligands.

Second, higher oxidation stated metals which have d^0 center are diamagnetic which allows NMR methods as a means to follow reactions and identify compounds.

As an example, our group previously reported the preparation of W(VI) complexes with $(^iPr)_2$-DAN and $\{3,5\text{-}(Me)_2\text{-}C_6H_3\}_2$-DAN (**Scheme 1.1**)[28].

Scheme 1.1

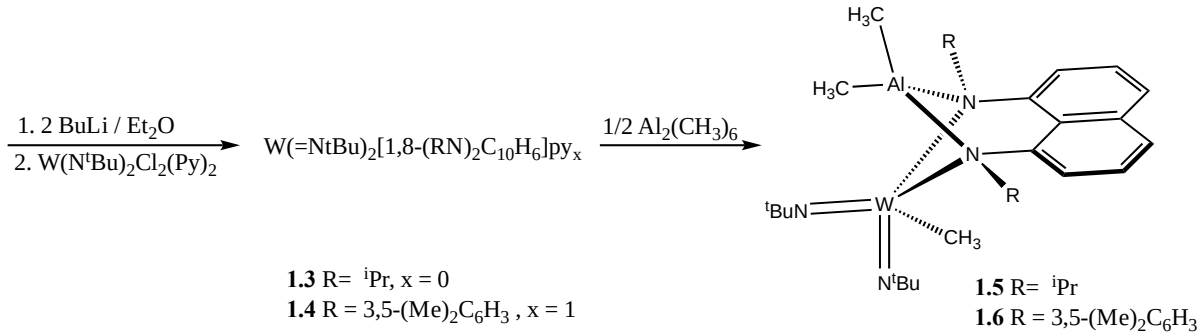

1.3 R= ^{i}Pr, x = 0
1.4 R = 3,5-$(Me)_2C_6H_3$, x = 1

1.5 R= ^{i}Pr
1.6 R = 3,5-$(Me)_2C_6H_3$

The nature of these complexes was confirmed by NMR spectroscopy, X-ray structural studies as well as computational analysis. As shown in **Figure 1.1**, it was worthy to note that non-planar coordination of $(^iPr)_2$-DAN ligand to the W(IV) center, with the W center being ca. 1.14 Å out of the naphthyl plane. Our analysis revealed that this type of metal-ligand interaction actually increased electron donation from the N centers and that nonplanar coordination provided additional π electron donation from the ligand to the metal.

Figure 1.1 X-ray structure of **1.3** (Hydrogen atoms have been omitted for clarity)

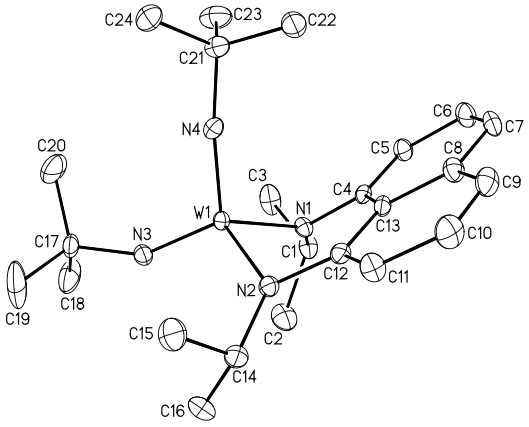

Another fascinating feature of **1.3** and **1.4** is that fruitful results were found in the reactions with $AlMe_3$, leading to the methylation of W and isolation of the heterobimetallic species **1.5** and **1.6** through μ^2-bridging interaction of R,R'-DAN ligand (**Scheme 1.1**).

Our group has also published on the application of R,R'-DAN ligands with Ta(V) complexes[29,30] supported by $(Ph)_2$-DAN, $\{(3,5\text{-}(Me)_2\text{-}C_6H_3)_2\}$-DAN, and $(^iPr)_2$-DAN. As seen in **Scheme 1.2**, one of the first interesting features of this chemistry is that with careful selection of the ligands on the metal starting material, in this case Ta-Me groups, the R,R'-DAN ligand can be incorporated into the metal coordination sphere without a prior deprotonation step of N-H protons. However, interestingly Ta-Me group was found to be able to activate methyne proton of the isopropyl substituents and lead to the formation of $[\{\mu^3\text{-}(Me_2CN)(Me_2CHN)C_{10}H_6\}TaCl_2]_2$, **1.7.** The nature of this complex was confirmed by NMR and fully characterized with single crystal X-ray diffraction analysis (**Figure 1.2**). Subsequent reaction with the nitrogen donor ligand 2-methylpyrroline led to cleavage of the Ta-Cl bond in **1.7**, and formation of **1.8** (**Scheme 1.2**). The chloro ligands in these Ta species can be replaced by benzyl groups using a Grignard reagent giving **1.9**. In the same manner, metathesis of Ta-Cl was also observed by adding 2 equivalents of LiCp* and forming the pentamethycyclopentadienyl compound **1.10**.

Scheme 1.2

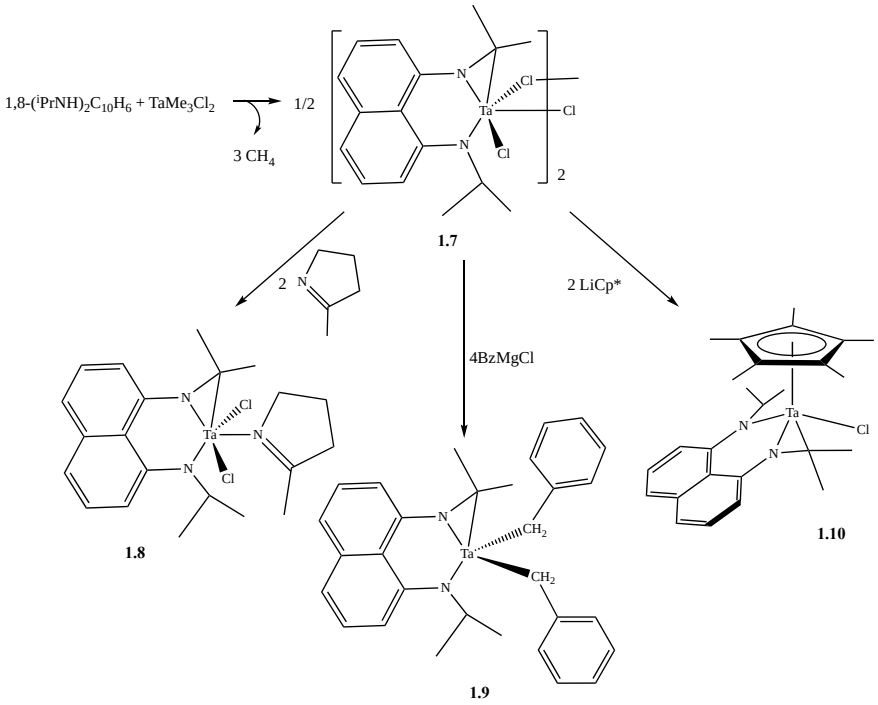

Figure 1.2 X-ray structure of **1.7** (Hydrogen atoms have been omitted for clarity)

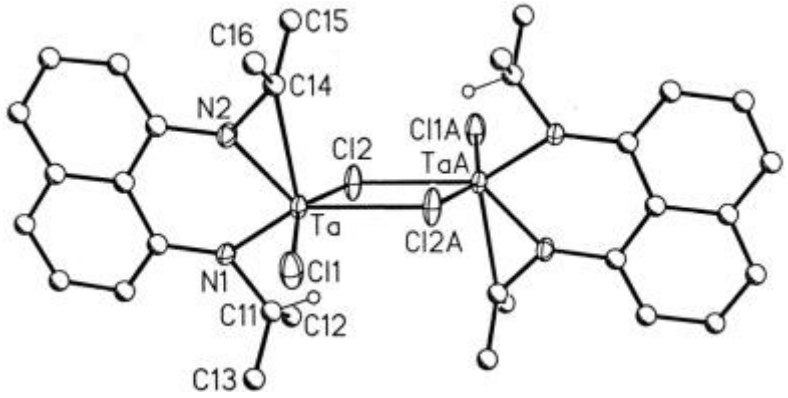

On top of the applications of R,R'- DAN with transition metals, our group also initiated an examination of the use of these ligands with main group elements. First, we examined the use of (^{i}Pr)$_2$-DAN with divalent 14 group elements such as Sn and Ge. For the preparation of the Sn(II) complex[31,32], two possible routes were demonstrated as seen in **Scheme 1.3**. First, Sn(NSiMe$_3$)$_2$ can be used as a reagent as well as base to protonate both N-Hs. The other way is to apply the

dilithium salt of DAN ligand (**1.11**) to the $SnCl_2$. Both approaches generate the desired product **1.12** successfully. From the X-ray structure of **1.12**, the geometry of Sn center was found to be pyramidal, which we attributed to a weak intermolecular donation of π electrons from the naphthyl group. From this chemistry, it is worthy to note that R,R'-DAN ligand support main group elements well.

Scheme 1.3

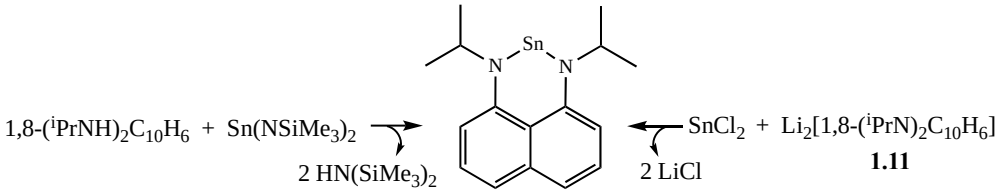

1.12

Successful results of the application of R,R'-DAN with Sn(II) encouraged the investigation of other main group elements. Therefore, another 14 group element Ge(II) was chosen. A mononuclear Ge(II) complex was isolated with two possible ways in **Scheme 1.4**. From these routes the desired product **1.13** was obtained, revealing a six membered heterocyclic ring. Therefore, steric impact of substituents is larger than the five membered ring. This is because α angle formed between C(substituent *C*H$(CH_3)_2$)-N-Ge is smaller in six-membered ring than in five-membered ring.

Scheme 1.4

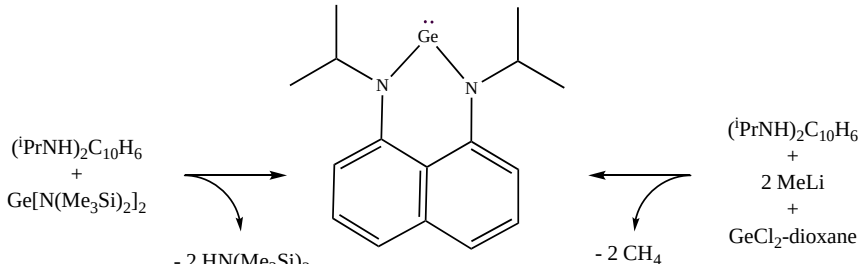

1.13

Furthermore, one of the most interesting factors of Ge(II) complex, **1.13** is that it could be used as a novel ligand for transition metals since Ge(II) center has a lone pair of electrons. This was demonstrated using Ni[COD]$_2$ with **1.13** as a neutral ligand and fortunately tetracoordinated Ni(0) complex was successfully obtained (**Scheme 1.5**)[33].

Scheme 1.5

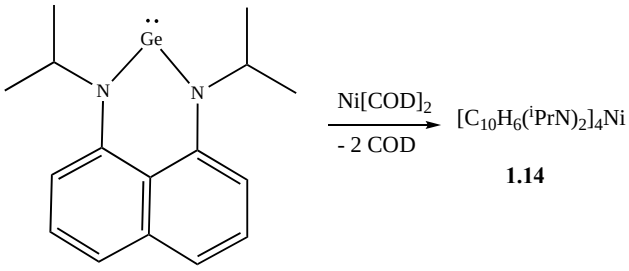

1.13 **1.14**

Furthermore, the single crystal X-ray structure was also obtained (**Figure 1.3**), showing that the Ge(II) center was coordinated to the Ni(0) and that the ligand exhibited a twisted heterometallocycle, possessing a cone angle 145º.

Figure 1.3 X-ray structure of **1.14** (Hydrogens have been omitted)

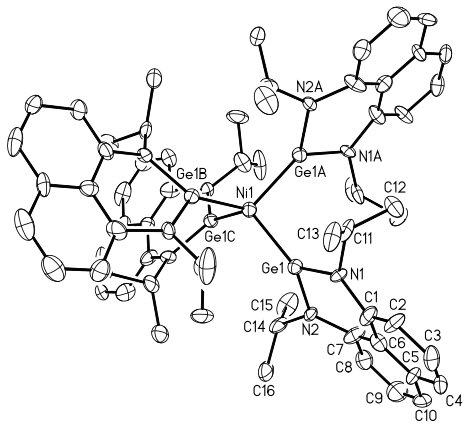

The development of compounds **1.12** and **1.13** gives evidence that main group, especially, 14 group elements can be supported by R,R'-DAN.

III. Overview of Thesis

As described, R,R'-DAN has been used as a ligand for both transition metals and main group elements. In this regard, we set the goal of further developing the coordination chemistry of R,R'-DAN with a focus on using derivatives having robust N-substituent groups, considering the anticipated potential of this architecture as a versatile ligand platform.

Specifically, synthesis of new R,R'-DAN ligand, having both alkyl and aryl substituents was developed. With these species in hand, we next examined the ability of these ligands to support complexes with 13 group elements (B, Al, Ga, and In) as well as methods to incorporate these ligands with these element centers.

In addition to R,R'-DAN functioning as a ligand, the chemistry revealed for Sn(II) and Ge(II) provided an avenue to focus on the development of other group 14 divalent compounds and in particular on carbene compounds derived from R,R'-DAN.

Finally, the last project of the thesis was on the use of carbene supported by disubstituted-DAN as a new ligand system for Pd(II) complexes.

In summary, in **Chapter II**, a few different preparation methods of N,N'-1,8-disubstituted-diaminonaphthalene ligands will be discussed depending on the different substituents. Additionally, characterization in terms of structure will be introduced too.

Chapter III introduces the reaction of group 13 elements B, Al, Ga, and In with R,R'-DAN ligands with both dialkyl and diaryl substituents. Furthermore, the Li salt of $(Ph)_2$-DAN is examined as well. This project is mainly focused on the application of R,R'-DAN with main group elements. Finally, the detailed characterizations of these compounds are provided.

In **Chapter IV**, unique properties of carbene with R,R'-DAN scaffold will be discussed. In addition, some comparisons with classic NHCs will be provided. Synthetic methods to prepare the carbene precursors as well as free carbene will be introduced.

The last chapter, **Chapter V** will introduce the applications of the prepared carbenes from the R,R'-DAN ligand framework as a new neutral ligand family**.** The explanation on the reactivity of the free carbenes with several different Pd(II) compounds will be given as well. Additionally, unique features of each complexes as well as interesting results of characterizations will be provided.

IV. References

[1] V. C. Gibson, S. K. Spitzmesser, *Chem. Rev*., 2003, **103**, 283.

[2] Z. J. Tonzetich, A. J. Jiang, R. R. Schrock, P. Müller, *Organometallics*, 2006, **25**, 4725.

[3] K. Aoyagi, P. K. Gantzel, K. Kalai, T. D. Tilley, *Organometallics*, 1996, **15**, 923.

[4] K. Aoyagi, P. K. Grantzel, T. D. Tilley, *Polyhedron*, 1996, **15**, 4299.

[5] G. Jiménez Pindado, M. Thornton-Pett, M. Bochmann, *J. Chem. Soc. Dalt. Trans.*, 1998, **4**, 393.

[6] T. W. Hayton, J. M. Boncella, B. L. Scott, K. A. Abboud, R. C. Mills, *Inorg. Chem.*, 2005, **44**, 9506.

[7] R. C. Mills, K. A. Abboud, J. M. Boncella, *Chem. Commun.*, 2001, **16**, 1506.

[8] R. C. Mills, S. Y. S. Wang, K. A. Abboud, J. M. Boncella, *Inorg. Chem.*, 2001, **40**, 5077.

[9] T. M. Cameron, K. A. Abboud, J. M. Boncella, *Chem. Commun.*, 2001, **7476**, 1224.

[10] T. M. Cameron, S. Gamble, K. A. Abboud, J. M. Boncella, *Chem. Commun.*, 2002, **734**, 1148.

[11] M. V. Jiménez, E. Sola, A. C. Francisco, L. A. Oro, F. J. Lahoz, A. P. Martínez, *Inorganica Chim. Acta.*, 2003, **350**, 266.

[12] M. V. Jiménez, E. Sola, M. A. Egea, A. Huet, A. C. Francisco, F. J. Lahoz, L. A. Oro, *Inorg. Chem.*, 2000, **39**, 4868.

[13] W. Clegg, L. Horsburgh, R. E. Mulvey, R. Rowlings, R. *Chem. Commun.*, 1996, 1739.

[14] C. Nachtigal, S. Al-Gharabli, K. Eichele, E. Lindner, H. A. Mayer, *Organometallics*, 2002, **21**, 105.

[15] P. Umapathy, R. A. Harnesswala, C. S. Dorai, *Polyhedron*, 1985, **4**, 1595.

[16] H. Matsuzaka, T. Kamura, K. Ariga, Y. Watanabe, T. Okubo, T. Ishii, M. Yamashita, M. Kondo, *Organometallics*, 2000, **19**, 216.

[17] J. A. Cabeza, H. Nöth, M. D. J. Rosales-Hoz, G. Sánchez-Cabrera, *Eur. J. Inorg. Chem.*, 2000, **11**, 2327.

[18] G. Kaupp, M. R. Naimi-Jamal, V. Stepanenko, *Chem. - A Eur. J.*, 2003, **9**, 4156.

[19] F. F. Caserio Jr., J. J. Cavallo, R. I. Wagner, *J. Org. Chem.*, 1961, 2157.

[20] S. S. Chissick, M. J. S. Dewar, P. M. Maitlis, *J. Am. Chem. Soc.*, 1961, **83**, 2708.

[21] R. Goetze, H. Noth, *J. Organomet. Chem.*, 1978, **145**, 151.

[22] F. Farzaneh, M. Majidian, M. Ghandi, *J. Mol. Catal. A Chem.*, 1999, **148**, 227.

[23] J. P. Collman, M. Zhong, C. Zhang, S. Costanzo, *J. Org. Chem.*, 2001, **66**, 7892.

[24] S. E. Denmark, Y. Ueki, *Organometallics*, 2013, 8.

[25] P. C. Keller, J. V. Rund, *Inorg. Chem.*, 1979, **18**, 3197.

[26] J. S. Hartman, J. A. W. Shoemaker, *Polyhedron*, 2000, **19**, 165.

[27] C. D. Schaeffer, J. J. Zuckerman, *J. Am. Chem. Soc.*, 1974, **96**, 7160.

[28] N. Lavoie, T. Ong, S. I. Gorelsky, I. Korobkov, G. P. A. Yap, D. S. Richeson, *Organometallics*, 2007, 6586.

[29] N. Lavoie, S. I. Gorelsky, Z. Liu, T. J. Burchell, G. P. A. Yap, D. S. Richeson, *Inorg. Chem.*, 2010, **49**, 5231.

[30] P. Bazinet, G. P. A. Yap, D. S. Richeson, *Organometallics*, 2001, **20** , 4129.

[31] I. Nowik, H. A. Spinney, D. S. Richeson, R. H. Herber, *J. Organomet. Chem.*, 2007, **692**, 5680.

[32] P. Bazinet, G. P. A. Yap, G. A. DiLabio, D. S. Richeson, *Inorg. Chem.*, 2005, **44**, 4616.

[33] P. Bazinet, G. P. A. Yap, D. S. Richeson, *J. Am. Chem. Soc.*, 2001, **123**, 11162.

Chapter II

Ligand synthesis

I. Introduction

This project has as a central requirement the preparation of 1,8-disusbstituted diaminonaphthalene compounds (R,R'-DAN) and this process relies on the formation of C-N bonds. This transformation is a key reaction to prepare commonly used organic compounds as well as compounds used in the pharmaceutical field.[1] We chose to focus on three different approaches depending on whether aromatic or alkyl substituents were in the target compounds.

The first approach we employed was based on a classic reductive amination which is one of the most common methods for controlled alkylation of amines. This approach begins with a carbonyl species and converts it to an intermediate imine followed by a reduction reaction, affording the final alkylated amine compound (**Scheme 2.1**).[2] This approach provides a simple method to prepare a variety of alkylated amines but does not allow for the introduction of an aryl substituent.

Scheme 2.1

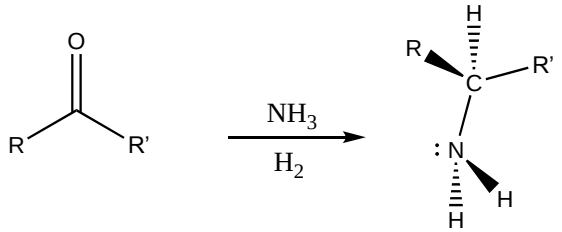

The second method is the amidation with acyl halide for preparing (Np)(^{i}Pr)-DAN. This method is reacts an acyl halide with an amine group as a nucleophile, leading a nucleophilic substitution reaction (S_n). Following this, a reduction of the carbonyl function of the amide is performed forming the desired akyl amine product (**Sheme 2.2**).

Scheme 2.2

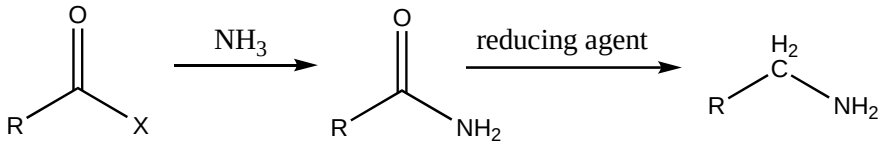

The third synthetic method we employed, a copper catalyzed coupling reaction, was to allow access to aryl substituted species. This approach is a catalytic amidation of aryl halides and is a powerful synthetic process. While such reactions can be catalyzed using Cu and Pd species, we have chosen to focus on Cu catalysts due to the lower catalyst cost and apparent ease in isolation of final product (**Scheme 2.3**).[3] Specifically, our focus was to employ the reported use of copper(I)/diamine mixtures for coupling of aryl iodide with nitrogens in the urea intermediate **2.9** as nucleophiles (**Scheme 2.7**).

Scheme 2.3

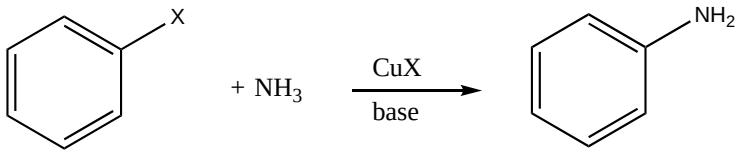

In order to clearly provide numeric labels to the compounds in this thesis I have decided to make separate labels in each chapter. The goal is to make it easier for readers to follow the reaction schemes. Each chapter will have a self-consistent numbering scheme. Therefore, there might be some cases that repeated compounds have different labels in different chapters.

II. Results and Discussion

A. Reductive Amination Routes to (Alkyl)$_2$-DAN

The initial concept for applying the reductive amination approach to preparing 1,8-dialkyldiaminonaphthalene was envisioned to proceed by the simple route outlined in **Scheme 2.4**. However, it was quickly determined that this route was not operable. The condensation of an 1,8-diaminonaphthalene with anhydrous acetone under reflux did not yield the anticipated diimine (**Scheme 2.4**) but rather the aminal product, 2,2-dimethyl-2,3- dihydroperimidine (**2.3**), was formed from this reaction (**Scheme 2.5**). This compound was identified by ^{13}C NMR spectroscopy which display the quaternary carbon at δ 64.3 ppm, as well as an observation of lack of downfield signal for NH(^{i}pr) in ^{1}H NMR. On top of that, a symmetric molecule is confirmed by not only the same *ortho* protons on the naphthyl rings but also single resonance for identical methyl groups in isopropyl group.

Scheme 2.4

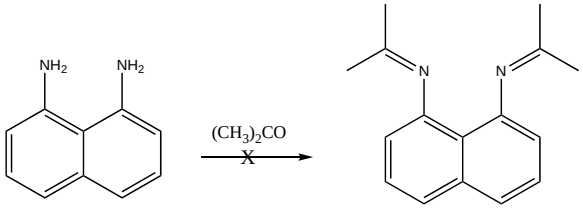

2.1 2.2

Scheme 2.5

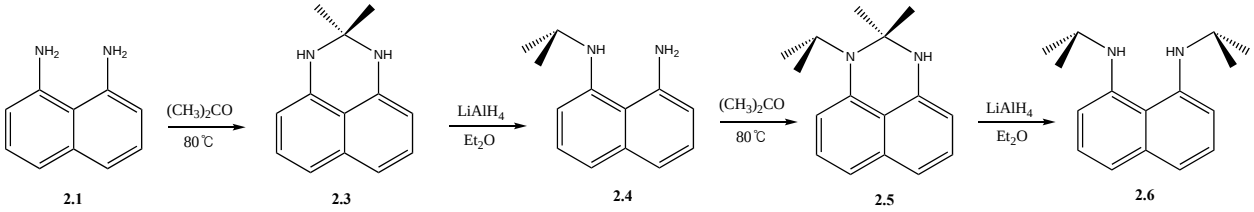

2.1 2.3 2.4 2.5 2.6

Although this was not the anticipated product, a successful reduction, with excess of $LiAlH_4$, resulted in the formation of the monoalkylated amine. Given the reactivity of $LiAlH_4$, this reaction was performed under strict anhydrous conditions. Due to the vigor of this reaction, the ether suspension of $LiAlH_4$ was cooled to 0°C before the slow dropwise addition of the aminal solution using a syringe. Furthermore, this reaction proceeded with vigorous generated of hydrogen gas which required that the reaction be vented during the addition, the reaction is stirred overnight to be complete. At this point the excess hydride reagent was quenched by adding excess of isopropanol followed by water while holding the reaction in ice at 0 °C. During the quenching, generation of hydrogen gas resulted in the pressure of the Schlenk flask being quite high and requiring venting. After the completion of the quenching, diethyl ether solvent was added to dissolve the final products which were separated from the byproduct salt by filtration through a Celite plug. After drying and removing the reaction solvent, the final product

is isolated as a purple oil. The key characteristic of this produce is that the ^{1}H NMR has a unique signal for the isopropyl peak at δ 3.6 ppm as a single septet.

Fortunately, a second substituent can be introduced using the same approach. By following the same procedure using the monoalkyl intermediate with acetone, a single isopropyl substituent was added to each of the amine centers to generate ($^{i}Pr)_2$-DAN **2.6** as the final desired product. Once again, the isopropyl groups provided characteristic ^{1}H NMR data by showing one septet signal, indicating the symmetrical condition.

The monoalkylated diaminonaphthalene can also be used as a precursor to introduce a second, different alkyl group. For example, reaction of the adduct **2.4** with pivaloylchloride, $(CH_3)_3CCOCl$, led to the formation of trimethylacetamide intermediate **2.7**, (^{i}PrNH)(^{t}BuCONH)$C_{10}H_6$ (**Scheme 2.6**). Following an analogous reduction procedure with $LiAlH_4$ solution in anhydrous ether led to the formation of **2.8** (Np)(^{i}Pr)-DAN.

Scheme 2.6

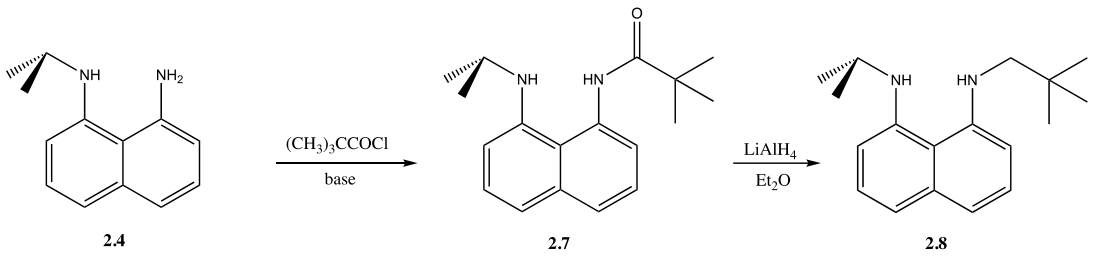

2.4 **2.7** **2.8**

B. Copper Catalyzed Aryl Iodide Coupling Route to $(Ph)_2$-DAN

With the goal of preparing $(Ph)_2$-DAN, we first protected the parent diamine as a 1H,3H-perimidin-2-one (**2.9**).[4] Therefore, a reaction was carried out between 1.8-diaminonaphthalene and the carbonyl group in diphenyl carbonate (**Scheme 2.7**). This reaction was completed by heating to 75 °C. This product was combined with 2 equivalent of iodobenzene, catalytic amount of CuI, excess of K_2CO_3, N,N'-dicyclohexylethane-1,2-diamine and diphenyl ether as solvent in a Schlenk flask and the reaction mixture was heated to 160°C overnight under nitrogen atmosphere.[5] The product was isolated using solvent extraction and column chromatography to give the diphenyl urea intermediate (**2.10**). The free diamine was formed by reaction of this intermediate with 4 equivalent of $NaNH_2$ at 90 °C for 18 hours, leading the final expected product (**2.11**). At the end, further purification is completed by extraction with dichloromethane as well as column chromatography with hexane and dichloromethane mixture. Although the preparation of $(Ph)_2$-DAN requires a quite complicated procedure including two applications of column chromatography, the anticipated compound was isolated successfully and characterized by ^{1}H NMR, ^{13}C NMR, and single crystal X-ray diffraction as well.

^{1}H and ^{13}C NMR spectroscopy was successfully obtained and was identical to the anticipated result. Since it has same substituents at the nitrogen atoms, it has symmetrical condition. Therefore, the identical peaks for both protons at *ortho* in naphthyl ring were observed in ^{1}H NMR. In addition, in the phenyl ring substituted at nitrogen, only three peaks are detected instead of six peaks in ^{13}C NMR, which represent *ortho, meta*, and *para* protons. Another interesting feature found was N-H peak in ^{1}H NMR, revealing a single (broad) peak at δ 7.15 ppm. The fact that $(Ph)_2$-DAN has significantly deshielding N-H peak compared to $(^iPr)_2$-DAN

and (Np)(^{i}Pr)-DAN can be explained by substitution effect at the nitrogen atoms. Due to electron withdrawing phenyl group at nitrogens, it has a lot more downfield peak at δ 7.15 ppm.

Scheme 2.7

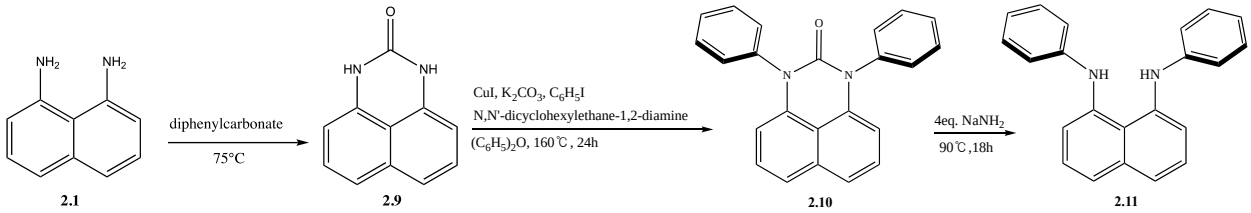

Compound **2.11** $(Ph)_2$-DAN could be characterized by X ray structure as well. The structure obtained from this analysis is shown in **Figure 2.1**. In the X-ray structure of $(Ph)_2$-DAN (**Table 2.2**), a bond length of 1.4332(3) Å was detected for the C1-N1 bond. The C11-N1 bond length is 1.413(3) Å, which is quite similar to the C1-N1 bond length. One of the most interesting features is the geometry. At the nitrogen atom, C11-N1-C1, C11-N1-H1A, and C1-N1-H1A are respectively 122.04(17)°, 113.3(13)°, and 110.0(13)°. From these bond angles, the fact that this structure has distorted tetrahedral around the nitrogen atom is found out. Therefore, with this geometry $(Ph)_2$-DAN can possess steric protections even though they are less than isopropyl group. Regarding this, the ability of the $(Ph)_2$-DAN to stabilize 13 group elements will be introduced in **Chapter III**.

III. Conclusion

Synthesis of disubstituted R,R'-DAN is successfully completed by using reductive amination and copper catalyzed coupling reaction. In addition, these species were easily characterized by NMR due to some unique and characteristic resonances. Furthermore, single

crystal X-ray diffraction confirmed the detailed connectivity of these compounds. Depending on the size and orientation of substituents, disubstituted R,R'-DAN is expected to show different reactivity as a ligand. In the following chapter, the reactivity of these R,R'-DAN with different substitutions will be introduced.

Experimental section

General: Unless otherwise noted, all manipulations are carried out in either a nitrogen filled glovebox or under nitrogen using standard Schlenk techniques. Reaction solvents were sparged with nitrogen then dried by passage through column of activated alumina using an apparatus purchased from Anhydrous Engineering. Deuterated benzene, chloroform, and toluene were purchased from Aldrich Chemical Company. Acetone, Toluene, Anhydrous diethyl ether, Isopropanol, Diethyl ether, 1,8-diaminonaphthalene, formic acid, and $LiAlH_4$, were purchased from Aldrich Chemical Company and used without further purification. ^1H and spectra were run on either a Bruker 400 MHz, or a Bruker 600MHz spectrometer, and $^{13}C\{^1H\}$ NMR was on a Bruker 100 MHz or a Bruker 150 MHz using the residual protons of the deuterated solvent for reference. Elemental analyses were performed by Midwest micro lab in Indianapolis, IN, USA.

The crystal of **2.11** $(Ph)_2$-DAN was mounted on thin glass fibers using paratone oil. Prior to data collection, the crystals were cooled to 201(2) K. The data were collected on a Bruker AXS single-crystal diffractometer equipped with a sealed Mo tube (wavelength 0.71073 Å) and APEX II CCD detector. The raw data collection and reduction were done with the Bruker APEXII

software package. 1 Semi-empirical absorption corrections based on equivalent reflections were applied using SADABS. Systematic absences in the diffraction dataset and unit-cell parameter were consistent with triclinic space groups. The structures were solved by direct methods and refined with full-matrix least-squares procedures based on F^2, using SHELXL and WinGX. All non-H atoms were refined anisotropically. All hydrogen atoms were placed in idealized positions. Displacement ellipsoid plots were produced using ORTEP.

Preparation of 2,2-dimethyl-2,3-dihydroperimidine (2.3):

Acetone (37g, 638 mmol) was first dried in a round bottom flask, by addition of activated molecular sieves (10.0g) and allowing this to sit at room temperature overnight. To a Teflon screw cap-sealed flask was added 1,8-diaminonaphthalene (**2.1**) (10.0g, 63.2 mmol) and dried acetone. The reaction was heated to 80°C overnight. The reaction mixture was filtered and the solids were washed with diethyl ether. The ether solutions were combined and all of the volatiles were removed under vacuum to give 10.17g (94%) of a red/purple solid that was identified as the aminal, 2,2-dimethyl-2,3- dihydroperimidine (**2.3)**.

^{1}H NMR ($CDCl_3$, 400MHz): δ 7.17-7.32 (m, 4H, CH), 6.45 (d, 2H, CH), 4.18 (br, 2H, NH), 1.40 (s, 6H, CH_3) $^{13}C\{^1H\}$ NMR ($CDCl_3$, 100 MHz): δ 140.3, 134.4, 126.9, 116.6, 112.6, 105.6 (C_{arom}), 64.3 (N_2CMe_2), 28.4 (CH_3)

Analysis Calcd $C_{13}H_{14}N_2$ C, 78.75; H, 7.12; N,14.13; Found C, 78.79; H, 7.23; N, 13.98

Preparation of N-(isopropyl)-1,8-diaminonaphthalene, (^{i}PrNH)(NH_2)$C_{10}H_6$ (2.4):

A sample of compound **2.3** (5.0g, 25.2 mmol) was dissolved in diethyl ether and added dropwise to a suspension of $LiAlH_4$ (2.9g, 76 mmol) in 100 ml of diethyl ether that was maintained at 0°C. Since significant pressure develops during the addition, a needle should be added through rubber septum to allow the gas to vent. After addition, the reaction was allowed to warm to room temperature and stirred for an additional 12 hrs. The reaction was then quenched, at 0°C, with isopropanol followed by water. This mixture was extracted with diethyl ether and dried under vacuum to give **2.4** as a purple oil (4.12g, 82%).

^1H NMR ($CDCl_3$, 400MHz): δ 7.17-7.26 (m, 4H, CH), 6.55-6.59 (m, 2H, CH), 4.89 (br, 3H, NH), 3.6 (sept, 1H, $CHMe_2$, J=6.84Hz), 1.26 (d, 6H, CH_3, J=6.84Hz) $^{13}C\{^1H\}$ NMR ($CDCl_3$, 100 MHz): δ 145.3, 144.1, 137.1, 126.2, 125.9 119.9, 118.7, 117.3, 112.1, 108.5(C_{arom}), 48.5 ($CHMe_2$), 22.7 (CH_3).

Analysis Calcd $C_{13}H_{16}N_2$ C, 77.96; H, 8.05; N,13.99; Found C, 78.21; H, 8.35; N, 14.32

Preparation of N,N'-diisopropyl-1,8-diaminonaphthalene, (^{i}PrNH)$_2$C$_{10}$H$_6$ (2.6):

Compound **2.4** (5.0g, 25 mmol) was mixed with dried acetone (29.0g, 500 mmol) in a flask sealed with a Teflon screw cap. The reaction was heated to reflux overnight. The product was isolated as a purple oil. A sample of the resulting aminal (15.0g, 62.5 mmol) was allowed to react with $LiAlH_4$ (6.0g, 160 mmol) and stirred overnight. The reaction was then quenched, at 0°C, with isopropanol followed by water. The resulting mixture was extracted with diethylether, dried and the solvent evaporated to yield **2.6** as a purple oil (10.5g, 70%). This product can be further purified by silica gel column chromatography using mixture of hexanes and diethylether (7:3 ratio) as the eluent.

^{1}H NMR ($CDCl_3$, 400MHz): δ 7.19-7.24 (m, 4H, CH), 6.58 (m, 2H, CH), 5.36 (br, 2H, NH), 3.58 (sept, 2H, $CHMe_2$, J=6.28Hz), 1.24 (d, 12H, CH_3, J=6.28Hz) ^{13}C{^{1}H} NMR ($CDCl_3$, 100 MHz): δ 145.0, 137.3, 125.9, 119.3, 117.9, 110.3 (C_{arom}), 46.4 ($CHMe_2$), 22.6 (CH_3).

Analysis Calcd $C_{16}H_{22}N_2$ C, 79.29; H, 9.15; N,11.56; Found C, 79.53; H, 9.35; N, 11.19

Synthesis of N-(isopropyl)-N'-(neopentyl) -1,8-diaminonaphthalene, (^{i}PrNH)(NpNH)$C_{10}H_6$ (2.8):

Reaction of pivaloylchloride (1.90g, 15.7mmol) with **2.4** in the presence of excess base (triethyl amine) generated the trimethylacetamide intermediate, (^{i}PrNH)(^{t}BuCONH)$C_{10}H_6$ (**2.7**) 4.37 g, 15.3 mmol) which was used in the following reaction without further purification. In a Schlenk flask, lithium aluminum hydride (1.46 g, 38.4 mmol) was dissolved in 50 mL of dry ether, cooled in an ice bath and stirred for 1 h. Compound **2.7** (4.37 g, 15.3 mmol) was added slowly as a solid to this solution under nitrogen and allowed to stir for 2 h. The reaction was stirred for 18 h at room temperature, and quenched with wet ether. The organic layer was extracted with water, dried with sodium sulfate, and purified by flash chromatography to yield a purple solid (**2.8**) (3.85 g, 93%).

^{1}H NMR ($CDCl_3$, 400MHz): δ7.19 (m, 4H), 6.60 (m, 2H), 5.23 (br, 2H), 3.65 (sept, 1H, J=6.4Hz), 2.91 (s, 2H), 1.12 (s, 9H) ^{13}C{^{1}H} NMR ($CDCl_3$, 100 MHz): 147.2, 144.8, 136.8, 126.1, 125.6, 119.3, 117.8, 117.3, 109.3, 105.4 (C_{arom}), 57.2 (CH_2Me_3), 45.2 ($CHMe_2$) 31.2 (CMe_3), 27.9 (CH_3), 22.7 (CH_3).

Analysis Calcd $C_{18}H_{26}N_2$ C, 79.95; H, 9.69; N,10.36; Found C, 79.63; H, 10.01; N, 10.39

Preparation of [1,8-(NHC_6H_5) $C_{10}H_6$](2.11):

To a Schlenk-flask was added **2.9** 1H,3H-perimidin-2-one (3.91 g, 21.7 mmol), iodobenzene (9.30g, 45.6mmol), CuI (0.83g, 4.36mmol), K_2CO_3 (8.99 g, 65.1 mmol), N,N'-dicyclohexylethane-1,2-diamine (0.50 g, 4.37mmol) and diphenyl ether (14.78 g, 86.8mmol). The reaction mixture was heated to 160 ℃ overnight under a nitrogen atmosphere. The reaction mixture was cooled to room temperature and extracted with dichloromethane. The solvent was removed under reduced pressure to give a brown solid. This material was further purified by column chromatography (silica gel, 1:1 hexane: dichloromethane) to afford an intermediate product diphenyl urea **2.10**. This product was then allowed to react with 4 equiv of $NaNH_2$ in 40 mL pyridine at 90℃ for 18 hours under a nitrogen atmosphere. The pyridine solvent was removed at 50℃ to afford a black solid which was cooled in an ice bath and a mixture of CH_2Cl_2 and water was added. This mixture was extracted with dichloromethane. The CH_2Cl_2 was removed under vacuum to give a gray solid. Purification by column chromatography (silica gel, 70:30 hexane: dichloromethane) afforded a light green solid (**2.11**) (3.98 g, 50 %).

^{1}H NMR (C_6D_6, 600MHz): δ 7.42 (dd, 2H, J=9.37, 1.30Hz), 7.15 (s, 2H, NH), 7.13 (m, 2H), 7.08 (d, 1H, J=1.14Hz), 7.07 (d, 1H, J=1.02Hz), 16.99-7.02(m, 4H), 6.74-6.77(m, 6H) ^{13}C{^{1}H} NMR (C_6D_6, 150 MHz): δ 144.99, 140.61, 137.41, 129.28, 126.11, 123.39, 122.10, 121.09, 118.21, 117.01 (C_{arom}).

Structural determinations

Table 2.1 Crystal data and structure refinement for **2.11**

Empirical formula	C_{22} H_{18} N_2
Formula weight	310.38
Temperature (K)	200(2)
Wavelength (Å)	0.71073
Crystal system	Triclinic
Space group	P -1
a (Å)	8.7479(17)
b (Å)	10.0156(19)
c (Å)	10.193(2)
α (deg)	94.308(2)
β (deg)	97.785(2)
γ (deg)	114.049(2)
Volume (Å ^{3})	799.6(3)
Z	2
Density (calculated) (Mg/m^3)	1.289
Absorption coefficient (mm^{-1})	0.076
F(000)	328
Crystal size (mm^3)	0.277 x 0.166 x 0.150
Theta range for data collection	2.038 to 28.490
Index ranges	-11<=h<=11, -11<=k<=12, -13<=l<=13
Reflections collected	7333
Independent reflections	3784 [R(int) = 0.0407]
Completeness to theta = 25.242	99.6 %
Refinement method	Full-matrix least-squares on F^2
Data / restraints / parameters	3784 / 0 / 225
Goodness-of-fit on F^2	0.925
Final R indices [I>2sigma(I)]	R1 = 0.0545, wR2 = 0.1035
R indices (all data)	R1 = 0.1181, wR2 = 0.1306
Extinction coefficient	n/a
Largest diff. peak and hole	0.185 and -0.213 e^{-3}

Figure 2.1 X-ray structure of **2.11** (Carbon bonded hydrogen atoms have been removed for clarity)

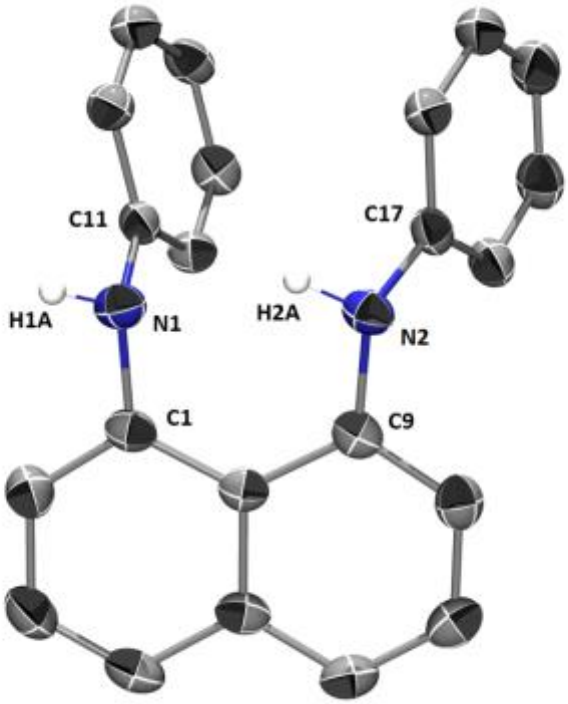

Table 2.2 Selected Bond Lengths [Å] and Angle [°] for **2.11**

Bond lengths (Å)		**Bond Angle (°)**	
C1-N1	1.433(2)	C1-N1-C11	122.04(17)
C11-N1	1.413(2)	C2-N2-C17	125.25(17)
C2-N2	1.414(2)	C1-N1-H1A	110.0(13)
C17-N2	1.406(2)	C11-N1-H1A	113.3(13)

IV. References

[1] J. F. Hartwig, S. Shekhar, Q. Shen, F. Barrios-Landeros, *In Chemistry of Anilines*, 2007, **1**, 455.

[2] A. F. Abdel-Magid, K. G. Carson, B. D. Harris, C. A. Maryanoff, R. D. Shah, *J. Org. Chem.*, 1996, **61**, 3849.

[3] S. Zhang, Y. Ding, *Organometallics,* 2011, **30**, 633.

[4] F. Sachs, *Liebigs Ann. Chem*., 1909, **365**, 136.

[5] J. C. Antilla, S. L. Buchwald**,** *Org. Lett.*, 2001, **3** ,2077.

Chapter III
Group 13 Compounds Supported by N,N'-Disubstituted-1,8-diaminonaphthalene (R,R'-DAN)

I. Introduction

Boron hydrides and alkyl aluminum species are among the core functional groups in the chemistry of the group 13 elements. They can be exploited from both fundamental and applied perspectives and employed for their reactivity and as building blocks in synthesis. In general, the chemistry of these and other group 13 element functionalities is modulated by the ligand environment. An excellent example has been the application of β-diketiminate ligands, which has vitalized the synthetic chemistry of group 13 elements.[1–4] As supporting ligands, β-diketiminates exhibit strong and diverse binding modes combined with adjustable steric demands through variation of the NR substituents and these features have promoted their application across the periodic table. These observations provided an impetus for our efforts to design and implement

ligands designed around the dianions of N,N'-disubstituted-1,8-diaminonaphthalene (R,R'-DAN). This ligand family presents a scaffold for preparing rigid dianionic ligands (R_2DAN^{2-}) with delocalized π-electrons that are reminiscent of the β-diketiminate scaffold in both geometry and frontier orbital topology. Dianionic diaminonaphthalene-type ligands have seen some application with borohydride and alkylaluminum chemistry with particularly noteworthy examples being silyl-substituted tetraminoperylene and 1,8-bis(trialkylsilylamino)naphthalene group 13 compounds represented by **A**-**D**.[5–9] Importantly, all reports with the R_2DAN framework are restricted to trialkylsilyl, R_3Si, substituents and are therefore limited by the electronic, steric and potential N-silyl reactivity of these groups.

Chart 3.1

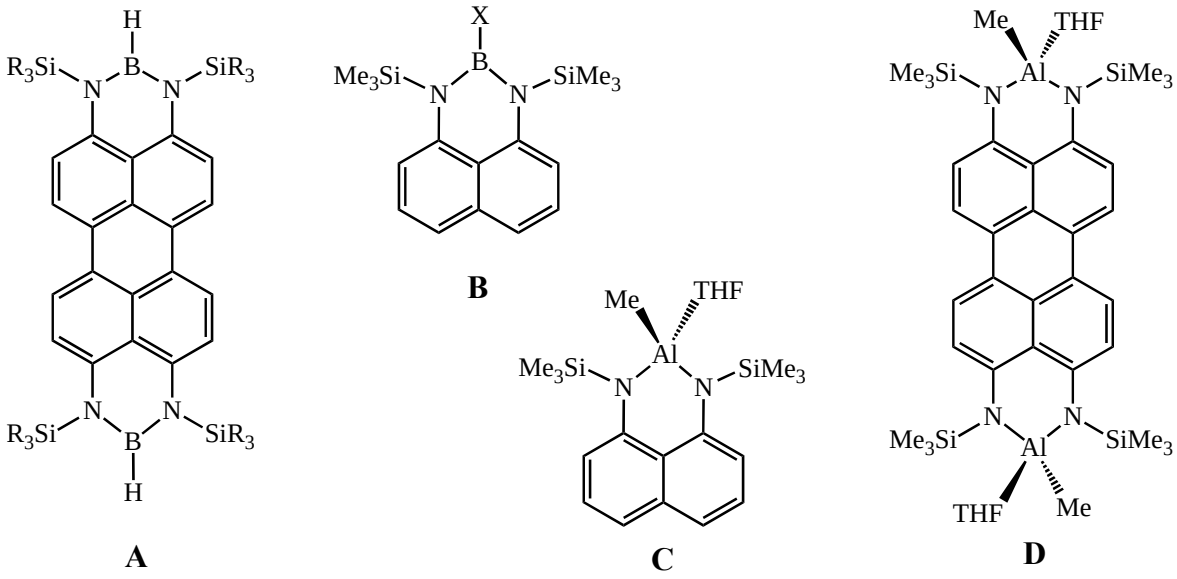

Our desire is to explore changes to the steric and electronic features of R'R-DAN framework by introduction and variation of the N-substituents to include both alkyl and aryl groups. We previously reported the syntheses of **3.1**, through a multi-step reductive amination method,[10] and **3.2**, using a Cu catalyzed coupling reaction,[11–13] from diaminonaphthalene in good

yields (**Scheme 3.1**). This framework has been successfully applied to group 14 divalent species[10,14,15] and to low coordinate group 15 cations. [16,17]

Scheme 3.1

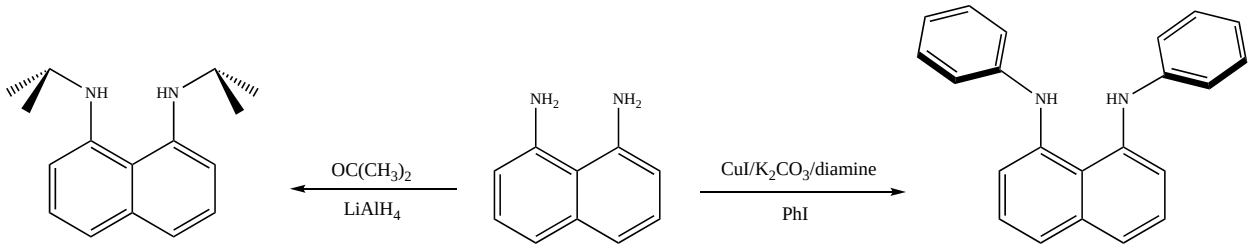

3.1 **3.2**

In this chapter, we report the use of **3.1** and **3.2** for the preparation of mononuclear three coordinate boron hydrides, with unusual air stability, mono- and dinuclear methylaluminum complexes, and the synthesis and isolation of the dilithium salt of the diphenyl species. In addition, application of dilithium salt of $(iPr)_2$-DAN to Ga and In compound will be presented. These new compounds make a substantial and fundamental contribution to the limited number of compounds and represent potential building blocks for further synthetic chemistry of these elements.

II. Results and Discussion

Both of the diaminonaphthalene-based ligands **3.1** and **3.2** possess reactive NH protons allowing for the direct reaction with inorganic and organometallic compounds that possess basic groups. In the reactions reported here these compounds are borohydride, with reactive BH groups, trimethylaluminum and methyllithium, with strongly basic AlMe and LiMe functions. For example, both **3.1** and **3.2** react directly with $BH_3(SMe_2)$ as summarized in **Scheme 3.2**. From these reactions, compounds **3.3** and **3.4** were isolated as colorless and light orange crystals,

respectively. The multinuclear NMR spectra and microanalyses of these two new 1,3,2-diazaborine species provide clear indications for the structures proposed for **3.3** and **3.4**. Specifically, both compounds exhibited ^{1}H and ^{13}C NMR resonances indicating a symmetrical ligation for the R_2DAN^{2-} group. A broad resonance for the BH group was observed in each of the ^{1}H NMR spectra at δ 4.74 ppm (**3.3**) and 4.26 ppm (**3.4**). These values are comparable to silylated N,N′;N″,N″-diborylene-3,4,9,10-tetraaminoperylenes (**A**) with corresponding B-H resonances observed at δ = 4.71–4.75 ppm.[8] The ^{11}B NMR spectra further support the proposed formulations with compound **3.3** displaying a proton decoupled ^{11}B resonance at δ 28.4 ppm while compound **3.4** showed such a resonance at δ 25.92 ppm. For comparison, the perylene analogue **A** (R = Me) showed a ^{11}B resonance at δ = 29.8.[7] Although they are not strictly analogous, the monomeric species **B**, $BX[(NSiMe_3)_2C_{10}H_6]$, gave ^{11}B resonances in a similar range with X=Cl at δ = 32.1 ppm and X=Br at δ = 28.04 ppm (X = Br) [6]

Interestingly, both **3.3** and **3.4** are stable to air in both solid state and in solution and NMR solutions can be prepared in the air using untreated deuterated solvents. This observation is in sharp contrast with the reactivity for the diazaborine species represented by **A** which are sensitive in both solid state and solution.[8] Similarly, five-membered 2-hydrido-1,3,2-diazaboroles are reported to be colorless air- and moisture-sensitive solids.[18]

Scheme 3.2

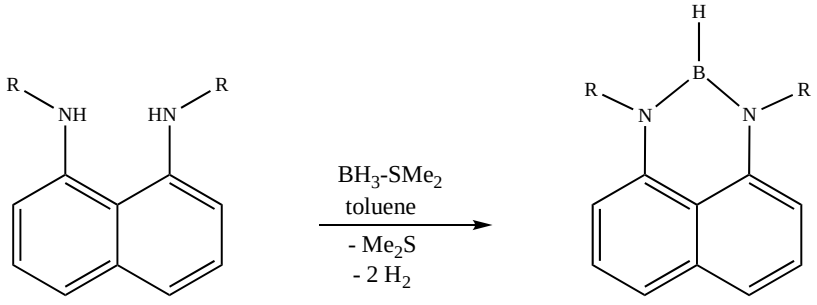

3.1 R = ^{i}Pr
3.2 R = Ph

3.3 R = ^{i}Pr
3.4 R = Ph

Definitive confirmation for the structural features of **3.3** and **3.4** was obtained from the single crystal X-ray analyses with results summarized in **Figures 3.1** and **3.2** and selected bond lengths and angles are given in **Table 3.2**. Both structures display a diaminonaphthylenediyl group chelating to a trigonal planar B center. The NBN unit is coplanar with the naphthyl backbone with the angle between these two planes of 4.5° (**3.3**) and 8.2° (**3.4**). For both **3.3** and **3.4**, the H atoms of the BH functions were refined freely and yielded average B-H bond distances of 1.11 Å. The two compounds exhibited similar N-B-N bite angles of 120.8(3)° and 119.2(1)° as expected for an sp^2 hybridized boron center. The B-N distances in **3.3** are equal to each other at 1.41 Å and those in compound **3.4** are only slightly longer on average at 1.417 Å. These bond lengths are slightly shorter than those reported for the tetraaminoperylene compounds **A**, which averaged to 1.43 Å.[8] Reported six-membered compounds with saturated rings, $HB(RR'C_6H_3NCHMe)_2CMe_2$ (R = R' = ^{i}Pr; R = ^{i}Pr, R' = H), displayed B-N distances that ranged from 1.396(4) Å to 1.414(5) Å and these distances were judged to be optimize B–N pπ–pπ interactions.[19]

In order to reveal some bonding details for these two compounds, we decided to examine the computational optimization of compound **3.3**. Starting with the crystal structure data, compound **3.3** was optimized using DFT and the Gaussian 09 program with the B3LYP functional and a 6-311+G(d,p) basis set.[20] The resulting structure was well aligned with the experimentally determined X-ray data with a comparison of selected bond distances and angles compared in **Table 3.11**.

The frontier orbitals obtained from these computations show a clear NBN π bonding interaction as shown in **Chart 3.2**. While the HOMO and LUMO molecular orbitals are non-bonding with respect the BN linkages, the occupied HOMO-2 and HOMO-1 orbitals show the contribution to NBN π–bonding. Taken together the experimental as well as the theoretical data agree with a significant delocalization of the nitrogen lone pairs and *p* electrons into the vacant $2p_z$ orbital of the boron atom in **3.3** and provide a rationalization for the air stability of these species.

Chart 3.2 Frontier Orbitals of 3.3 computed as described in the text.

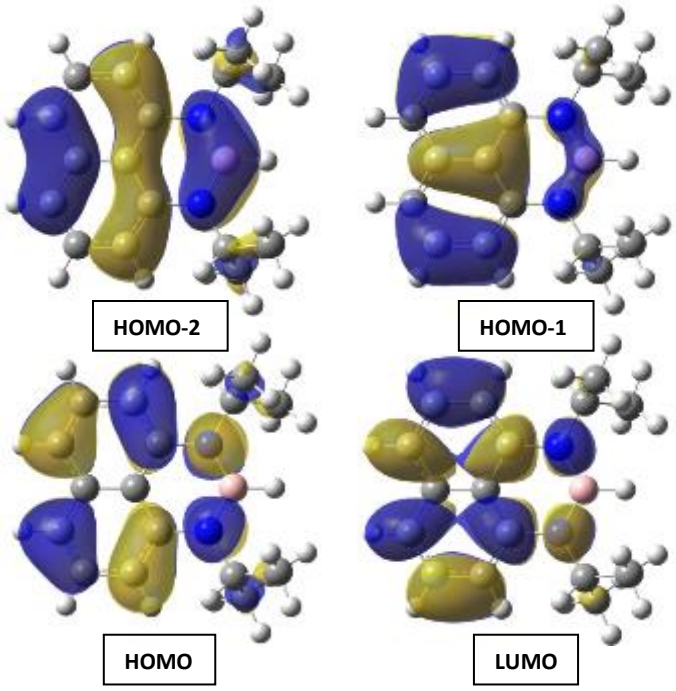

An analogous method for introducing the $(Ph)_2$-DAN^{2-} group in aluminum chemistry involved a proton transfer reaction between **3.2** and trimethylaluminum in toluene as shown in

Scheme 3.3. The red crystalline product obtained from this reaction gave ^{1}H NMR data indicative of a 1:1 CH_3Al:ligand ratio with nine aromatic carbon resonances in the ^{13}C NMR consistent with a symmetrical ligand environment. A ^{1}H NMR resonance at δ 0.24 ppm was assigned the Al-CH_3 and is comparable to compounds **C** and **D**, the only reported analogues, which displayed Al-CH_3 resonances at δ = –0.55 ppm .[5] and δ = -0.53ppm[7], respectively.

Scheme 3.3

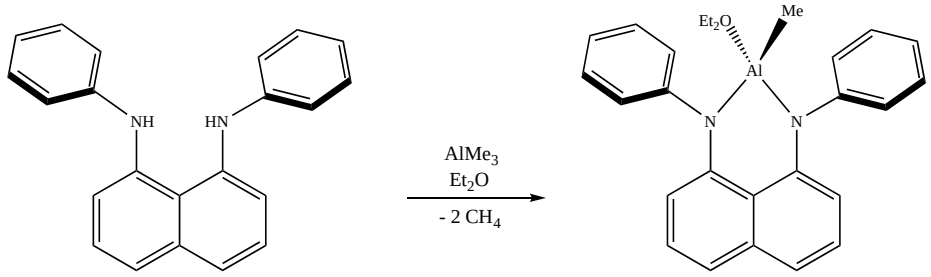

3.2 **3.5**

The NMR spectra showed variable traces of Et_2O and this provided further motivation to perform the single crystal X-ray analysis of **3.5**. The results of this analysis are summarized in **Figure 3.3** with selected bond distances and angles in **Table 3.4**. Compound **3.5** was the anticipated mononuclear Al species possessing one chelating diphenyldiaminonaphthalene ligand, one methyl group and a coordinated diethyl ether to give a pseudo-tetrahedral coordination geometry. The presence of the coordinated ether is consistent with the fact that crystals of **3.5** were removed from mother liquor and immediately frozen in Paratone oil for data collection. The N(1) and N(2) centers in **3.5** are planar with a sum of angles around these N-centers equal to 360° in both cases. Of the six angles around the Al center, the smallest is represented by the ligand bite angle N(1)-Al(1)-N(2), 98.84(11)°. The average of these six angles is 109.3° supporting a distorted tetrahedral assignment.

The four bond lengths associated with the Al center, C23-Al1 = 1.939(3) Å, N1-Al1 = 1.812(2) Å, N2-Al1 =1.816(2) Å, and Al1-O1 = 1.895(2) Å, are slightly shorter than in the analogue [1,8-$(Me_3SiN)_2C_{10}H_6$]Al(Me)THF (**C**) (Al-C 1.9482(16), av. Al–N = 1.830 Å, Al-O = 1.920 Å,).[5] Further comparison can be made to the silylated tetraaminoperylenes species, $[AlMe(THF)]_2[(Me_3Si)_4N_4C_{20}H_8]$ (**D**), with Al-C = 1.954(3) Å, average Al-N = 1.826 Å, and Al-O = 1.910(2) Å.[7]

Reaction of $AlMe_3$ with ligand **3.1** followed a different path than for the synthesis of **3.5**. The direct reaction of equimolar ratio of **3.1** and $AlMe_3$ proceeded smoothly to yield the bimetallic product **(**$AlMe_2)_2$[1,8-($^iPrN)_2C_{10}H_6$] (**3.6**) as shown in **Scheme 3.4**. The first indication of a bimetallic species was the appearance of two equal intensity proton NMR signals at δ -0.10 ppm and -1.18 ppm consistent with four Al-CH_3 groups. This product was the only isolated species regardless of the reaction stoichiometry and an improved synthesis was achieved using 2 equiv of $AlMe_3$ to yield white crystals of **3.6**.

Scheme 3.4

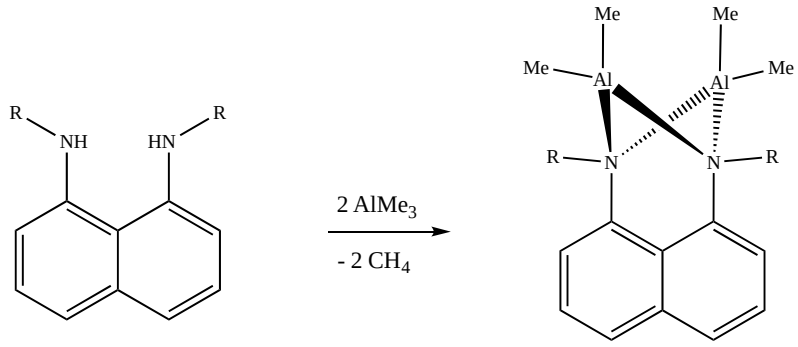

3.1 R = ^{i}Pr
3.2 R = Ph

3.6 R = ^{i}Pr
3.7 R = Ph

In the ^{1}H NMR of **3.6,** two doublet peaks at δ 1.38 ppm and 1.28 ppm indicative of four methyl groups in $CH(CH_3)_2$ and two peaks for isopropyl protons at δ 4.03 and 3.58ppm were

found, revealing a slightly unsymmetrical structure. Another feature is one of the isopropyl protons gave a signal that was slightly deshielded by 0.5 ppm from the starting $(iPr)_2$-DAN, which might be because of weak interaction between isopropyl proton and Al center.

Crystallization of the reaction mixture from cold (-25°C) ether gave colorless crystals of compound **3.6**. An X-ray diffraction study was performed which confirmed the connectivity with the molecular structure shown in **Figure 3.4**. The corresponding values for selected bond distances and angles are shown in **Tables 3.6**.

Compound **3.6** is a bimetallic Al species, $[\mu\text{-}1,8\text{-}(^{i}PrN)_2C_{10}H_6](AlMe_2)_2$, with each aluminum center possessing a four-coordinate distorted tetrahedral geometry consisting of two methyl groups, and the two nitrogens of a R,R'-DAN ligand. Each of the anionic nitrogen centers of the ligand donates a lone pair of electrons to the two different Al centers. The result is a puckered Al_2N_2 metallacycle in a butterfly shape with approximate C_{2v} symmetry. A similar structure has been reported from the related trimethylsilyl ligand, $[\mu\text{-}1,8\text{-}(Me_3SiN)_2C_{10}H_6](AlMe_2)_2$ (**E**).[9]

The four Al-N bond lengths in **3.6** range from 1.9710(15) Å to 1.9873(15) Å and are considerably longer than in the mononuclear species **3.5** yet slightly shorter than in **E** with Al-N of 2.00 Å. The butterfly shape of the bimetallic core positions the two methyls in inequivalent environments consistent with the NMR observations. Crystallographically there are four Al-C bond lengths ranging from 1.9554(19) Å to 1.9627(19) Å. In **3.6** the two N-Al-N bite angles were 80.74(6)° and 80.73(6)° which are much smaller than the corresponding angle in **3.5** but only slightly smaller than the angle of 83.0(2)° observed for compound **E**.

Following this same stoichiometric ratio but using ligand **3.2** generated the analogous species **3.7** (**Scheme 3.4**). Again two equal intensity signals were observed for the inequivalent Al-CH_3 groups in **3.7** at δ -0.37 and -0.64 ppm. Furthermore, single crystal X-ray analysis confirmed a similar structure as represented in **Figure 3.5** and with the selected bond distances and angles in **Table 3.6**.

In this case, the molecule exhibited formal C_2 symmetry with the axis through the center of the Al_2N_2 cycle. The structural features of **3.7** parallel those of **3.6** with small differences in bond lengths and bond angles (**Table 3.6**).

Compounds **3.3-3.7** represent interesting species as well as building blocks for further group 13 chemistry. These compounds were readily prepared by exploiting the basicity of the B and Al substituents. Another synthetically powerful reagent for the introduction of R_2DAN^{2-} ligands would be the lithium salt of the R,R'-DAN dianion. We targeted this species using the reaction of **3.1** and **3.2** with 2 equivalents of MeLi as shown in **Scheme 3.5**. Regarding this, isolation of dilithium salt **3.8** as well as implications of **3.8** as ligand was already known. Therefore, our initial effort was made on the isolation of **3.9**.

The identity of compound **3.9** was first suggested by the NMR data. Specifically, disappearance of N-H peaks (δ 7.15 ppm) of **3.2** can give evidence for the deprotonation of **3.2** $(Ph)_2$-DAN.

Scheme 3.5

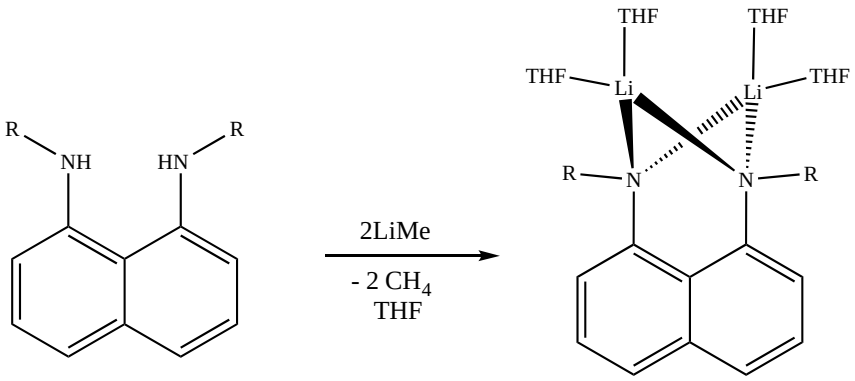

3.1 R = ^{i}Pr
3.2 R = Ph

3.8 R = ^{i}Pr
3.9 R = Ph

Fortunately, an X-ray structure of **3.9** was obtained (**Figure 3.6**), and the generality of the structural features of **3.6** and **3.7** was observed for **3.9**. In addition, four THF were coordinated to the two Li centers with bond lengths 1.988(4)Å, 2.050(4)Å, 1.965(5)Å, and 1.979(5)Å as Li1-O1, Li1-O2, Li2-O3, and Li2-O4 (**Table 3.8**). Li1-N1, Li1-N2, Li2-N1, and Li2-N2 were found as 1.999(4) Å, 2.038(4) Å, 2.041(4) Å, and 2.020(4) Å. In addition, N1-Li1-N2 and N1-Li2-N2 were 85.30(16)º and 84.70(16)º. Around Li1 center, bond angles were 104.9(4)º, 125.3(2)º, 111.7(3)º, and 85.30(16)º as O1-Li1-O2, O1-Li1-N1, O2-Li1-N2, N1-Li1-N2, revealing pseudo tetrahedral geometry.

However, the ^{1}H NMR spectra of **3.9** gave integrated values for the THF coordinated to Li center that were low in intensity. This can be understood by some loss of coordinated THF during NMR sample preparation. Since crystals are formed in the solution and X-ray measurement removed from the mother liquor and immediately covered in Paratone oil, all four

coordinated THF molecules were captured and kept well. However, for the NMR spectroscopy, vacuum is required to dry and in this process, various THF ratios are possible.

The preparation of dilithium salt of $(Ph)_2$-DAN was proved by X-ray structure and NMR spectroscopy. In addition, the successful isolation of boron and aluminum complexes led us to investigate the reaction of the dianion ligands R,R'-DAN^{2-} with the heavier members of group13, Ga(III) and In(III). While the previous approach used R,R'-DAN without deprotonation of the N-H groups, the reactions with $GaCl_3$ and $InCl_3$ require the preparation of the dilithium salt of $(^iPr)_2$-DAN, (**3.8**) as a ligand due to the lack of the basic group in metal compound. Therefore, **3.8** was first synthesized by the deprotonation reaction of $(^iPr)_2$-DAN with 2 *equiv* of MeLi. This was followed by *in situ* reaction carried out by addition of $GaCl_3$ to the reaction mixture of $(^iPr)_2$-DAN/MeLi Unfortunately, instead of the desired three coordinated Ga(III) supported by $(^iPr)_2$-DAN, **3.10** was obtained (**Scheme 3.6**). The identity of **3.10** was confirmed by a single crystal X-ray structure with the results show in **Figure 3.7**.

Scheme 3.6

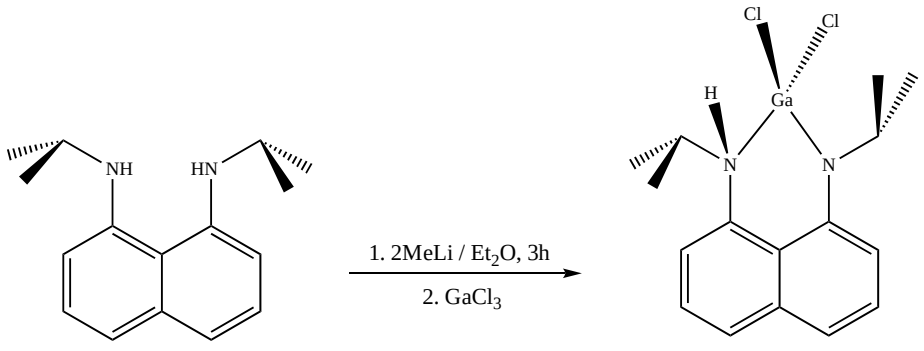

3.1 **3.10**

As seen in the structure of **3.10**, one of nitrogen centers possesses an N-H group (N1 in **Table 3.10**) the other N center (N2) and the two chlorides are anionic ligands for the Ga center. When it comes to the X-ray structure, around Ga center, the bond angles were found as 109.98(3)°, 116.86(7)°, 100.30(7) °, and 106.35(6)°, which are Cl1-Ga1-Cl2, Cl2-Ga1-N2, N1-Ga1-N2, and Cl1-Ga1-N1 respectively. This result indicates that the Ga(III) center in complex **3.10** has a distorted tetrahedral geometry. This can be explained by an additional electron donation from the lone pair of nitrogen (N1). The difference in the two Ga-N bonds can be clearly seen in the structural data. Specifically Ga1-N2 was found to be 1.8543(17) Å, while Ga1-N1 was 1.9652(17) Å. This is consistent with the fact that N1 was not successfully deprotonated.

Two possibilities can be proposed to explain why the ligand in **3.10** was not deprotonated successfully. The first is that some water impurities in the solvent system can give proton sources to the dilithium salt of ligand **3.8**, leading to the formation of **3.10**. The second possible reason for the isolation of **3.10** is that the amount of MeLi was not enough to deprotonate two N-Hs for some sources of error.

We also attempted to use $InCl_3$ for the coordination chemistry with $(^{i}Pr)_2$-DAN via the analogous pathway for the preparation of Ga(III) complexes (**3.10**) and this is summarized in **Scheme 3.7**. Once again, the issue with residual ligand protons was observed. This was confirmed by single crystal X-ray analysis (**Figure 3.8**). In this case, the structure is a five coordinate complex with two equivalents of ligand **3.1** $(^{i}Pr)_2$-DAN supporting the $InCl_3$ starting material as shown in **Figure 3.8**. This coordination complex (**3.11**) with two additional ligands is possible due to the bigger size of In compared to Al and B.

Scheme 3.7

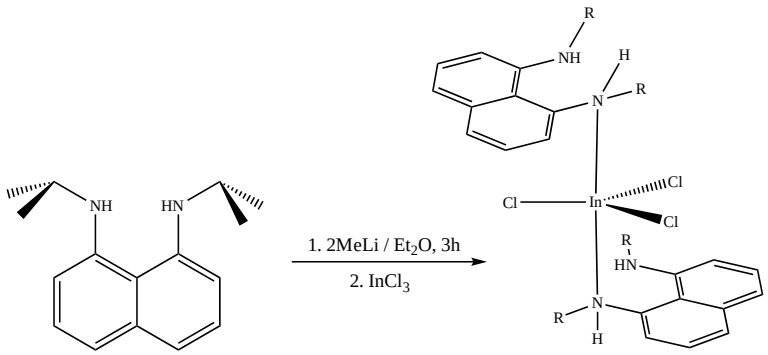

3.1 **3.11** R = ^{i}Pr CH(CH$_3$)$_2$

Bond angles around In center were 127.620(11)°, 127.620(11)°, and 104.76(2)° as Cl1-In1-Cl2, Cl1-In1-Cl2_i, and Cl2-In1-Cl2_i, revealing that the three chlorides lie in the same plane. In addition, (^{i}Pr)$_2$-DAN ligand was perpendicular to the plane of the $InCl_3$, having 90.20(3) ° bond angle as N15-In1-Cl1, which indicates trigonal bipyramidal geometry for the In center in **3.11**.

Again, this failure of preparing of the desired anion substituted In complex can possibly be solved by the isolation of dilithium salt (**3.8**) first to make sure of preparation of dianion ligand. Moreover, usage of more purified and dried anhydrous solvent can be another solution to prevent any proton sources. Since the final product was a mixture of some leftover ligand with the final product and some other intermediates, analysis of NMR data of **3.10** and **3.11** was not possible. Although I was not able to isolate the targeted complexes in the case of **3.10** and **3.11**, this issue could be further investigated in the future. Additionally, more efforts will be made on the reaction of **3.9** as a ligand for Ga and In compounds.

III. Conclusion

Applications of dianionic ligand R,R'-DAN with 13 group elements were successfully investigated, showing the fact that R,R'-DAN^{2-} can stabilize BH and AlMe moieties and can lead to both mononuclear (**3.3**, **3.4**, and **3.5**) and dinuclear complexes (**3.6** and **3.7**). Additionally, preparation of the dilithium salts of R,R'-DAN expands the chemistry in terms of the development of a new class of ligand and their use for main group element as well as transition metal compounds. Regarding this, by using the dilithium salt of (^{i}Pr)$_2$-DAN **3.8**, synthesis of Ga and In complexes supported by (^{i}Pr)$_2$-DAN was attempted. However, unfortunately, the desired complexes were not isolated. This challenge will likely be solved by future lab members.

Experimental section

General: All manipulations were carried out in either a nitrogen filled dry box or under nitrogen using standard Schlenk techniques. Reaction solvent (anhydrous diethyl ether) was sparged with nitrogen then dried by passage through column of activated alumina using an apparatus purchased from Anhydrous Engineering. Deuterated benzene was purchased from Aldrich Chemical Company and was dried by vacuum transfer from potassium. MeLi, $BH_3{\cdot}SMe_2$, and $AlMe_3$, $GaCl_3$, $InCl_3$, anhydrous toluene, and anhydrous hexane were purchased from Aldrich Chemical Company and used without further purification. ^{1}H, spectra were run on either a Bruker 300 MHz or Bruker 600 MHz spectrometer, ^{13}C{^{1}H} NMR spectra were run on either a Bruker 75 MHz or Bruker 150 MHz, and ^{11}B{^{1}H} NMR were on a Bruker 96 MHz using the residual protons of the deuterated solvent for reference. Elemental analyses were performed by Midwest micro lab in Indianapolis, IN, USA.

The crystal of **3.3**-**3.7** and **3.9**-**3.11** were mounted on thin glass fibers using paratone oil. Prior to data collection, the crystals were cooled to 201(2) K. The data were collected on a Bruker AXS single-crystal diffractometer equipped with a sealed Mo tube (wavelength 0.71073 Å) and APEX II CCD detector. The raw data collection and reduction were done with the Bruker APEXII software package. 1 Semi-empirical absorption corrections based on equivalent reflections were applied using SADABS. Systematic absences in the diffraction dataset and unit-cell parameter were consistent with orthorhombic (**3.3**, **3.9**), monoclinic (**3.4**, **3.5**, **3.7**, **3.11**) triclinic (**3.6**, **3.10**) space groups. The structures were solved by direct methods and refined with full-matrix least-squares procedures based on F^2, using SHELXL and WinGX. All non-H atoms were refined anisotropically. All hydrogen atoms were placed in idealized positions. Displacement ellipsoid plots were produced using ORTEP.

Preparation of HB[1,8-(N^{i}Pr)C$_{10}$H$_6$] (3.3)

The diamine (^{i}PrNH)$_2$C$_{10}$H$_6$ **1** (0.40g, 1.65 mmol) was dissolved in approximately 30 ml of toluene and transferred to a Schlenk vessel equipped with a teflon screw cap. To this solution was added $BH_3 \cdot SMe_2$ (0.140g, 1.84 mmol) pre-dissolved in toluene. The solution was heated to 60°C overnight. The volatiles were removed under vaccum and the crude product was crystallized by dissolving in hexane and cooling to -25°C. The product was isolated as colorless crystals and dried under vacuum (0.397g, 1.57 mmol, 95 %).

^{1}H NMR (C_6D_6, 300 MHz): with ^{11}B decoupling δ 7.20-7.22 (m, 4H, CH), 6.36-6.41 (m, 2H, CH), 4.74 (s br, 1H, BH), 3.67(sep, 2H, J= 6.03 Hz, $CHMe_2$), 1.12 (d, 12H, J=6.54, CH_3).

$^{13}C\{^{1}H\}$ NMR (C_6D_6, 75 MHz): δ 141.85, 137.28, 127.70, 127.10, 118.20, 102.97(C arom), 46.69 ($CHMe_2$), 22.86 (CH_3).

$^{11}B\{^{1}H\}$ NMR (C_6D_6, 96 MHz): with ^{1}H decoupling δ 25.92 (s BN_2H)

Analysis Calcd $C_{16}H_{21}BN_2$ C, 76.21; H, 8.39; N,11.11; Found C, 75.84; H, 8.37; N, 11.05

Preparation of HB[1,8-(NC_6H_5)$C_{10}H_6$] (3.4)

The diamine $(C_6H_5NH)_2C_{10}H_6$ (0.320g, 1.03 mmol) was dissolved in approximately 30 ml of toluene and transferred to a Schlenk vessel equipped with a teflon screw cap. To the solution was added $BH_3{\cdot}SMe_2$ (0.14ml, 1.115 mmol) pre-dissolved in toluene. The solution was heated to 60°C overnight. The volatiles were removed under vacuum and the crude product was crystallized by dissolving in ether and cooling to -25°C. The product was isolated as light orange color crystals and dried under vacuum (0.303g, 0.95mmol, 92%).

^{1}H NMR ($CDCl_3$, 300 MHz): δ 7.44-7.50 (m, 4H, CH), 7.30-7.37 (m, 6H, CH), 7.03-7.14 (m, 4H, CH), 6.15 (dd, 2H, CH), 4.26 (s br, 1H, BH).

$^{13}C\{^{1}H\}$ NMR ($CDCl_3$, 75 MHz): δ 143.88, 142.97, 136.32, 129.90, 128.25, 127.06, 126.78, 120.32, 118.90, 106.15 (C arom)

$^{11}B\{^{1}H\}$ NMR ($CDCl_3$, 96 MHz): with ^{1}H decoupling δ 28.4 (s, BN_2H)

Analysis Calcd $C_{22}H_{17}BN_2$ C, 82.52; H, 5.35; N, 8.75; Found C, 82.18; H, 5.67; N, 8.52

Preparation of [μ-1,8-$C_{10}H_6(NC_6H_5)_2$](AlMe)(OEt_2) (3.5)

The diamine $(C_6H_5NH)_2C_{10}H_6$ (0.310g, 1.0 mmol) was dissolved in approximately 15 ml of diethyl ether in a round bottom flask equipped with a stir bar. To the solution was added a 2.0 M hexanes solution of $AlMe_3$ (0.5 ml, 1.0 mmol). The solution was stirred overnight and turned green, reddish brown, and then red color solution. The volatiles were removed and the product was recrystallized from ether at -25°C, giving red crystals (0.314g, 0.74mmol, 0.74%).

^{1}H NMR ($CDCl_3$, 300 MHz): δ 7.37 (dd, 2H, CH, J=8.16, 1.32Hz), 7.13-7.11 (m, 2H, CH), 6.93-7.07 (m, 6H, CH), 6.67-6.73 (m, 6H, CH), 0.24(s, 3H, CH_3Al).

$^{13}C\{^1H\}$ NMR ($CDCl_3$, 75 MHz): δ 144.93, 140.06, 137.45, 129.09, 126.01, 123.30, 121.10, 118.09, 116.92 (C_{arom}), 1.39(CH_2Al)

Preparation of [μ-1,8-$C_{10}H_6(N^iPr)_2$]($AlMe_2$)$_2$ (3.6)

The diamine $(^iPrNH)_2C_{10}H_6$ (0.242g, 1.0 mmol) was dissolved in approximately 15 ml of hexane in a round bottom flask equipped with a stir bar. To the solution was added a 2.0 M hexanes solution of $AlMe_3$ (1.0 ml, 2.0 mmol). The solution was stirred overnight and turned black, then brown. The volatiles were removed to yield a beige solid. The product was recrystallized from ether at -25°C, affording colorless crystals (0.0174g, 49%).

^{1}H NMR (toluene, 300MHz): δ 7.31-6.68 (m, 6H), 4.03 (sept, 1H, J=7.14Hz), 3.58 (m, 1H), 1.38 (d, 6H, J= 7.05Hz), 1.28 (d, 6H, J=6.33Hz), -0.10 (s, 6H), -1.18 (s, 6H).

$^{13}C\{^1H\}$ NMR (C_6D_6, 75 MHz): δ 125.31, 123.25, 122.16, 119.74, 113.44, 111.66(C_{arom}), 47.41($CHMe_2$), 47.13($CHMe_2$), 22.49(CH3), 19.08(CH3), -5.23($AlMe_2$), -10.95($AlMe_2$).

Analysis Calcd $C_{20}H_{32}Al_2N_2$ C, 67.77; H, 9.10; N,7.90; Found C, 66.84; H, 9.31; N, 7.75

Preparation of [μ-1,8-$C_{10}H_6(NC_6H_5)_2$]$(AlMe_2)_2$ (3.7)

The diamine $(C_6H_5NH)_2C_{10}H_6$ (0.105g, 0.5 mmol) was dissolved in approximately 15 ml of diethyl ether in a round bottom flask equipped with a stir bar. To the solution was added a 2.0 M hexanes solution of $AlMe_3$ (0.5 ml, 1.0 mmol). The solution was stirred overnight and turned green, then red color. The volatiles were removed and the product was recrystallized from ether at -25°C, providing red crystals (0.135g, 0.32mmol, 65%).

^{1}H NMR (C_6D_6, 600 MHz): δ 7.18-7.28 (m, 9H), 7.11-7.13 (m, 2H), 6.93 (t, 3H, J=7.89Hz), 6.36(dd, 2H, J=7.72, 1.00Hz), -0.37 (s, 6H, $AlMe_2$), -0.64 (s, 6H, $AlMe_2$).

$^{13}C\{^1H\}$ NMR (C_6D_6, 150 MHz): δ 152.14, 144.11, 135.85, 130.99, 130.03, 126.96, 126.76, 123.39, 121.82, 118.04, 113.85 (C_{arom}), -8.15 (CH_2Al), -10.04 (CH_2Al).

Preparation of Li_2[1,8-(NPh)$C_{10}H_6$](THF)$_4$ (3.8)

Addition of MeLi (2.5 ml, 1.6M in ether, 4 mmol) to a dark yellow solution of 1,8-$[HN(C_6H_5)]_2C_{10}H_6$ (0.620g 2mmol) in ether let to a color change to green color with gas evolution. The reaction mixture was stirred overnight and then all volatiles were removed under vacuum. The crude product was purified by crystallization from THF at -35 °C, giving yellowish orange color crystals (1.011g, 1.66mmol, 83%.)

^{1}H NMR ($CDCl_3$, 300 MHz): δ 7.53 (dd, 1H, CH), 7.29-7.44 (m, 5H, CH), 7.14-7.26 (m, 5H, CH), 6.89- 6.94 (m, 5H, CH), 3.76 (br, 10H, THF), 1.87 (br, 10H, THF)

$^{13}C\{^1H\}$ NMR ($CDCl_3$, 75 MHz): δ 129.44, 129.30, 126.69, 126.08, 125.17, 123.33, 121.28, 120.65, 118.50, 116.71 (C_{arom}), 68.47(THF), 25.85(THF)

Structural determinations

Table 3.1 Crystal data and structure refinement for **3.3** and **3.4**

	3.3	**3.4**
Empirical formula	$HB[(^{i}PrN)_2C_{10}H_6]$	$HB[(PhN)_2C_{10}H_6]$
Formula weight	252.16	320.18
Temperature (K)	200(2)	201(2)
Wavelength (Å)	0.71073	0.71073
Crystal system	Orthorhombic	Monoclinic
Space group	$P\ 2_1\ 2_1\ 2_1$	$P\ 2_1\ c$
a (Å)	8.6579(8)	9.2859(3)
b (Å)	9.2253(9)	20.6308(6)
c (Å)	18.0067(19)	9.3938(3)
α (deg)	90	90
β (deg)	90	111.3220(10)
γ (deg)	90	90
Volume($Å^3$)	1438.2(2)	1676.44(9)
Z	4	4
Density (calculated) (Mg/m^3)	1.165	1.269
Absorption coefficient (mm^{-1})	0.068	0.074
Reflections collected	17625	24573
Independent reflections	3439 [R(int) = 0.0439]	4244 [R(int) = 0.0229]
Refinement method	Full-matrix least-squares on F^2	Full-matrix least-squares on F^2
Data / restraints / parameters	3439 / 39 / 204	4244 / 0 / 230
Goodness-of-fit on F^2	0.955	1.012
Final R indices [I>2sigma(I)]	R1 = 0.0702, wR2 = 0.1878	R1 = 0.0411, wR2 = 0.1022
R indices (all data)	R1 = 0.0868, wR2 = 0.2037	R1 = 0.0570, wR2 = 0.1154

Figure 3.1 Structural representation of **3.3**, (Hydrogen atoms bonded to carbon have been omitted for clarity)

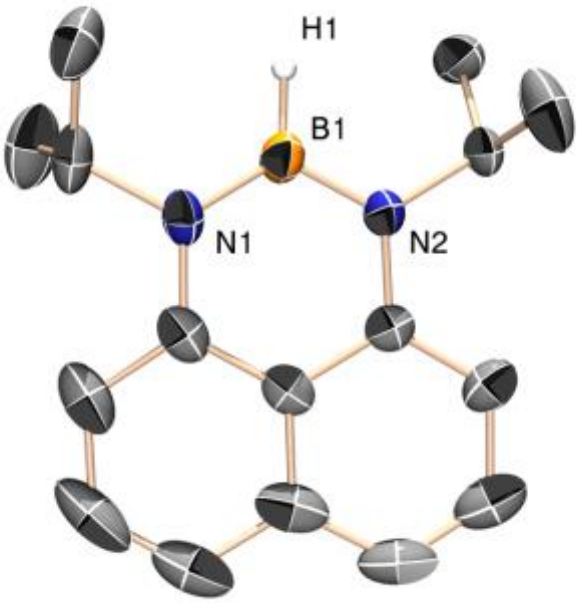

Figure 3.2 Structural representation of **3.4** (Hydrogen atoms bonded to carbon have been omitted for clarity)

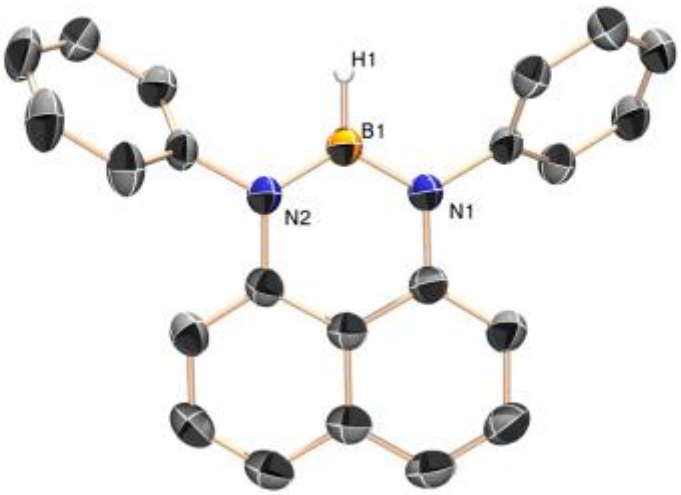

Table 3.2 Selected Bond Lengths [Å] and Angles [°] for **3.3** and **3.4**

3.3		**3.4**	
Bond lengths (Å)			
N1-B1	1.405(5)	B1-N1	1.4163(16)
N2-B1	1.409(5)	B1-N2	1.4186(16)
B1-H1	1.11(4)	B1-H1	1.112(13)
Bond Angle (°)			
N1-B1-N2	120.8(3)	N1-B1-N2	119.21(11)
N1-B1-H1	123(2)	N1-B1-H1	119.5(7)
N2-B1-H1	115(2)	N2-B1-H1	121.3(7)

Table 3.3 Crystal data and structure refinement for **3.5**

Empirical formula	$C_{27}H_{29}AlN_2O$
Formula weight	424.50
Temperature (K)	200(2) K
Wavelength (Å)	0.71073
Crystal system	Monoclinic
Space group	P 2_1/n
a (Å)	8.4606(8)
b (Å)	14.5062(13)
c (Å)	19.2089(17)
α (deg)	90
β (deg)	97.9680(10)
γ (deg)	90
Volume ($Å^3$)	2334.8(4)
Z	4
Density (calculated) (Mg/m^3)	1.208
Absorption coefficient (mm^{-1})	0.108

F(000)	904
Crystal size (mm^3)	0.206 x 0.076 x 0.067
Theta range for data collection (∞)	1.765 to 25.249
Index ranges	-10<=h<=10, -17<=k<=17, -23<=l<=23
Reflections collected	23062
Independent reflections	4233 [R(int) = 0.0799]
Completeness to theta = 25.242	100.0 %
Refinement method	Full-matrix least-squares on F^2
Data / restraints / parameters	4233 / 0 / 283
Goodness-of-fit on F^2	1.010
Final R indices [I>2sigma(I)]	R1 = 0.0526, wR2 = 0.1212
R indices (all data)	R1 = 0.1160, wR2 = 0.1586
Extinction coefficient	n/a
Largest diff. peak and hole	0.276 and -0.242 e^{-3}

Figure 3.3. The molecular structure for **3.5** (Hydrogen atoms bonded to carbon have been omitted for clarity)

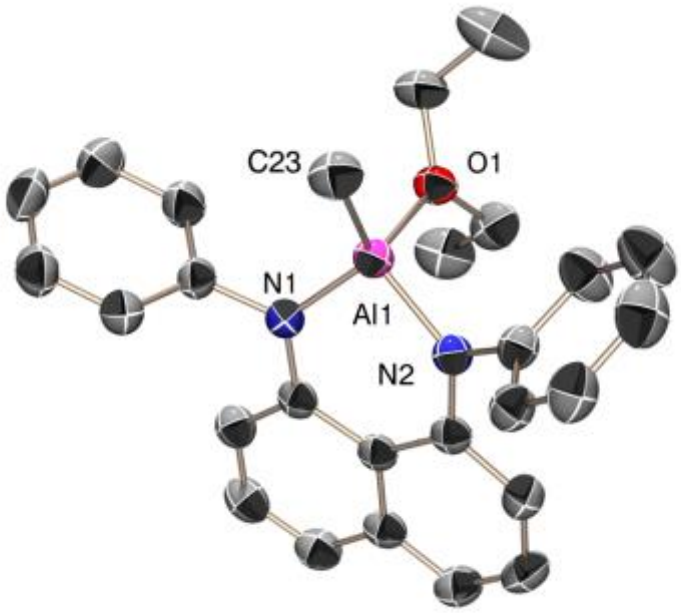

Table 3.4 Selected Bond Lengths [Å] and Angles [°] for **3.5**

Bond lengths (Å)		**Bond Angle (°)**	
C23-Al1	1.939(3)	N1-Al1-N2	98.84(11)
N1-Al1	1.812(2)	N1-Al1-O1	108.21(10)
N2-Al1	1.816(2)	N1-Al1-C23	117.73(13)
Al1-O1	1.895(2)	N2-Al1-O1	103.83(10)
		N2-Al1-C23	119.84(13)
		O1-Al1-C23	107.17(12)

Table 3.5 Crystal data and structure refinement for **3.6** and **3.7**

	3.6	**3.7**
Empirical formula	$C_{20}H_{32}Al_2N_2$	$C_{26}H_{28}Al_2N_2$
Formula weight	354.43	422.46
Temperature (K)	200(2)	200(2)
Wavelength (Å)	0.71073	0.71073
Crystal system	Triclinic	Monoclinic
Space group	P -1	C 2/c
a (Å)	8.4035(6)	13.0565(13)
b (Å)	8.5065(5)	11.3712(12)
c (Å)	14.8030(10)	17.0996(18)
α (deg)	86.745(3)	90
β (deg)	80.172(3)	108.4110(10)
γ (deg)	78.409(3)	90
Volume ($Å^3$)	1021.11(12)	2408.8(4)
Z	2	4
Density (calculated) (Mg/m^3)	1.153	1.165
Absorption coefficient (mm^{-1})	0.146	0.135
F(000)	384	896

Reflections collected	13493	14310
Independent reflections	4829 [R(int) = 0.0351]	2975 [R(int) = 0.0184]
Refinement method	Full-matrix least-squares on F^2	Full-matrix least-squares on F^2
Data / restraints / parameters	4829 / 0 / 225	2975 / 0 / 139
Goodness-of-fit on F^2	1.027	1.075
Final R indices [I>2sigma(I)]	R1 = 0.0465, wR2 = 0.1220	R1 = 0.0404, wR2 = 0.1178
R indices (all data)	R1 = 0.0712, wR2 = 0.1350	R1 = 0.0482, wR2 = 0.1250

Figure 3.4. The molecular structure for **3.6** (Hydrogen atoms bonded to carbon have been omitted for clarity)

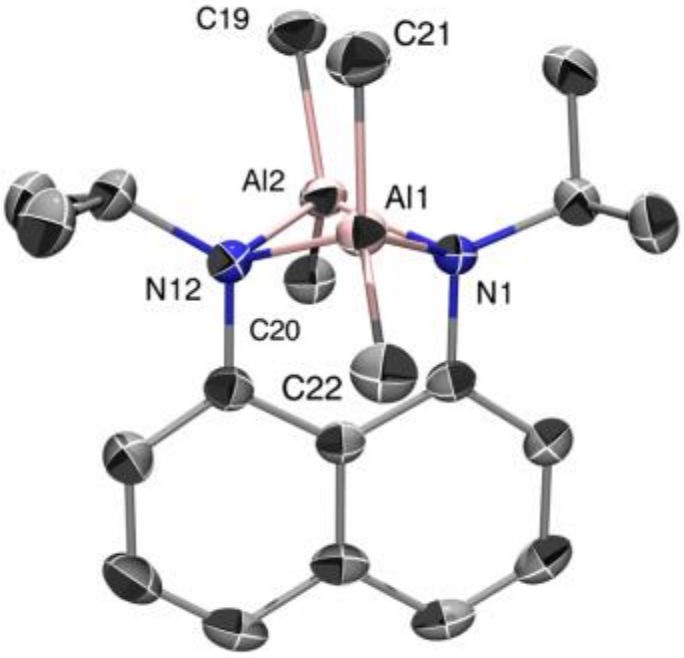

Figure 3.5. The molecular structure for **3.7** (Hydrogen atoms bonded to carbon have been omitted for clarity and thermal ellipsoids are only shown for selected atoms)

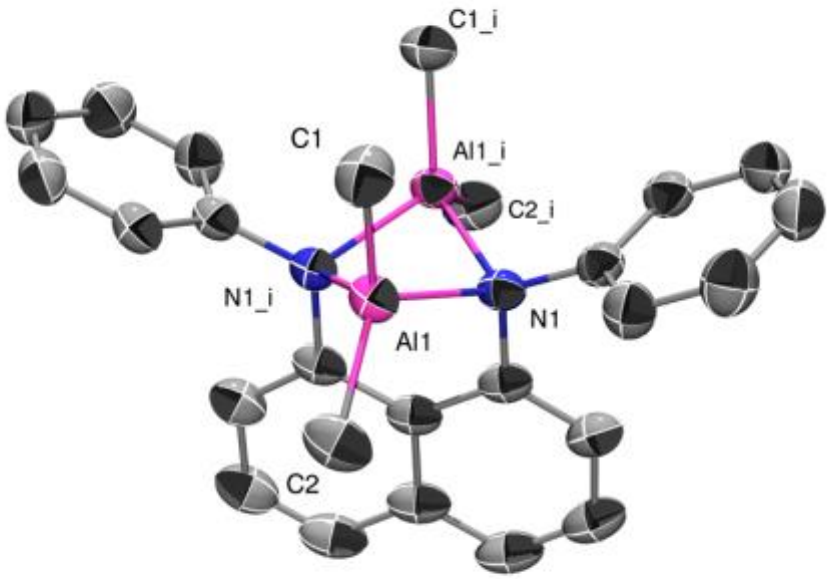

Table 3.6. Selected Bond Lengths [Å] and Angles [°] for **3.6** and **3.7**

3.6		**3.7**	
Bond lengths (Å)			
Al1-C21	1.962(2)	C1-Al1	1.9544(16)
Al1-C22	1.9627(19)	C2-Al1	1.9542(16)
Al1-N12	1.9744(17)	N1-Al1	1.9868(12)
Al(1)-N1	1.9836(15)	N1-Al1_i	1.9966(12)
Al1-Al2	2.8465(8)		
Al2-C19	1.9554(19)		
Al2-C20	1.957(2)		
Al2-N12	1.9710(15)		
Al2-N1	1.9873(15)		
Bond Angle (°)			
N1-Al1-N12	80.74(6)	C1-Al1-C2	118.16(8)
N1-Al1-C21	115.90(8)	C1-Al1-N1	111.38(6)

N1-Al1-C22	113.85(8)	C1-Al1-N1_i	114.29(6)
C21-Al1-N12	112.00(8)	N1-Al1-N1_i	79.43(6)
C22-Al1-N12	113.17(8)	Al-N1-Al_i	90.96(5)
C22-Al1-C21	116.15(10)	C2-Al1-N1	115.05(7)
C19-Al2-C20	114.93(9)	C2-Al1-N1_i	112.44(6)
C19-Al2-N12	109.74(8)		
C20-Al2-N12	114.90(8)		
C19-Al2-N1	119.14(8)		
C20-Al2-N1	112.81(8)		

Table 3.7 Crystal data and structure refinement for **3.9**

Empirical formula	$C_{38}H_{48}Li_2N_2O_4$
Formula weight	610.66
Temperature (K)	201(2)
Wavelength (Å)	0.71073
Crystal system	Orthorhombic
Space group	P n a 2_1
a (Å)	16.6442(12)
b (Å)	11.1358(8)
c (Å)	18.8591(13)
α (deg)	90
β□(deg)	90
γ (deg)	90
Volume ($Å^3$)	3495.5(4)
Z	4
Density (calculated) (Mg/m^3)	1.160
Absorption coefficient(mm^{-1})	0.073
F(000)	1312

Crystal size (mm^3)	0.978 x 0.538 x 0.464
Theta range for data collection	2.124 to 27.810
Index ranges	-21<=h<=21, -14<=k<=14, -24<=l<=24
Reflections collected	40167
Independent reflections	8238 [R(int) = 0.0235]
Completeness to theta = 25.242	100.0 %
Refinement method	Full-matrix least-squares on F^2
Data / restraints / parameters	8238 / 507 / 611
Goodness-of-fit on F^2	1.036
Final R indices [I>2sigma(I)]	R1 = 0.0410, wR2 = 0.1074
R indices (all data)	R1 = 0.0570, wR2 = 0.1176
Absolute structure parameter	-0.2(2)
Extinction coefficient	n/a
Largest diff. peak and hole	0.117 and -0.138 e^{-3}

Figure 3.6 The molecular structure for **3.9** (Hydrogen atoms bonded to carbon have been omitted for clarity and thermal ellipsoids are only shown for selected atoms)

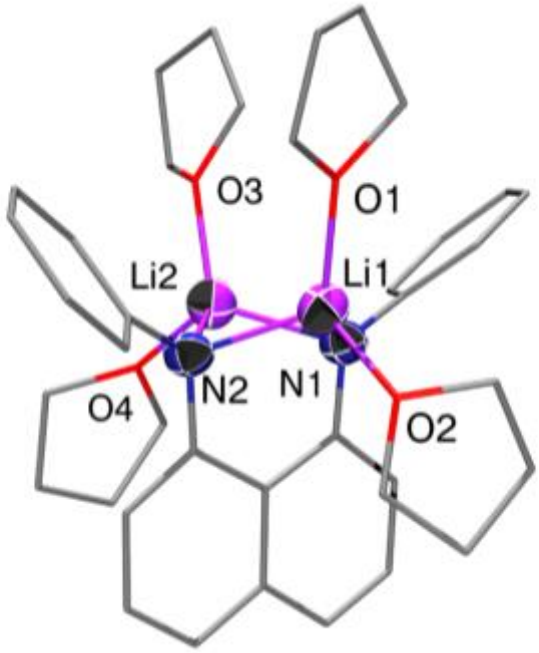

Table 3.8 Selected Bond Lengths [Å] and Angles [°] for **3.9**

Bond lengths (Å)		**Bond Angle (°)**	
Li1-O1	1.988(4)	O1-Li1-N1	125.3(2)
Li1-N1	1.999(4)	O1-Li1-N2	115.4(2)
Li1-N2	2.038(4)	N1-Li1-N2	85.30(16)
Li1-O2	2.050(10)	O1-Li1-O2	104.9(4)
Li2-O3	1.965(5)	N1-Li1-O2	113.3(4)
Li2-O4	1.979(5)	N2-Li1-O2	111.7(3)
Li2-N2	2.020(4)	O3-Li2-O4	100.37(19)
Li2-N1	2.041(4)	O3-Li2-N2	127.0(2)
		O4-Li2-N2	109.9(2)
		O3-Li2-N1	115.8(2)
		O4-Li2-N1	120.6(2)
		N2-Li2-N1	84.70(16)
		C2-N1-C11	118.05(18)
		Li1-N1-Li2	84.82(17)
		Li2-N2-Li1	84.38(17)

Table 3.9 Crystal data and structure refinement for **3.10** and **3.11**

	3.10	**3.11**
Empirical formula	$C_{20}H_{31}Cl_2GaN_2O$	$C_{32}H_{44}Cl_3InN_4$
Formula weight	456.09	705.88
Temperature (K)	201(2)	200(2)
Wavelength (Å)	0.71073	0.71073
Crystal system	Triclinic	Monoclinic
Space group	P -1	C 2/c
a (Å)	9.9270(2)	19.086(3)
b (Å)	14.1359(4)	8.7509(15)
c (Å)	17.3849(4)	20.563(3)

α (deg)	101.4110(10)	90
β (deg)	90.3710(10)	106.988(8)
γ (deg)	108.5660(10)	90
Volume ($Å^3$)	2260.55(10)	3284.5(10)
Z	4	4
Density (calculated) (Mg/m^3)	1.340	1.427
Absorption coefficient (mm^{-1})	1.465	0.991
F(000)	952	1456
Crystal size (mm^3)	0.236 x 0.145 x 0.143	0.348 x 0.294 x 0.283
Theta range for data collection	1.555 to 27.997	2.071 to 28.365
Index ranges	-12<=h<=13, -18<=k<=18, -22<=l<=22	-24<=h<=25, -11<=k<=11, -27<=l<=27
Reflections collected	34219	19025
Independent reflections	10857 [R(int) = 0.0302]	4089 [R(int) = 0.0234]
Completeness to theta = 25.242	100.0 %	99.9 %
Refinement method	Full-matrix least-squares	Full-matrix least-squares on
Data / restraints / parameters	10857 / 112 / 579	4089 / 0 / 194
Goodness-of-fit on F^2	1.007	1.067
Final R indices [I>2sigma(I)]	R1 = 0.0362, wR2 =	R1 = 0.0187, wR2 = 0.0462
R indices (all data)	R1 = 0.0692, wR2 =	R1 = 0.0202, wR2 = 0.0471
Extinction coefficient	n/a	n/a
Largest diff. peak and hole	0.542 and -0.438 e^{-3}	0.288 and -0.250^{-3}

Figure 3.7 X-ray structure of **3.10.** (Hydrogen atoms bonded to carbon and nitrogen have been omitted for clarity)

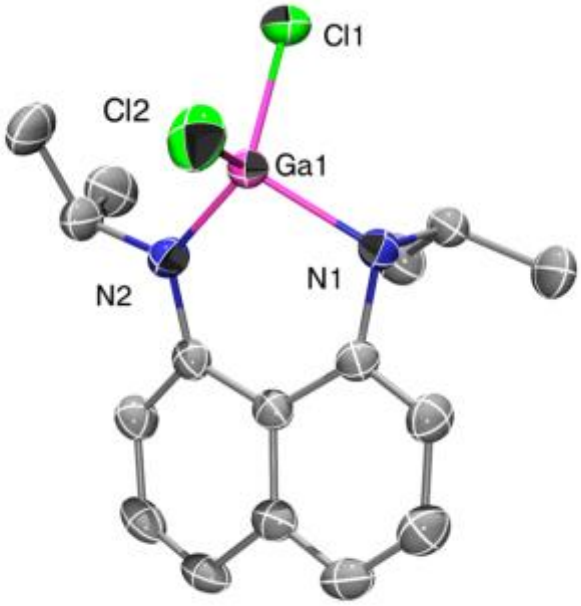

Figure 3.8 X-ray structure of **3.11.** (Hydrogen atoms bonded to carbon and nitrogen have been omitted for clarity)

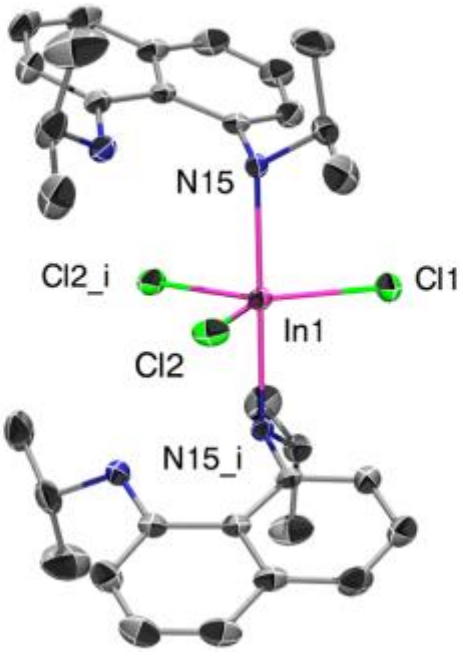

Table 3.10 Selected Bond Lengths [Å] and Angles [°] for **3.10** and **3.11**

3.10		**3.11**	
Bond lengths (Å)			
Ga1-Cl1	2.1691(7)	In1-Cl1	2.3784(6)
Ga1-Cl2	2.1528(7)	In1-Cl2	2.3767(4)
Ga1-N1	1.9652(17)	In1-Cl2_i	2.3767(4)
Ga1-N2	1.8543(17)	In1-N15	2.3747(11)
		In1-N15_i	2.3747(11)
Bond Angle (°)			
N2-Ga1-N1	100.30(7)	Cl1-In1-Cl2	127.620(11)
Cl1-Ga1-N1	106.35(6)	Cl1-In1-Cl2_i	127.620(11)
Cl2-Ga1-N2	116.86(7)	Cl2-In1-Cl2_i	104.76(2)
Cl1-Ga1-N2	115.86(6)	N15-In1-N15_i	179.59(5)
Cl1-Ga1-Cl2	109.98(3)	N15-In1-Cl1	90.20(3)

Table 3.11. A comparison of selected experimental and computed Bond Distances [Å] and Angles [°] of **3.3**

	Experimental	**Computed**
B-N	1.41Å	1.422 Å
B-H	1.11 Å	1.18 Å
NBN	120.8°	120.91°
$C_{naphthyl}$-N-B	120.6(3)°	120.01°
CH-N-B	120.6(3)°	121.17°

IV. References

[1] C. Camp, J. Arnold, *Dalt. Trans.*, 2016, **45**, 14462.

[2] Y. C. Tsai, *Coord. Chem. Rev.*, 2012, **256**, 722.

[3] M. Asay, C. Jones, M. Driess, *Chem. Rev*,. 2011, 354.

[4] L. Bourget-Merle, M. F. Lappert, J. R. Severn, *Chem. Rev.*, 2002, **102**, 3031.

[5] Z. Yang, X. Ma, H. W. Roesky, Y. Yang, V. M. Jiménez-Pérez, J. Magull, A. Ringe, P. G. Jones, *Eur. J. Inorg. Chem.*, 2007, **31**, 4919.

[6] V. M. Jimenez-Perez, B. M. Munoz-Flores, H. W. Roesky, H. T. Schulz, A. Pal, T. Beck, Z. Yang, D. Stalke, R. Santillan, M. Witt, *Eur. J. Inorg. Chem.*, 2008, **13**, 2238.

[7] T. Riehm, H. Wadepohl, L. H. Gade, *Inorg. Chem.*, 2008, **47**, 11467.

[8] S. C. Martens, T. Riehm, H. Wadepohl, L. H. Gade, *Eur. J. Inorg. Chem.*, 2012, 3039.

[9] C. H. Lee, Y. -H. La, S. J. Park, J. W. Park, *Organometallics*, 1998, **17**, 3648.

[10] P. Bazinet, G. P. A. Yap, G. A. DiLabio, D. S. Richeson, *Inorg. Chem.*, 2005, **44**, 4616.

[11] G. Rimmler, C. Krieger, F. A. Neugebauer, *Chem. Ber.*, 1992, **125**, 723.

[12] N. Lavoie, S. I. Gorelsky, Z. Liu, T. J. Burchell, G. P. A. Yap, D. S. Richeson, *Inorg. Chem.*, 2010, **49**, 5231.

[13] H. A. Spinney, I. Korobkov, G. A. DiLabio, G. P. A Yap, D. S. Richeson, *Organometallics*, 2007, **26**, 4972.

[14] P. Bazinet, G. P. A. Yap, D. S. Richeson, *J. Am. Chem. Soc.,* 2001, **123**, 11162.

[15] P. Bazinet, T. G. Ong, J. S. O'Brien, N. Lavoie, E. Bell, G. P. A. Yap, I. Korobkov, D. S. Richeson, *Organometallics,* 2007, **26**, 2885.

[16] H. A. Spinney, I. Korobkov, D. S. Richeson, *Chem. Commun.,* 2007, **16**, 1647.

[17] H. A. Spinney, G. P. A. Yap, I. Korobkov, G. DiLabio, D. S.Richeson, *Organometallics,* 2006, **25**, 3541.

[18] L. Weber, E. Dobbert, H. Stammler, B. Neumann, R. Boese, D. Bläser, *Eur. J. Inorg. Chem.,* 1999, 491.

[19] D. T. Carey, F. S. Mair, R. G. Pritchard, J. E. Warren, R. J. Woods, *Dalt. Trans.,* 2003, 3792.

[20] M. J. Frisch, G. W. Trucks, H. B. Schlegel, G. E. Scuseria, M. A. Robb, J. R. Cheeseman, G. Scalmani, V. Barone, B. Mennucci, G. A. Petersson, Gaussian 09, Revision A.02.

[21] A. J. Blake, N. L. Gillibrand, G. J. Moxey, D. L. Kays, *Inorg. Chem.,* 2009, **19**, 10837.

Chapter IV

Carbene chemistry

I. Introduction

A carbene displays a neutral carbon center having two valences involved in bonding with substituents and two unshared electrons. The general geometries of disubstituted carbenes are linear or bent (**Figure 4.1**). For a linear arrangement, the carbene center would have an approximate sp-hybridization with the two remaining p orbitals remaining perpendicular to each other as well as to the axis of the molecule. In this case, the carbene would show a triple ground state with one unpaired electron each of the non-bonding p orbitals as expected by Hund's rule. When the carbene center has a bent geometry, perhaps as an effect of the substituents, the carbon would now be assigned a valence bond description of sp^2 hybridization. This results in the non-bonding orbitals being inequivalent and possessing different orbital energies. Obviously, the difference in energies between these orbitals will determine whether this carbene prefers the singlet or triplet state in terms of energy. Regarding this, the size of the energy gap between the sp^2 and p orbitals is the key to clarify the most stable state. When the energy gap between the sp^2 and p orbitals is larger than the pairing energy for the doubly occupied orbital, the singlet state is

preferred. Usually, a singlet-triplet gap of 7.6 x 10^{-23}Kcal or more results in a singlet ground state and a gap less than 5.7 x 10^{-23}Kcal yields a triplet ground state.[1]

Figure 4.1 Simple orbital pictures for linear and bent carbenes

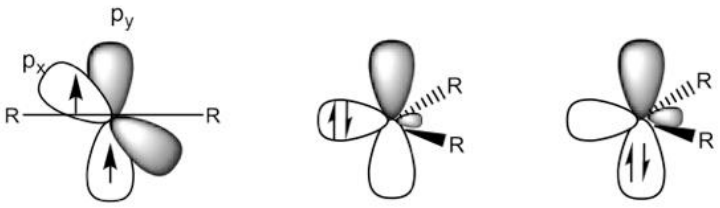

$(sp^2)^2$-bent p^2-bent

Linear Geometry Bent Geometry

The first room-temperature stable carbene, reported in the early 1990's, was the five membered heterocyclic species 1,3-di-1-adamantylimidazol-2-ylidene (**Chart 4.1**).[2] This species is a singlet carbene. From this discovery, several examples of related N-heterocycle carbenes (NHCs) were introduced. Since the development of the first examples, there have been significant success in NHC chemistry, leading to isolable and commercial compounds.[3,4] Even though a carbene has only 6 electrons, making it an electron deficient compound, the carbene center of an NHC is typically used as a nucleophile since it possesses a pair of nonbonding electrons that could interact with an electrophilic center. As a result, carbenes behave as ligands, donating their lone electron pairs to a metal and can stabilize transition metal compounds. The applications of NHCs as ligands rapidly expanded and today NHCs have become rather ubiquitous donor ligands putting them in the same class of ligands as phosphines in transition metal catalyzed reactions.[5,6]

Chart 4.1

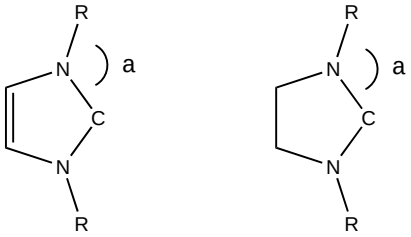

A **B**

The most common NHCs in the literature are represented by **A** and **B** (**Chart 4.1**) and have five-membered ring architectures. In terms of the stability of five-membered ring structures, carbenes having an unsaturated structure like **A** are more stable, a feature that has been attributed to the 6π electrons/ extended aromatic nature of these compounds. However, both types of carbenes are considered as stable ligands since the empty p_z orbital on the carbene center can be stabilized by π overlap with the flanking nitrogen non-bonding electrons. On top of that, the five-membered heterocycle forces the carbene to have a bent structure with an ideal angle of approximately 108°. Therefore, the fact that singlet state is the preferred electron arrangement can be explained by these factors.

Chart 4.2

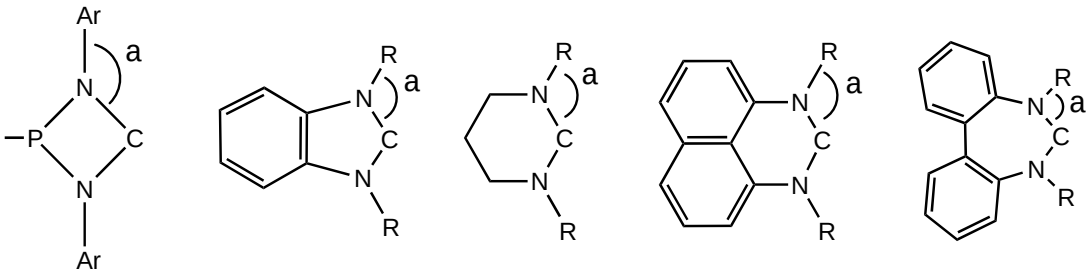

C **D** **E** **F** **G**

This successful discovery of stable five-membered ring carbenes has attracted chemists to design of new stable carbenes such as **C**[7], **D**[8], **E**[9,10], **F**[11,12], and **G**[13,14]. In addition to changing the direct angle of the carbene substituents, these different scaffold structures, also possess different α angles. For example, the larger ring sizes increases the steric impact of the nitrogen substituents by having a smaller α angle. We have focused on carbenes with **F** framework. This idea was originally prompted from the R,R'-DAN frame presented in **Chapter I**. Therefore, we decided to apply the R,R'-DAN frame as a scaffold to synthesize carbenes with the **F** architecture. Regarding this, there are several reasons why our lab has been working with this particular framework. First of all, compared to most commonly used carbenes, it has six-membered ring which has smaller α angle than five membered ring carbenes so that it can hold larger steric protection. The second reason for this is that this framework has the naphthalene backbone. Therefore, carbene center is placed in a formally fourteen π electron heterocycle by forming extended aromatic system of naphthalene backbone, causing this carbene to have more nucleophilic character.

II. Results and Discussion

A. Perimidinium Salts

To obtain the desired carbenes, we targeted the perimidium cations as precursor compounds so that we could deprotonate these compounds to reach the final stable carbene products. Regarding this, we have tried two different approaches. The first method, shown in **Scheme 4.1**, was to use R,R'-DAN and cyclize in an acid reaction with excess of triethylorthoformate to form perimidinium salts. The second approach to the perimidium salt was

to prepare a monosubstituted perimidine and then quaternize the unsubstituted N center using an alkyl halide. This approach is summarized in **Scheme 4.3**.

Given the variety of substituents that could be applied to N,N'-disubstituted-perimidinium salt family of ligands, a shorthand notation for identifying these species is useful. With this in mind, I have chosen to use the notation R,R'-PERI^{+}X^{-} (X=anion). For example, N,N'-diisopropyl-perimidinium salt and N,N'-Benzyl,isopropyl-perimidinium salt will be called (^{i}Pr)$_2$-PERI^{+}HCOO^{-} and (Bn)(^{i}Pr)-PERI^{+}Br^{-}. In the case of monosubstituted perimidinium I will use the notation R-PERI. In order to follow this same pattern I will follow a similar short-hand notation for the N,N'-disubstituted free carbene which will be called "R,R'-carbene".

As **Scheme 4.1** shows, the first method resulted in compounds that possessed counter anions that were determined by the acid that have been utilized for reaction This can lead to issues with the targeted deprotonation step. For example, with the formate salt, **4.3** (^{i}Pr)$_2$-PERI^{+}HCOO^{-} prepared using formic acid, we found that exchanging the formate anion to a chloride was required for effective deprotonation reactions. This anion exchange step was done by washing a methylene chloride solution of the **4.3** (^{i}Pr)$_2$-PERI^{+}HCOO^{-} with a concentrated NaCl solution.

Scheme 4.1

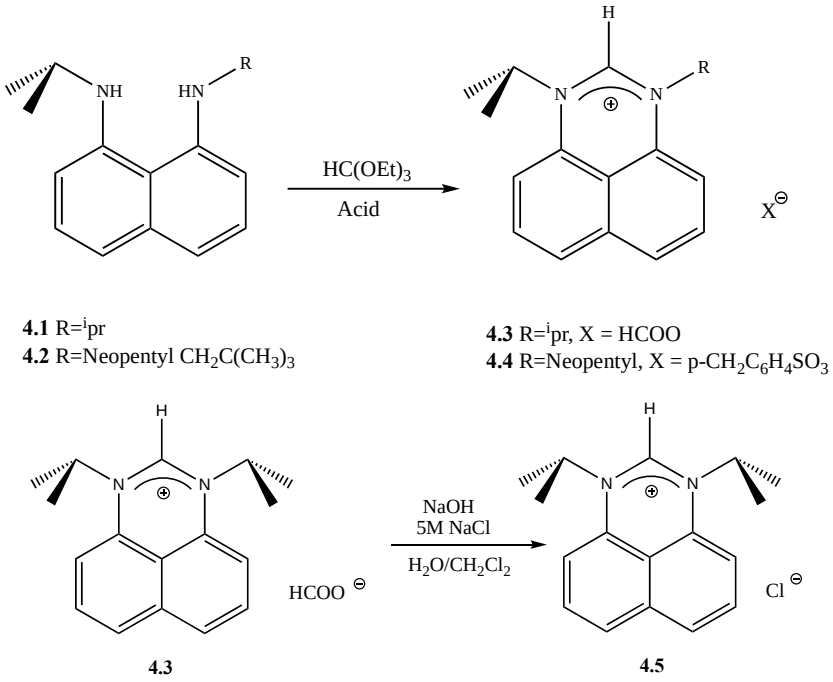

Accordingly, in order to skip this extra step for exchanging anions, we tried replacing the organic acids with NH_4Br as shown in **Scheme 4.2**. With this approach, the **4.6** $(^iPr)_2$-PERI$^+$Br$^-$ was successfully obtained which was successfully characterized by NMR and single crystal X-ray diffraction. The ^{1}H NMR spectrum showed a single septet peak at 4.84 ppm indicative of two symmetric isopropyl protons as expected. Additionally, ^{13}C NMR results were also consistent with the symmetrical structure. Similarly, the **4.4** (Np)(^{i}Pr)-PERI$^+CH_3C_6H_5SO_3^-$ was also successfully characterized by NMR and X-ray. Unique features in the ^{1}H NMR spectrum of **4.4** is a singlet peak at δ 9.15 ppm, indicating proton on the cationic of N-C(H)-N unit. A septet signal was also observed for the isopropyl CH proton at δ 4.45 ppm.

When it comes to X-ray structures (**Table 4.4**), for **4.4** (Np)(^{i}Pr)-PERI^{+}$CH_3C_6H_4SO_3^{-}$, the C11-N2 and C11-N1 bond lengths are 1.318(3) Å and 1.313(3) Å respectively. Moreover, the compound (^{i}Pr)$_2$-PERI^{+}Br^{-} **4.6** has 1.330(8) Å and 1.346(9) Å for C12-N11 and C12-N13 bond lengths. Consistent with the fact that both C-N bond lengths are almost identical in each structure, we suggest that the cationic charge is delocalized along the N-C(H)-N unit. This represent that a C-N bond order is 1.5.[15] In addition, the N2-C11-N1 bond angle in **4.4** and N11-C12-N13 in **4.6** were 123.3(7)º and 125.1(2)º, and the average of α angles both precursors were 120º.

Scheme 4.2

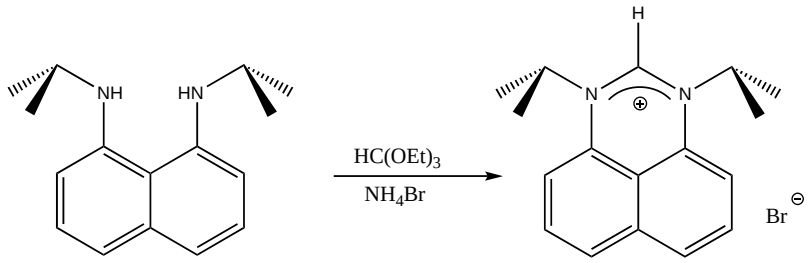

4.1 **4.6**

As stated, the second approach to synthesize perimidinium precursors was to prepare a monosubstituted R-PERI and add then another substituent. For example, by using **4.7** (^{i}Pr)-DAN with triethylorthoformate and formic acid, **4.8** (^{i}Pr)-PERI was successfully synthesized and fully characterized. Reaction of benzyl bromide with **4.8** (^{i}Pr)-PERI led to high conversion to **4.9** (Bn) (^{i}Pr)-PERI^{+}Br^{-} (**Scheme 3**). This desired compound **4.9** was also characterized by X-ray diffraction (Figure 4.3). The fact that N3-C2 (1.316(3) Å) and N1-C2 (1.318(3) Å) bond lengths are same confirms that cation is delocalized thorough N-C(H)-N. Another interesting feature is the α angles which are C21-N3-C2 and C14-N1-C2. Since steric impact of the isopropyl group is larger, the α angle at nitrogen having the isopropyl substituent turns out to be larger (119.3(2)°) than the nitrogen having the benzyl substituent (118.39(19)°).

Scheme 4.3

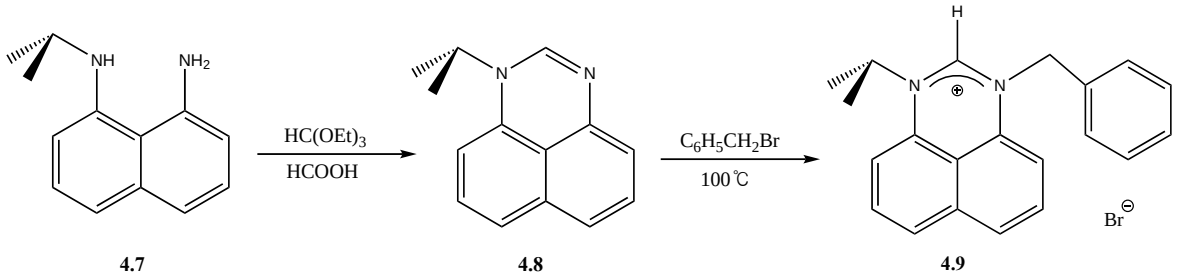

B. Generation of Free Carbenes from Perimidinium Salts

Using the methods outlined in **Scheme 4.2** and **Scheme 4.3**, we had prepared the R,R'-PERI^{+}Br^{-} that could function as carbene precursors. To synthesize the desired carbenes, we initially considered bulkier and less nucleophilic bases for the deprotonation step of the R,R'-PERI^{+}Br^{-}. For example, co-workers in our lab attempted to use tert-butoxide anion, since the tert-butoxide anion is one of the most common bases used for the preparation of NHCs. However, it was realized that this approach converts the perimidinium salts to a σ-diamino ether instead of a stable free carbene (**Scheme 4.4**).

Scheme 4.4

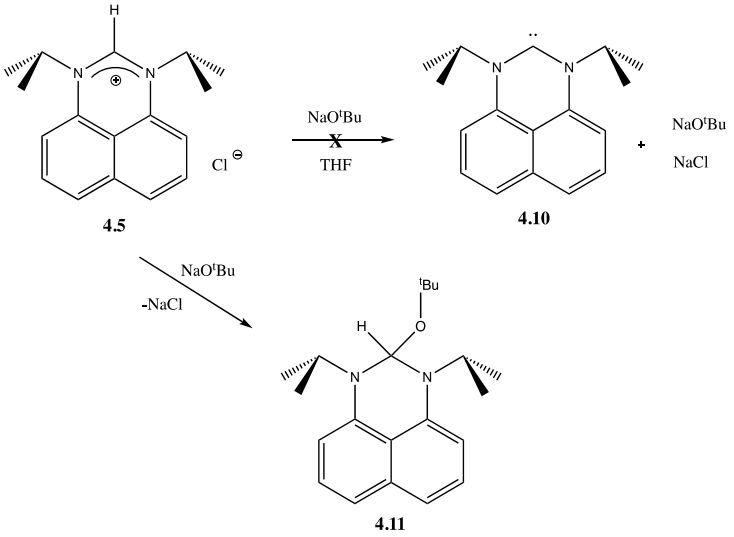

We next attempted the deprotonation of the bromide salts **4.6** and **4.9** using one equivalent of lithium hexamethyldisilazide (LiHMDS). This approach is based upon a published procedure originating in our lab using R,R'-PERI^{+}Cl^{-}.[16]

However, we have experienced difficulties preparing and isolating the desired stable carbenes with LiHMDS. The reason for this issue might be explained by the different anions. While LiHMDS was successful to deprotonate the R,R'-PERI^{+}Cl^{-}. Analogous reactions using a bromide salt did indicate deprotonation, confirmed by the disappearance, in the ^{1}H NMR, of the C-H peak of N-C(H)-N at δ 10.21 ppm and δ 9.69 ppm for **4.9** (Bn)(^{i}Pr)-PERI^{+}Br^{-}, and **4.6** (^{i}Pr)$_{2}$-PERI^{+}Br^{-} respectively. Nonetheless, isolation of free carbene was not possible. We attributed the isolation problem to solubility of LiBr in THF/chlorobenzene solution as well as the potential for residual base from the reaction. Another difficulty was the filtration step where we have used Celite to capture the LiBr salts formed in the deprotonation step. Specifically, when we filtered the crude solution of the free carbene through the Celite, a large amount of solvent was required in order to liberate the carbene. In addition, the large amounts of solvent create potential issues with solvent impurities.

As a result of these concerns, we chose to make a slight change in the base and to employ KN(SiMe$_{3}$)$_{2}$ (KHMDS) in the deprotonation reactions (**Scheme 4.5**). We anticipated that KBr product from this reaction would be less soluble than LiBr leading to cleaner precipitation out from the solution. Indeed, exchanging the base from LiHMDS to KHMDS enabled us to deprotonate R,R'-PERI^{+}Br^{-} as well as isolate the resulting carbene species. In addition, the use of a syringe filtration enables us to filter crude products without using Celite thus significantly reducing the volume of solvent.

Scheme 4.5

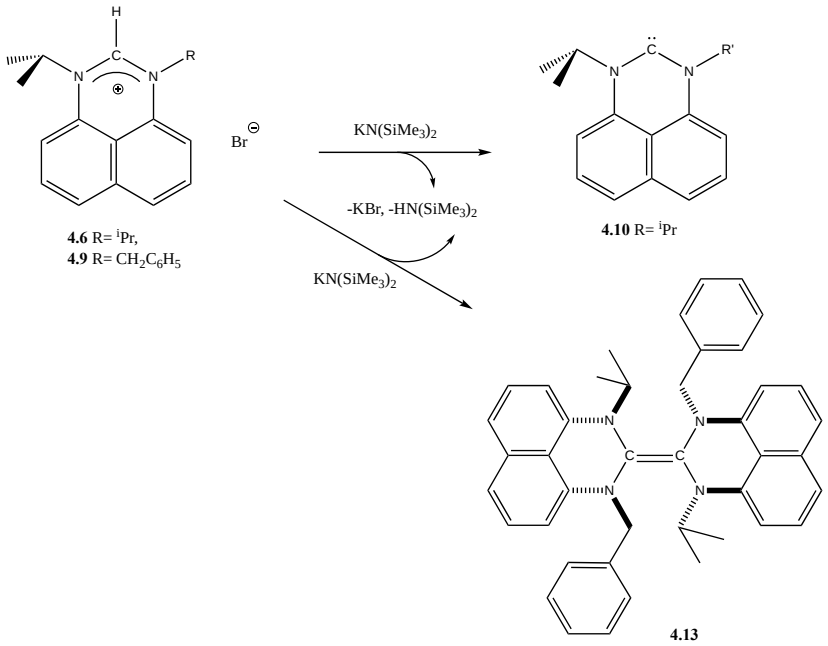

Transformation of starting material (R,R'-PERI^{+}X^{-}) can be easily confirmed by the disappearance of C-H peak of N-C(H)-N unit in ^{1}H NMR around at δ 10 ppm. Another outstanding difference between the perimidinium salts and the free carbenes is that $C_{carbene}$ signal is shifted extremely downfield in the free carbenes at around δ 240 ppm in ^{13}C NMR, which used to be at approximately δ 150 ppm in the R,R'-PERI^{+}Br^{-} starting materials. The appearance of $C_{carbene}$ signal at around δ 240 ppm can give an evidence of synthesis of free carbenes. In addition, for the **4.10** (^{i}Pr)$_2$-carbene, a symmetrical structure is observed, revealing a single septet signal in ^{1}H NMR indicating of the N-^{i}Pr groups. Additionally, there are only three ^{1}H resonances from the naphthalene backbone ring, also indicative of a symmetrical structure. On the contrary, the (Bn)(^{i}Pr)-carbene shows an NMR spectrum for an unsymmetrical condition as expected. Particularly, the ^{1}H NMR shows six resonances for the naphthalene backbone ring and five

different signals for the benzyl ring, which is much more complicated compared to the diisopropyl symmetrical carbene.

Interestingly, when we tried to isolate this free (Bn)(^{i}Pr)-carbene to verify structure by X-ray, this compound yielded a enetetraamine, the formal dimerization of the carbene (**4.13**). This can be justified in terms of the steric properties of the benzyl compound compared to the diisopropyl species. The reduced steric impact of the benzyl substituent compared to isopropyl makes it possible to form the dimerized dicarbene. The X-ray structure (**Table 4.6**) of this compound was obtained and the olefin linkage formed through a C11 - C11' bond showed a bond length of 1.333(3) Å. This bond length is typical for a carbon-carbon double bond length.

From this X-ray structure, presence of enetetraamine was found instead of free carbene. Therefore, (Bn)(^{i}Pr)-enetetraamine will be used as a short notation from now on instead of (Bn)(iPr)-carbene.

Another distinct feature is that the C11-N1 and C11-N2 bond lengths increased in the (Bn)(^{i}Pr)-enetetraamine (**4.13)**, which are 1.419(2) Å and 1.432(2) Å compared to 1.318(3) Å, and 1.316(3) Å in the R,R'-PERI^{+}Br^{-} (**Table 4.2**). From the sum of the angles around the N1 center (C12-N1-C11, C1-N1-C11, and C12-N1-C1) we see that N1 which has the benzyl substituent is found to have a planar geometry (**Table 4.6**). On the other hand, N2 possessing the isopropyl substituent has a pyramidal structure. In addition, α angle was 122.35° at N1 and 114.90(13)° at N2, which is consistent with the fact that the isopropyl substituent has larger steric effects.

This X-ray result helps to understand the complicated ^{1}H NMR and ^{13}C NMR obtained for this enetetraamine. Taking into account that there are two possible orientations for the substituents, which are *cis* and *trans* form, we expect a doubling of the NMR signals due to formation of two structural isomers. Therefore, four different septet signals for isopropyl CH proton were found as well as 8 peaks of each benzyl CH_2 protons as doublet peaks were found. In the same manner, ^{13}C NMR technically, maximum 64 signals can be found in aromatic region. However, some peaks had overlapped each other, which lead to observance of 50 signals which are less than 64 signals.

The carbene dimerization can be understood by thermodynamic factors applied as the driving force. Specifically, forming a C=C double bond lead to an energy gained of approximately 172 kcal/mol. Therefore, if the sum of the energy gap between a triplet/singlet states for two carbene compounds is less than the energy gain (172 kcal/mol) from the formation of the C=C double bond, the dimerization of the carbenes is observed. In the case of (Bn)(^{i}Pr)-enetetraamine **4.13**, singlet/triplet gap energy gap could be computed through a DFT optimization of **4.13** using the B3LYP functional and the TZVP basis set. From this computation, the difference in the free energies of the singlet and triplet forms of **4.13** (the singlet/triplet gap) was determined to be 57.7 kcal/mol. As a result, approximate 56.6 kcal/mol energy can be gained by forming the dimer as both triplet states. Thus, the formation of (Bn)(^{i}Pr)-enetetraamine **4.13** can be understood in terms of relative energy of the carbene compared to the free carbene species.

Using the same basis set and functional in DFT optimization, the singlet/triplet gap of (^{i}Pr)$_2$-carbene **4.10** was found to be 54.7 kcal/mol which is smaller than that of (Bn)(^{i}Pr)-enetetraamine **4.13**. In the case of (^{i}Pr)$_2$-carbene **4.10**, even if there is an energy gain forming a C=C double bond, free carbene is found. This can be understood by the fact that steric hindrances of isopropyl substituents prevent it from dimerizing the free carbenes.

III. Conclusion

By using the R,R'-DAN framework, stabilization of a unique carbene compounds are accessible and consequently, design of the new stable carbenes was successfully achieved. The use of ^{i}Pr substituents on the N atoms makes the verification of the targeted compound by NMR easier due to the distinctive septet CH signals. On top of that, indication of success in the synthesis of the free carbenes was given from not only the disappearance of C-H peak of N-C(H)-N in ^{1}H NMR but also a new peak for $C_{carbene}$ at approximate δ 245ppm. Another interesting result is dimerization of carbenes was also obtained when the steric demand of one of the substituents was changed. Specifically, by exchanging one of isopropyl substituents to the less sterically bulky benzyl substituent led to coupling of the carbenes to yield an enetetraamine. Regarding this, further investigation will be discussed in Chapter **V** on the reactivity of the free carbenes as ligands to stabilize several Pd(II) compounds. Additionally, research on enetetraamine which is used as a precursor of free carbene ligand for Pd(II) compound will be discussed as well.

Experimental section

General: Unless otherwise noted, all manipulations were carried out in either a nitrogen filled glovebox or under nitrogen using standard Schlenk techniques. Reaction solvents were sparged with nitrogen then dried by passage through column of activated alumina using an apparatus purchased from Anhydrous Engineering. Deuterated benzene, chloroform, and toluene were purchased from Aldrich Chemical Company. Acetone, benzyl bromide, 1,8-diaminonaphthalene, formic acid, $LiAlH_4$, MeLi, $KN(SiMe_3)_2$, $LiN(SiMe_3)_2$ and triethylorthoformate were purchased from Aldrich Chemical Company and used without further purification. ^1H and spectra were run on either a Bruker 300 MHz, a Bruker 400 MHz, a Bruker 600MHz spectrometer $^{13}C\{^1H\}$ NMR were run on a Bruker 75 MHz, a Bruker 100 MHz, or a Bruker 150 MHz using the residual protons of the deuterated solvent for reference. Elemental analyses were performed by Midwest micro lab in Indianapolis, IN, USA.

The crystal of **4.4, 4.6, 4.8, 4.9,** and **4.13** were mounted on thin glass fibers using paratone oil. Prior to data collection, the crystals were cooled to 201(2) K. The data were collected on a Bruker AXS single-crystal diffractometer equipped with a sealed Mo tube (wavelength 0.71073 Å) and APEX II CCD detector. The raw data collection and reduction were done with the Bruker APEXII software package. 1 Semi-empirical absorption corrections based on equivalent reflections were applied using SADABS. Systematic absences in the diffraction dataset and unit-cell parameter were consistent with monoclinic (**4.4**, **4.6**, **4.8**, **4.9**) triclinic (**4.13**) space groups. The structures were solved by direct methods and refined with full-matrix least-squares procedures based on F^2, using SHELXL and WinGX. All non-H atoms were refined

anisotropically. All hydrogen atoms were placed in idealized positions. Displacement ellipsoid plots were produced using ORTEP.

Preparation of 1-isopropylperimidine, $C_{10}H_6N(^iPrN)CH$ (4.8):

In a 250ml round bottom flask was added (^{i}Pr)-DAN **4.7** (2.0g, 10 mmol), triethyl orthoformate (14.8g, 100 mmol) and formic acid (0.02 ml, 0.5 mmol) in the glovebox. The reaction was heated to 100°C under nitrogen for 4 hours and monitored by TLC. The product was purified by column chromatography using silica gel and a 1:1 ether:dichloromethane elution solvent mixture. Product **4.8** was isolated as a brown solid 1.8g (83%).

^{1}H NMR ($CDCl_3$, 400MHz): δ7.40 (s, 1H, CH), 7.21 (m, 1H, CH), 7.04-7.13 (m, 3H, CH), 6.80 (dd, 1H, CH J=9.4Hz), 6.21 (dd, 1H, CH, J=9.4Hz), 4.02 (sept, 1HM $CHMe_2$, J=8.72Hz), 1.42(d, 6H, CH_3, J=9.04Hz).

$^{13}C\{^1H\}$ NMR ($CDCl_3$, 400 MHz): δ 144.5 (CH), 143.3, 137.7, 135.6, 128.7, 127.3, 123.2, 120.2, 119.1, 114.8, 110.2(C_{arom}), 47.8 ($CHMe_2$), 20.8 (CH_3).

Analysis Calcd $C_{14}H_{14}N_2$ C, 79.97; H, 6.71; N,13.32; Found C, 79.60; H, 6.51; N, 13.00

Preparation of 1,3- diisopropylperimidinium bromide $\{C_{10}H_6(^iPrN)_2CH\}Br$ (4.6):

A round bottom flask equipped with stir-bar and a condenser was charged with (^{i}Pr)$_2$-DAN **4.1** (1.455g, 6.0mmol), ammonium bromide (0.588g, 6.0mmol), triethylorthoformate (21.0g, 141mmol) and ethanol (10g) and the atmosphere was exchanged for nitrogen by purging the

head space with N_2 gas. The reaction was heated to 80°C and refluxed for 2 hours. The reaction was stirred for an additional 12 hours at room temperature. All volatiles were removed under vacuum and the product was washed with ether and solid product was dried under vacuum. The product was isolated as a yellow powder (1.53g, 77%).

^{1}H NMR ($CDCl_3$, 400MHz): δ 9.69 (s, 1H, HCN_2), 7.50-7.39 (m, 4H, CH), 6.94 (m, 2H, CH), 4.84 (sept, 2H, $CHMe_2$ J=6.84Hz), 1.87 (d, 12H, CH_3, J=6.84Hz)

^{13}C{^{1}H} NMR ($CDCl_3$, 400 MHz): δ 149.9, 135.0, 132.3, 128.0, 124.3, 122.5, 108.0, 55.7, 19.8.

Synthesis of 1-isopropyl-3-neopentylperimidinium tosylate, {$C_{10}H_6$(^{i}PrN)(NpN)} {$O_3SC_6H_4CH_3$}(4.4):

In a round bottom flask, **4.2** (3.87g, 14.3 mmol), p-toluenesulfonic acid (monohydrate) (2.72g, 14.3 mmol), and triethylorthoformate (21.2g, 0.143 mol) were combined and stirred for 18h at 45 °C under N_2 gas. The solvent was dried, and the product recrystallized from methylene chloride was a yellow solid (**4.4**) (3.85g, 66%)

^{1}H NMR ($CDCl_3$, 400MHz): δ 9.15 (s, 1H, N_2CH) 7.78 (d, 2H, CH), 7.38 (m, 4H), 7.09 (d, 2H, CH) 6.90 (m, 2H, CH), 4.45 (sept, 1H, $CHMe_2$), 4.27 (s, 2H, CH_2), 2.30 (s, 3H, CH_3), 1.72 (d, 6H, CH_3), 1.08 (s, 9H, CH_3).

^{13}C{^{1}H} NMR ($CDCl_3$, 400 MHz): 152.0 (N_2CH), 143.7, 138.7, 135.0, 132.7, 131.4, 138.2, 128.1, 127.6, 125.8, 124.2, 124.0, 121.6, 108.4, 107.6 (C_{arom}), 59.4 (CH_2CCH_3), 53.5 ($CHCH_3$) 33.6 (tosylate CH_3), 27.7 (CH_2CCH_3), 21.1 (CH_2CCH_3) 19.8 ($CHCH_3$).

Analysis Calcd $C_{26}H_{32}N_2O_3S$ C, 69.00; H, 7.13; N,6.19; Found C, 68.88; H, 7.16; N, 6.34

Preparation of 1-^{i}Pr-3-benzylperimidinium bromide, {$C_{10}H_6$(BnN)(^{i}PrN)CH}Br (4.9): A round bottom flask equipped with a magnetic stir bar and a reflux condenser was charged with (^{i}Pr)-PERI^{+} **4.8** (5.0g, 23.8 mmol), benzyl bromide (8.0g, 46.8 mmol) and approximately 100 ml of toluene. The reaction was heated at 100°C overnight under N_2 gas. A yellow product precipitated from the reaction mixture and was isolated by filtration and drying under vacuum and determined to be pure **4.9** (8.2g, 90%).

^{1}H NMR ($CDCl_3$, 400MHz): δ 10.21 (s, 1H, N_2CH) 7.37-7.44 (m, 5H, CH), 7.28 - 7.32 (m,2H, CH), 7.22 – 7.26 (m, 2H, CH) 6.96 (d, 1H, CH), 6.75 (d, 1H, CH), 5.77 (s, 2H, CH_2), 4.62 (m, 1H, $CHMe_2$), 1.83 (d, 6H, CH_3).

^{13}C{^{1}H} NMR ($CDCl_3$, 400 MHz): 150.9 (N_2CH), 135.1, 132.2, 131.6, 131.4, 129.2, 128.6, 128.08, 128.07, 127.1, 124.5, 124.3, 121.8, 108.8, 107.9 (C_{arom}), 54.9 (CH_2), 54.3 (CH) 20.6 (CH_3).

Analysis Calcd $C_{21}H_{21}BrN_2$ C, 66.15; H, 5.55; N,7.35; Found C, 66.51; H, 5.62; N, 7.49.

Preparation of 1,3-(^{i}Pr)$_2$-perimidine-2 ylidene, $C_{10}H_6$(^{i}PrN)$_2$C(4.10):

(^{i}Pr)$_2$-PERI^{+}Br **2.6** (0.167 g, 0.5mmol) was dissolved in 10 mL of 1:1 chlorobenzene/THF in the glovebox, then added KHMDS (0.10 g, 0.5mmol) also dissolved in 7 mL of 1:1 chlorobenzene/THF to precursor solution. The reaction was stirred for 1 h, and the solvent was removed under vacuum. The product, a pale pink solid, was isolated by extraction with toluene and solution was dried drying under vacuum (0.045g, 0.25mmol, 50%).

^{1}H NMR (C_6D_6, 300MHz): *δ* 7.12 (m, 4H, *CH*), 6.29 (dd, 2H, *CH*), 4.08 (sept, 2H, *H*CMe_2),

1.41 (d, 12H, C*H*3).

$^{13}C\{^{1}H\}$ NMR (C_6D_6, 300MHz): δ 241.7 (N*C*N), 136.0, 133.7, 128.0, 122.7, 119.4, 102.9 (C_{arom}), 51.5 (*C*HMe2), 22.3 (*C*H3).

Anal. Calcd for $C_{17}H_{20}N_2$: C, 80.91; H, 7.99; N, 11.10. Found: C, 80.55; H, 8.01; N, 10.84

Preparation of 1-^{i}Pr-3-$CH_2C_6H_5$-perimidine-enetetraamine, $\{C_{10}H_6(BnN)(^{i}PrN)C\}_2$(4.13): (Bn)(^{i}Pr)-PERI^{+}Br **4.9** (0.5 g, 1.3 mmol) was dissolved in 15 mL of 1:1 chlorobenzene/THF in the glove box. To this was added KHMDS (0.26 g, 1.3 mmol) also dissolved in 5 mL of 1:1 chlorobenzene/THF. The reaction was stirred for 1 h, and the solvent was removed under vacuum. The product, **4.13**, a pale brown viscous liquid, was isolated by extraction with toluene and solution was dried under vacuum (0.53 g, 0.9 mmol, 70%).

^{1}H NMR (C_6D_6, 600MHz): δ 7.18-7.56 (m, 16H, CH) 7.06-7.15 (m, 10H, CH), 6.74-7.01 (m, 10H, CH), 6.20-6.61 (m, 6H, CH) 5.39-5.53 (m, 2H, CH), 5.52 (d, 1H, CH_2, J=13.41), 5.39 (d, 1H, CH_2, J=16.0Hz), 5.21 (d, 1H, CH_2, J=8.94 Hz) 5.12 (d, 1H, CH_2, J= 16.9 Hz) 5.0 (m, 1H, CH_2) 4.9 (d, 1H, CH_2, J=16.1 Hz) 4.44 (d, 1H, CH_2, J=16.09 Hz) , 4.23(d, 1H, CH_2, J=11.7 Hz) 3.87 (sept, 1H, $CHMe_2$, J=6.66 Hz), 3.37 (sept, 1H, $CHMe_2$, J=6.07 Hz), 3.30 (sept, 1H, $CHMe_2$, J=6.69), 3.27(sept, 1H, CHMe2, J=7.11 Hz), 1.49 (d, 6H, CH_3, J=6.97 Hz), 1.01-1.20 (m, 6H, CH_3), 0.85 (d, 6H, CH_3, J= 6.64 Hz), 0.74 (m, 6H, CH_3).

$^{13}C\{^{1}H\}$ NMR (C_6D_6, 150MHz): δ 162.9 (C=C), 144.9, 144.0,143.7, 143.2, 142.8, 141.3, 139.3, 138.6, 138.2, 137.9, 137.8, 137.2, 136.4, 136.3, 136.2, 136.1, 135.8, 135.4, 132.3, 131.52, 130.36, 129.0, 128.9, 128.7, 128.6, 128.5, 128.3, 127.4, 127.1, 127.0, 126.8, 122.6, 121.1, 119.8, 119.4, 119.3, 118.5, 117.6, 117.5, 117.4, 117.1, 116.4, 116.1, 114.8, 106.4, 105.3, 105.0, 104.79, 104.4

(C_{arom}), 59.4 (CH_2), 56.5 ($CHMe_2$), 55.8 (CH_2), 54.4 (CH_2), 53.4 ($CHMe_2$), 51.6 ($CHMe_2$), 47.3 ($CHMe_2$), 47.1 (CH_2), 23.3, 22.4, 22.3, 22.2, 21.4, 21.2, 18.9, 18.6 (CH_3).

Structural determinations

Table 4.1 Crystal data and structure refinement for **4.8** and **4.9**

	4.8	**4.9**
Empirical formula	$C_{14}H_{14}N_2$	$C_{21}H_{21}BrN_2$
Formula weight	210.27	381.31
Temperature (K)	200(2)	200(2)
Wavelength (Å)	0.71073	0.71073
Crystal system	Monoclinic	Monoclinic
Space group	P 2_1/c	P 2_1/n
a (Å)	8.5645(12)	14.1181(5)
b (Å)	11.5155(16)	13.5501(4)
c (Å)	11.1405(16)	18.2578(7)
α (deg)	90	90
β (deg)	92.008(2)	94.847(2)
γ (deg)	90	90
Volume ($Å^3$)	1098.1(3)	3480.3(2)
Z	4	8
Density (calculated) (Mg/m^3)	1.272	1.455
Absorption coefficient (mm^{-1})	0.076	2.366
F(000)	448	1568
Crystal size (mm^3)	0.826 x 0.540 x 0.303	0.445 x 0.189 x 0.132
Theta range for data collection	2.380 to 28.318.	1.753 to 28.364.
Index ranges	-11<=h<=11, -15<=k<=15, -14<=l<=14	-18<=h<=18, -18<=k<=18, -23<=l<=24
Reflections collected	12995	47276
Independent reflections	2696 [R(int) = 0.0344]	8678 [R(int) = 0.0563]
Completeness to theta = 25.242	99.8 %	100.0 %

Absorption correction	Semi-empirical from equivalents	Semi-empirical from equivalents
Max. and min. transmission	0.7457 and 0.7058	0.7457 and 0.5956
Refinement method	Full-matrix least-squares on F^2	Full-matrix least-squares on F^2
Data / restraints / parameters	2696 / 0 / 147	8678 / 0 / 437
Goodness-of-fit on F^2	1.046	1.015
Final R indices [I>2sigma(I)]	R1 = 0.0458, wR2 = 0.1131	R1 = 0.0439, wR2 = 0.0873
R indices (all data)	R1 = 0.0670, wR2 = 0.1265	R1 = 0.0950, wR2 = 0.1029
Extinction coefficient	n/a	n/a
Largest diff. peak and hole	0.139 and -0.242 e^{-3}	0.611 and -0.654 e^{-3}

Figure 4.2 X-ray structure of **4.8 (**Hydrogen atoms have been eliminated for clarity)

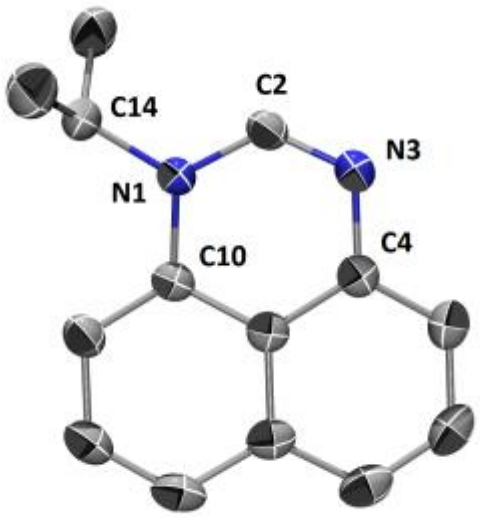

Figure 4.3 X-ray structure of **4.9** (Only one of the two independent molecules is shown and the counter anion, Br^- and hydrogen atoms have been omitted for clarity)

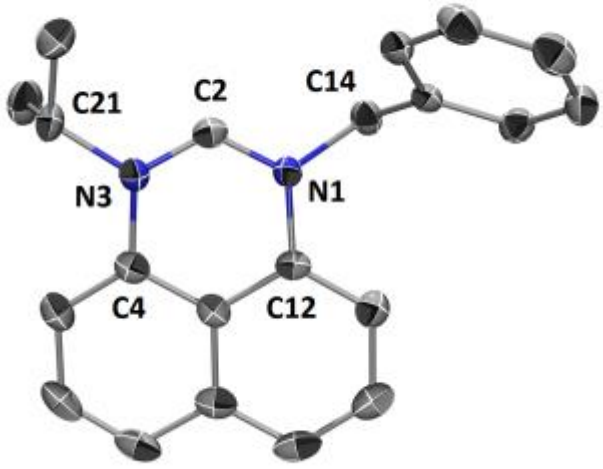

Table 4.2 Selected Bond Lengths [Å] and Angles [°] for **4.8** and **4.9**

4.8		**4.9**	
Bond lengths (Å)			
N1-C2	1.3640(15)	N3-C2	1.316(3)
N1-C14	1.4792(16)	N3-C4	1.428(3)
N1-C10	1.4070(15)	N3-C21	1.496(3)
N3-C2	1.2912(16)	N1-C2	1.318(3)
N3-C4	1.4035(16)	N1-C12	1.422(3)
		N1-C14	1.484(3)
Bond Angle (°)			
N1-C2-N3	127.31(11)	N3-C2-N1	124.5(2)
C14-N1-C2	121.10(10)	C21-N3-C2	119.3(2)
C14-N1-C10	119.72(10)	C21-N3-C4	120.3(2)
C2-N1-C10	119.18(10)	C2-N1-C14	118.39(19)
C2-N3-C4	116.84(10)	C2-N1-C12	120.1(2)
		C12-N1-C14	120.90(19)

Table 4.3 Crystal data and structure refinement for **4.4** and **4.6**

	4.4	**4.6**
Empirical formula	$C_{27}H_{34}Cl_2N_2O_3S$	$C_{17}H_{21}BrN_2$
Formula weight	537.52	333.27
Temperature (K)	200(2)	200(2)
Wavelength (Å)	0.71073	0.71073
Crystal system	Monoclinic	Monoclinic
Space group	P 2_1/n	P 2_1/c
a (Å)	10.0662(10)	20.399(5)
b (Å)	16.5788(16)	11.812(3)
c (Å)	16.9147(17)	13.441(3)
α (deg)	90	90
β (deg)	101.3860(10)	98.950(5)
γ (deg)	90	90
Volume (Å ^{3})	2767.3(5)	3199.3(13)
Z	4	8
Density (calculated) (Mg/m^3)	1.290	1.384
Absorption coefficient (mm^{-1})	0.341	2.563
F(000)	1136	1376
Crystal size (mm^3)	0.363 x 0.259 x 0.168	0.666 x 0.241 x 0.082
Theta range for data collection	1.737 to 28.554.	1.998 to 25.249.
Index ranges	-13<=h<=13, -21<=k<=22, -21<=l<=22	-24<=h<=24, -14<=k<=14, -16<=l<=16
Reflections collected	33285	70370
Independent reflections	6867 [R(int) = 0.0348]	70370 [R(int) = ?]
Completeness to theta = 25.242	100.0 %	98.1 %
Refinement method	Full-matrix least-squares on F^2	Full-matrix least-squares on F^2
Data / restraints / parameters	6867 / 42 / 352	70370 / 313 / 392
Goodness-of-fit on F^2	1.023	0.966
Final R indices [I>2sigma(I)]	R1 = 0.0493, wR2 = 0.1178	R1 = 0.0669, wR2 = 0.1606

R indices (all data)	R1 = 0.0938, wR2 = 0.1523	R1 = 0.1177, wR2 = 0.1841
Extinction coefficient	n/a	n/a
Largest diff. peak and hole	0.504 and -0.570 e^{-3}	0.783 and -0.373 e^{-3}

Figure 4.4 X-ray structure of **4.4. (**The co-crystallized solvent, counter anion**,** $CH_3C_6H_4SO_3^-$ and hydrogen atoms have been omitted for clarity)

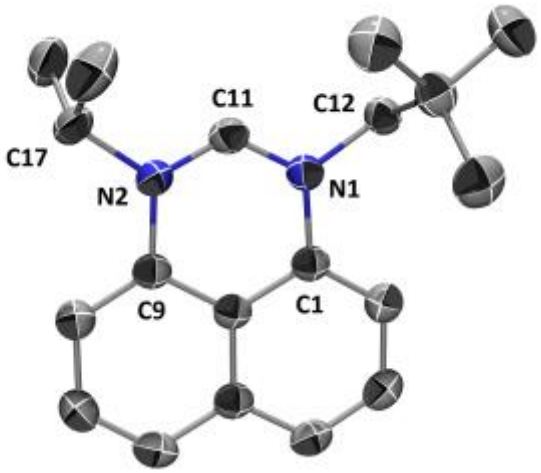

Figure 4.5 X-ray structure of **4.6. (**Only one of the independent molecules is shown and the counter anion Br^- and hydrogen atoms have been omitted for clarity)

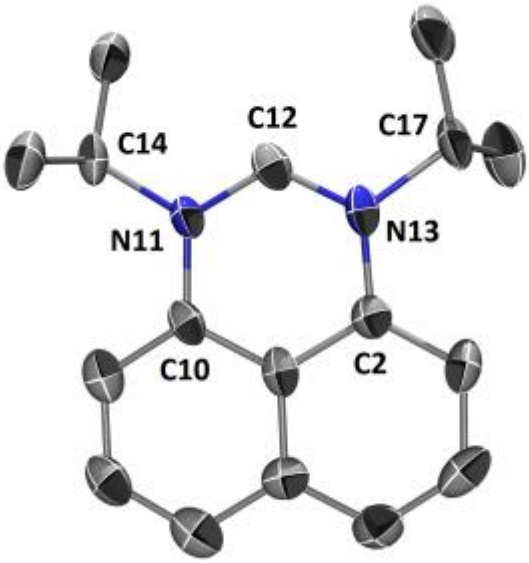

Table 4.4 Selected Bond Lengths [Å] and Angles [°] for **4.4** and **4.6**

4.4		**4.6**	
Bond lengths (Å)			
N2-C11	1.313(3)	N11-C12	1.330(8)
N2-C9	1.427(3)	N11-C10	1.411(10)
N2-C17	1.519(12)	N11-C14	1.499(9)
N1-C11	1.318(3)	N13-C12	1.346(9)
N1-C12	1.485(3)	N13-C2	1.415(10)
N1-C1	1.428(3)	N13-C17	1.513(9)
Bond Angle (°)			
N2-C11-N1	125.1(2)	N11-C12-N13	123.3(7)
C17-N2-C11	117.2(9)	C14-N11-C12	118.2(8)
C11-N2-C9	120.27(18)	C14-N11-C10	121.1(7)
C17-N2-C9	121.7(8)	C12-N11-C10	120.7(7)
C11-N1-C12	117.86(18)	C12-N13-C17	117.7(8)
C11-N1-C1	120.38(18)	C12-N13-C2	121.3(7)
C12-N1-C1	121.76(17)	C17-N13-C2	121.1(7)

Table 4.5 Crystal data and structure refinement for **4.13**

Empirical formula	$C_{42}H_{40}N_4$
Formula weight	600.78
Temperature (K)	200(2) K
Wavelength (Å)	0.71073
Crystal system	Triclinic
Space group	P -1
a (Å)	9.7596(3)
b (Å)	10.0259(3)
c (Å)	17.3380(5)
α (deg)	83.737(2)
β (deg)	89.541(2)

γ (deg)	73.797(2)
Volume (Å ^{3})	1618.95(9)
Z	2
Density (calculated) (Mg/m^3)	1.232
Absorption coefficient (mm^{-1})	0.072
F(000)	640
Crystal size (mm^3)	0.253 x 0.187 x 0.141
Theta range for data collection	2.129 to 28.061.
Index ranges	-12<=h<=12, -13<=k<=12, -22<=l<=22
Reflections collected	15763
Independent reflections	7794 [R(int) = 0.0434]
Completeness to theta = 25.242	99.7 %
Refinement method	Full-matrix least-squares on F^2
Data / restraints / parameters	7794 / 68 / 449
Goodness-of-fit on F^2	1.003
Final R indices [I>2sigma(I)]	R1 = 0.0530, wR2 = 0.1114
R indices (all data)	R1 = 0.1224, wR2 = 0.1372
Extinction coefficient	n/a
Largest diff. peak and hole	0.189 and -0.185 e^{-3}

Figure 4.6 X-ray structure of **4.13.** (Only one of the independent molecules is shown and hydrogen atoms have been omitted for clarity)

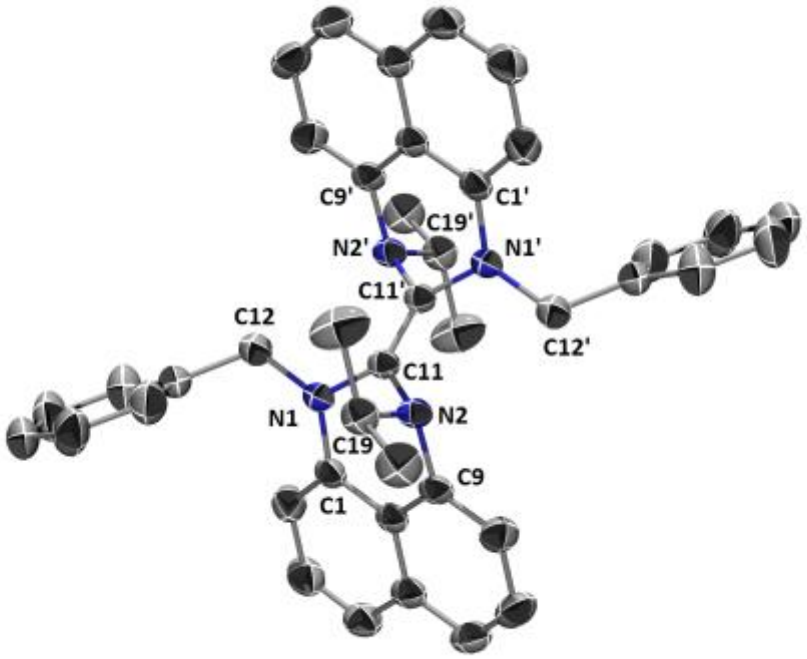

Table 4.6 Selected Bond Lengths [Å] and Angles [°] for **4.13**

Bond lengths (Å)		Bond Angle (°)	
C11-C11’	1.333(3)	N1-C11-N2	114.31(13)
C11-N1	1.419(2)	N2-C11-C11’	121.0(2)
C11-N2	1.432(2)	C12-N1-C11	122.35(13)
C1-N1	1.399(2)	C19-N2-C11	112.95(13)
C12-N1	1.462(2)	C11-N1-C1	114.84(13)
C9-N2	1.435(2)	C11-N2-C9	109.23(13)
C19-N2	1.496(2)	N1-C11-C11’	124.4(2)
		N2-C11-C11’	121.0(2)

IV. References

[1] R. Hoffmann, *J. Am.Chem. Soc.*, 1968, **90**, 1475.

[2] A. J. Arduengo III, R. L. Harlow, M. Kline, *J. Am. Chem. Soc.*, 1991, **113**, 361.

[3] P. Lei, G. Meng, M. Szostak, *ACS Catal*, 2017, **7**, 1960.

[4] C. Färber, M. Leibold, C. Bruhn, M. Maurer, U. Siemeling, *Chem, Commun.*, 2012, **48**, 227.

[5] W. A. Herrmann, M. Elison, J. Fischer, C. Köcher, G. R. J. Artus, Angew. *Chem., Int. Ed. Engl.*, 1995, **107**, 2602

[6] J. Schwartz, V. P. W. Böhm, M. G. Gardiner, M. Grosche, W. Herrmann, W. Hieringer, G. Raudaschl-Siebr, *Chem. Eur. J.*, 2000, **6**, 1773.

[7] E. Despagnet-Ayoub, R. H. Grubbs, *J. Am. Chem. Soc.*, 2004, **126**, 10198.

[8] F. E. Hahn, L. Wittenbecher, D. Le Van, R. Fröhlich, *Angew. Chemie - Int. Ed.*, 2000, **39**, 541.

[9] R. W. Alder, M. E. Blake, C. Bortolotti, S. Bufali, C. P. Butts, E. Linehan, E, J. M. Oliva, A. Guy Orpen, M. J. Quayle, *Chem. Commun.*, 1999, **3**, 241.

[10] F. Guillen, C. L. Winn, A. Alexakis, *Tetrahedron Asymmetry*, 2001, **12**, 2083.

[11] P. Bazinet, T. G. Ong, J. S. O'Brien, N. Lavoie, E. Bell, G. P. A. Yap, I. Korobkov, D. S. Richeson, *Organometallics*, 2007, **26**, 2885.

[12] P. Bazinet, G. P. A. Yap, D. S. Richeson, *J. Am. Chem. Soc*., 2003, **125**, 13314.

[13] C. C. Scarborough, B. V. Popp, I. A. Guzei, S. S. Stahl, *J. Organomet. Chem.*, 2005, **690**, 6143.

[14] C. C Scarborough, M. J. W. Grady, I. A. Guzei, B. A. Gandhi, E. E. Bunel, S. S. Stahl, *Angew. Chemie - Int. Ed.*, 2005, **44**, 5269.

[15] M. Burke-Liang, M. Liang, *Acta Crystallogr., Sect. B*, 1976, **32**, 3216.

[16] P. Bazinet, T. -G. Ong, J. S. O'Brien, N. Lavoie, E. Bell, G. P. A. Yap, L. Korobkov, D. S. Richeson, *Organometallics*, 2007, **26**, 2885.

Chapter V

Pd Complexes of Perimidine-Based Carbenes

I. Introduction

Application of NHCs (N-heterocyclic carbenes) as ligands to stabilize late transition metals is already well known.[1] Moreover, in transition metal catalyzed reaction, the role of NHCs is comparable to that of good donor ligand phosphines.[2,3,4,5] Regarding this, the design of NHC frameworks is a significant endeavor in that it affects donor properties to the transition metal as well as having the potential to modify the steric environment of a metal complex.[6,7,8] Therefore, strong σ donation abilities and better steric protections should be considered for preparing suitable ligands. In this regard, the six-membered ring perimidine-based carbenes have been chosen with several reasons. As stated in **Chapter IV**, the six-membered ring perimidine-based carbene has a smaller α angle, leading a change in the steric impact of the N-substituents compared to classic five-membered ring carbenes. In addition, by expanding to a six membered

ring, a more stable compound can be formed by the extended aromaticity. Indeed, (^{i}Pr)$_2$-carbene was found to form rigid metal ligand complexes with Rh(I) by using these steric and electronic features.[9] From this result, strong σ donation properties were found. Additionally, there could be some π back donation from the transition metal to the vacant π orbital of the singlet carbene.[10,11]

Our first effort was to find the appropriate late transition metals that would be exploited well with our perimidine-based carbenes. Regarding this, we decided to focus on Pd(II). The electron configuration of Pd(II) is [Kr]4d^8, leading to a strong tendency to be square planar coordination. In the case of the coordinately unsaturated Pd(II) compound, they can accept NHCs as ligands in the vacant orbitals. Furthermore, the literature presents a number of applications of Pd(II)-NHCs in catalyzed cross coupling reactions such as C-N cross coupling[12], and C-C cross coupling.[13] Examples are presented in **Charts 5.1** and **5.2**.

Chart 5.1 Example of C-N cross coupling reaction catalyzed by Pd-NHC[14]

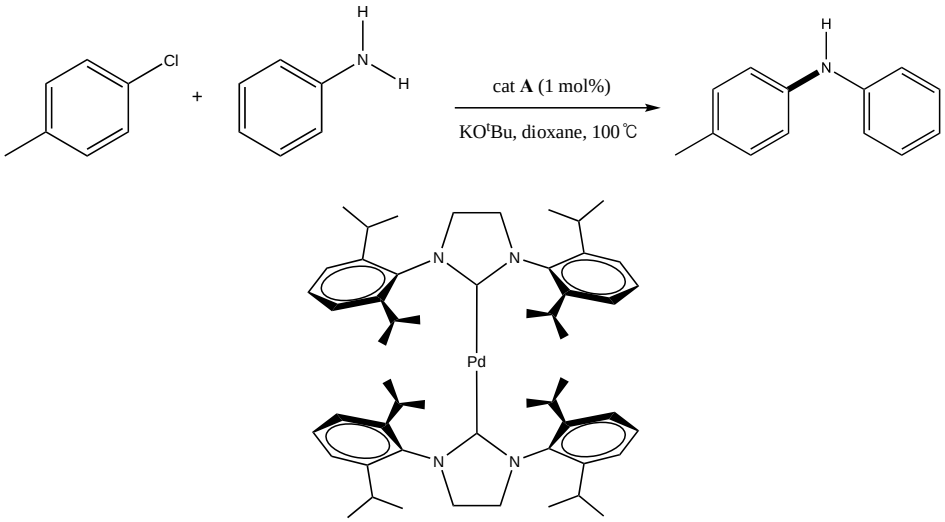

cat **A**

Chart 5.2 Example of C-C cross coupling reaction catalyzed by Pd-NHC[15]

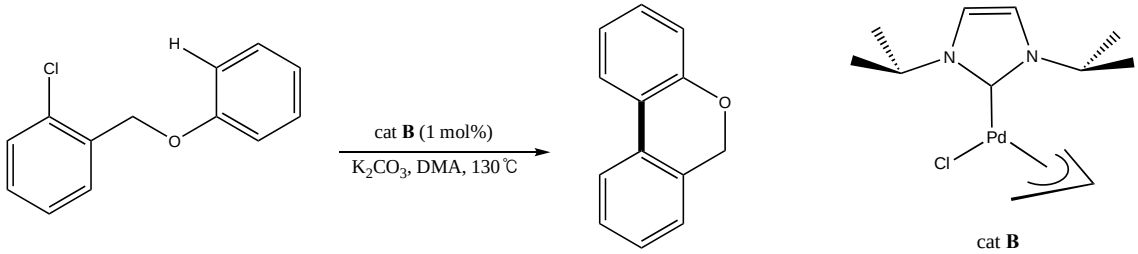

cat **B**

There are several advantages of Pd-NHCs for cross coupling reaction compared to Pd complexes with other donor ligand system such as phosphines. First of all, due to the strong σ donation of NHCs, Pd-NHCs facilitate oxidative addition reactions even into strongly bonded chloroarenes[16] or alkyl halides.[17,18] The second reason is that steric bulkiness of NHCs make Pd-NHCs capable of reductive elimination reactions as well.[19] Finally, the strong Pd-NHCs bond strength leads to increased stability of these complexes and limits the possibility of decomposition. As a result, Pd-NHCs are suitable for catalytic reactions in that they are not only

stable but also activated under proper conditions. These promising features of Pd-NHCs encouraged us to design new Pd(II) complexes with new scaffold carbenes employing our six-membered perimidine-based carbenes. In this chapter, the application of perimidine-based carbene ligands with Pd(II) compound will be described. Spectroscopic and structural analysis will be used to discuss the electronic and steric features within these compounds. Furthermore, by exchanging the substituents at nitrogen atom with alkyl and phenyl group, introduction of different degrees of steric protection and modulation of electronic features will be followed.

II. Results and Discussion

As mentioned earlier, our main goal was to design and synthesize new Pd(II) carbene complexes, which would be promising for some catalytic reactions. Regarding this, $Pd(OAc)_2$ and $[(allyl)PdCl]_2$ were chosen for following reasons. First of all, we were interested in attempting various coordination environments for the Pd(II) center. These could include compounds with one or more carbene ligands attached to the Pd(II) center. The proposed starting compounds, $Pd(OAc)_2$ and $[(allyl)PdCl]_2$, seem to be good candidates for our initial exploration of different coordination geometries. The second reason is the lability of acetate group of $Pd(OAc)_2$ and bridging chloride of $[(allyl)PdCl]_2$. Since acetate group is weakly coordinated due to the delocalized anion through acetate group, acetate group is labile and coordination of two equivalents of carbene doesn't require significantly high energy. In a similar manner, $[(allyl)PdCl]_2$ dimer possesses bridging chlorides, sharing electrons of chloride with another Pd. Therefore, cleavage of Pd-Cl bond could be accessible by adding the carbene ligand.

Given the variety of Pd(II) complexes, a shorthand notation for identifying these species is convenient. Regarding this, I have chosen to use the notation $[R,R'\text{-carbene}]_xPd(L)_y$ (L=ligand in Pd complex). For example, $\{C_{10}H_6(^iPrN)_2C\}_2Pd(OAc)_2$ and $\{C_{10}H_6(^iPrN)(BnN)C\}_2Pd(OAc)_2$ will be called $[(^iPr)_2\text{-carbene}]_2Pd(OAC)_2$ and $[(Bn)(^iPr)\text{-carbene}]_2Pd(OAC)_2$. Although $(Bn)(^iPr)$-carbene is not isolated as free carbene but as enetetraamine, the final Pd(II) complexes were found to have carbene as a ligand, I have decided to call $[(Bn)(^iPr)\text{-carbene}]_xPd(L)_y$. In the case of enetetraamine of $\{C_{10}H_6(^iPrN)(BnN)C\}_2$, $(Bn)(^iPr)$-enetetraamine will be used as a short notation as mentioned in **Chapter IV**.

The first reaction that was explored was between two equivalent of **5.1** $(^iPr)_2$-carbene and $Pd(OAc)_2$ and is shown in **Scheme 5.1**. At first, an *in situ* method was tried with $(^iPr)_2$-$PERI^+Br^-$ and $Pd(OAc)_2$ with the idea that acetate anion would function as base for deprotonation of the perimidinium salt. Unfortunately, this procedure did not lead to reaction. This fact was easily confirmed by ^1H NMR, due to the fact that a singlet resonance at δ 9.69 ppm for the N-C(H)-N in the starting perimidium salt appeared in the spectrum. This observation indicates that $Pd(OAc)_2$ is not basic enough to deprotonate $(^iPr)_2$-$PERI^+Br^-$. In the same manner, *in situ* reaction with Ag_2O and $Pd(OAc)_2$ also failed since Ag_2O was also unable to deprotonate $(^iPr)_2$-$PERI^+Br^-$. As a result, we decided to isolate the free carbene by deprotonation with KHMDS. Another factor that should be considered is stability of the free carbenes. Since I have experienced some failures due to decomposition, reaction with Pd compound should be followed right after the deprotonation step. when I isolate and leave the free carbene more than one day, the anticipated Pd(II) complex was not obtained.

Consequently, **5.3** [(^{i}Pr)$_2$-carbene]$_2$Pd(OAc)$_2$ was successfully obtained by using free carbene **5.1** (^{i}Pr)$_2$-carbene and Pd(OAc)$_2$ in the proper condition. Moreover, this desired compound **5.3** could be characterized by NMR as well as single crystal X-ray diffraction

In terms of NMR result, one of the most interesting features was the appearance of the isopropyl C-H peak at δ 8.34 ppm, which is highly deshielded from δ 4.08 ppm in **5.1** (^{i}Pr)$_2$-carbene. This result can be understood by the interaction between these two protons and Pd center. Since the isopropyl proton is in the diamagnetic field of Pd(II) center, it was 4.26 ppm deshielded. The NMR spectra indicate a symmetrical structure, therefore, two isopropyl protons were appeared at the same chemical shift. Additionally, ^{13}C NMR was consistent with the symmetrical structure, which is proved by X ray structure of **5.3**.

Scheme 5.1

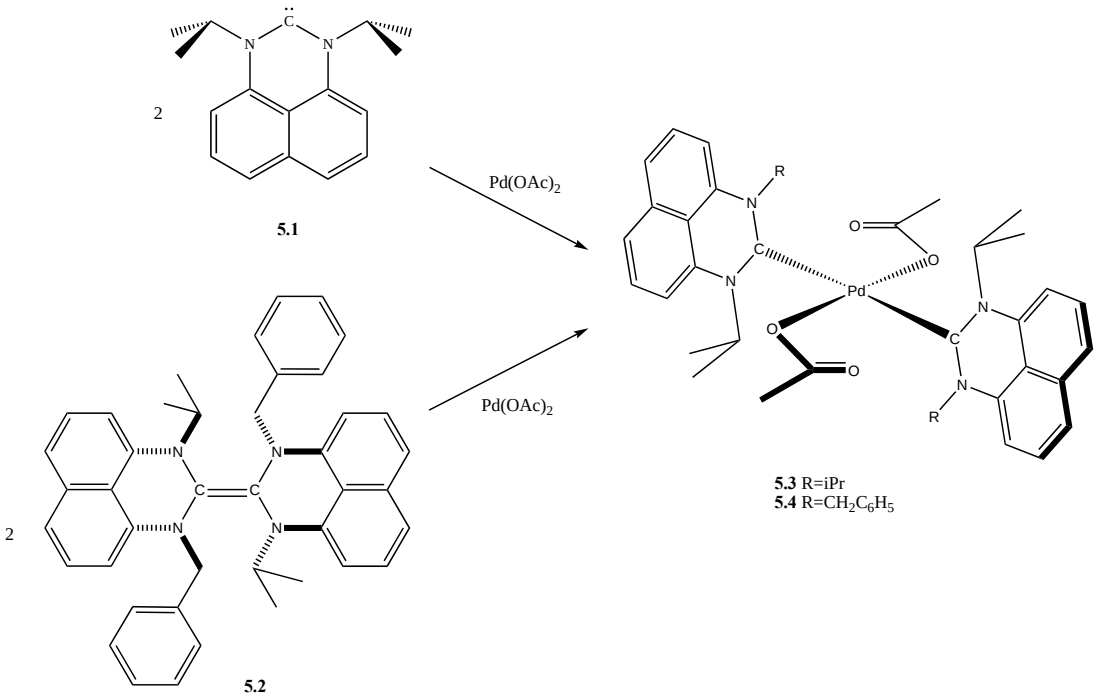

The results of X-ray analysis (**Table 5.2**) gave definite evidence of the connectivity of **5.3** and gave a complex with a square planar geometry around Pd1, with angles of 98.47(16)°, 81.53(16)°, 81.53(16)°, and 98.47(16)° respectively for O1-Pd1-C11, O1'-Pd1-C11, O1-Pd1-C11', and O1'-Pd1-C11'. Additionally, the sum of these four angles is 360°, which is consistent with classic pseudo-square planar complexes. Another interesting feature is the bond distance between Pd center and the $C_{carbene}$ center (C11), which is 2.064(2) Å, this value is close to the literature values found for square planar Pd(II)-NHC complex Pd-[(s)-4-($C_6H_5CH_2$)-1-(2,6-$^{i}Pr_2C_6H_3$)-3-(2,4,6-$Me_3C_6H_2CH_2$)-$C_3H_3N_2$](C_3H_5N)Cl_2 (1.951(3) Å).[20]

From the fruitful result for the preparation of **5.3** [(^{i}Pr)$_2$-carbene]$_2$Pd(OAc)$_2$, we were interested in exploiting a new carbene ligand for the Pd(OAc)$_2$ as well as comparing two different complexes. In this regard, we have decided to keep one isopropyl group and exchange only one substituent at the other nitrogen atom so that we can investigate the role of the substituent electronically and sterically. As a result, (Bn)(^{i}Pr)-carbene was chosen in that it has one benzyl group that possesses the decreased steric hindrance compared to isopropyl group. However, as described in **Chapter IV**, due to energy factors, dimeric (Bn)(iPr)-carbene is preferred. Due to this fact, we employed a slightly different approach to introducing a (Bn)(^{i}Pr)-carbene by using the enetetraamine as the carbene sources. Fortunately, the analogous synthetic procedure allowed for the successful isolation of **5.4** [(Bn)(^{i}Pr)-carbene]$_2$Pd(OAc)$_2$. Regarding this, the successful synthesis of **5.4** [(Bn)(^{i}Pr)-carbene]$_2$Pd(OAc)$_2$ reveals that dimeric carbene can be used as a precursor to a carbene ligand for Pd(II) compound. It is noteworthy that dimeric carbene can be cleaved and form Pd(II)-carbene complexes as this offers great potential of various kinds of dimerized carbenes as ligands. In fact, the use of enetetraamine as a ligand for

transition metal has already known.[21] For example, perimidine-based enetetramine, possessing 3,5-dimethyl phenyl substituents, $C[N(3,5\text{-}Me)C_6H_3]_2C_{10}H_6$ was found to react with $Rh(CO)_2Cl$ cleanly at room temperature.[21]

The NMR data for **5.4** $[(Bn)(^iPr)\text{-carbene}]_2Pd(OAc)_2$ was as expected. One of the most interesting features was that a septet peak for isopropyl CH proton appeared at δ 7.82, which is deshielded by 4.32 ppm compared to the isopropyl CH proton of the **5.2** $(Bn)(^iPr)$-enetetraamine. Additionally, the benzyl CH_2 resonance was found at δ 7.45 ppm and appeared as a doublet, which is deshielded by 2.45 ppm (it used to appear at around δ 5 ppm in $(Bn)(^iPr)$-enetetraamine). This observation could be understood by some interaction between Pd and these protons, which exist in the diamagnetic region of Pd center. Furthermore, when it comes to the degree of deshielding, the isopropyl proton was much more deshielded than the benzyl one. This fact suggests a stronger interaction between Pd center and isopropyl proton due to its orientation towards Pd center. The fact that benzyl and isopropyl proton appear as a single septet and doublet peak implies a symmetrical molecular structure.

The X-ray data (**Table 5.2**) allows a comparison of the bond distances of **5.4** $[(Bn)(^iPr)\text{-carbene}]_2Pd(OAc)_2$ with **5.3** $[(^iPr)_2\text{-carbene}]_2Pd(OAc)_2$. Bond distances between Pd and $C_{carbene}$ (C11) was 2.061(2) Å and between Pd and O1 of acetate was 2.0337(18) Å. Compared to the bond lengths of **5.3** $[(^iPr)_2\text{-carbene}]_2Pd(OAc)_2$, they are slightly shorter, which can be explained by less steric hindrance from the N-substituents. In terms of bond angles around Pd, O1'-Pd1-C11, O1-Pd1-C11, O1'-Pd1-C11', and O1-Pd1-C11' turned out to be 97.37(8)°, 82.63(8)°, 82.63(8)°, and 97.37(8)° respectively. As anticipated, square planar geometry is observed, having 360° as sum of the four angles around Pd.

We next broadened our examination of Pd(II) starting materials to $[PdCl(allyl)]_2$ and reactions of this Pd compound were investigated for both **5.1** $[(^iPr)_2$-carbene] and **5.2** [(Bn)(^{i}Pr)-enetetraamine], which is summarized in **Scheme 5.2**. As with $Pd(OAc)_2$, both perimidinium salts were not able to be used as ligand for $[PdCl(allyl)]_2$ unless they are first deprotonated with KHMDS. Two equivalents of $[(^iPr)_2$-carbene] were applied as a ligand to $[PdCl(allyl)]_2$, which led to the cleavage of bond between Pd and Cl. Consequently, the Pd(II) center can accept one carbene ligand, forming the desired complex **5.5** $[(^iPr)_2$-carbene]PdCl(allyl). Fortunately, complex **5.5** was obtained as a crystalline solid and investigated by NMR and single crystal X-ray diffraction.

In ^{1}H NMR of **5.5**, four different isopropyl C-H signals were detected at δ 6.22 ppm, 4.9 ppm, 4.51 ppm, and 3.42 ppm, indicating two unsymmetrical structures. This can be undertstood by different conditions around each isopropyl protons, with allyl group and Cl at Pd center. The fact that two different structures exist in the final product was also confirmed in X-ray structure, having two possible oreintations of the allyl group. In the X-ray structure of **5.5**, allyl group was found to attach to the Pd center in the two different ways.

In the X ray structure of **5.5** $[(^iPr)_2$-carbene]PdCl(allyl) (**Table 5.4**), it was intersting to note that Pd and carbene bond distance (Pd1-C11) is shorter than three Pd and C distances of Pd-allyl in the Pd(allyl)Cl dimer complex, which are 2.075(15) Å and 2.123 Å, 2.121 Å, and 2.108 Å respectively[22]. Furthermore, bond angle between allyl group, C18-C19-C20 is found to be 118(2)º, which is similar to 119.8º in the $[Pd(allyl)Cl]_2$ starting material. When it comes to the geometry, the Pd center had the angles 90.6(4) °, 99.8(6) °, 66.5(8) °, and 102.9(7)° as C11-Pd-Cl1, Cl1-Pd1-C18, C18-Pd1-C20, and C20-Pd1-C11, respectively. These angles indicate that

C11, Pd1, C18, and C20 are in one plane having 361.4° as a sum of angles. Furthermore, it can be explained as distorted square planar geometry. This is because the allyl group takes two coordination sites. Therefore, it has square planar geometry even though it has three ligands. Additionally, as shown in **Figure 5.3** allyl group was oriented perpendicular to the plane of Pd and the carbene. Another interesting feature is bond length between Pd center and three carbons in allyl gorup. Specifically, when comparing the bond lengths of C18-Pd1 and C20-Pd1, C18-Pd1 is longer than C20-Pd1 with respectively 2.181(15) Å and 2.111(19) Å. From the difference of two bond lenghts, the fact that C20-C19 has more single bond, coordinated directly to the Pd center, and C18-C19 has more double bond characters was found.

Scheme 5.2

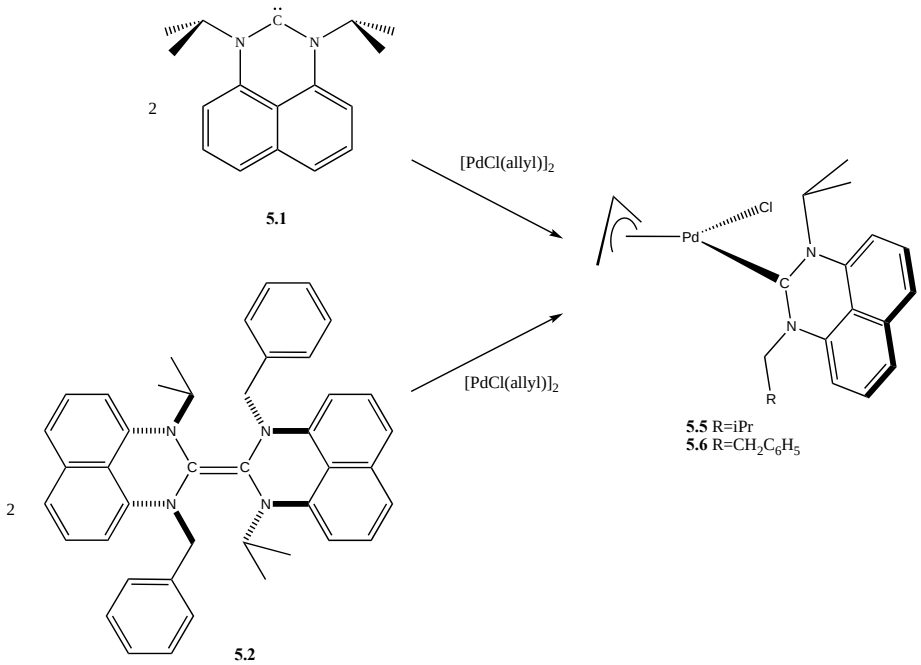

The NMR results of product **5.6** [(Bn)(^{i}Pr)-carbene]PdCl(allyl) revealed a more complicated spectrum than expected. It would appear that there are two different orientations of the allyl group. Indeed, the X-ray structure analysis showed two possible ways to attach the allyl

group. Therefore, when the allyl group bonds to the Pd(II) center in two different ways, two different chemical shifts were observed for each protons and carbons in ^{1}H NMR and ^{13}C NMR. As described for **5.4** [(Bn)(^{i}Pr)-carbene]$_2$Pd(OAc)$_2$, compound **5.6** also displayed benzyl CH_2 and isopropyl CH protons that were very deshielded compared to free carbene. However, in this case the deshielding was not as large as in **5.4** [(Bn)(^{i}Pr)-carbene]$_2$Pd(OAc)$_2$. This result can be understood by reduced steric impact. Compared to **5.4** which has two carbenes and two acetates around Pd center, **5.6** has only one carbene, an allyl ligand, and Cl around Pd center. Consequently, steric impact is less and therefore less interaction exist between carbene protons and metal center.

In the X-ray structure of **5.6** [(Bn)(^{i}Pr)-carbene]PdCl(allyl) (**Table 5.4**), it was worthy to note that Pd1-C11 bond distance of 2.065(5)Å is shorter than Pd-C11 distance (2.075(15) Å) in the **5.5** [(^{i}Pr)$_2$-carbene]PdCl(allyl) due to the less steric hinderance in **5.6**. In addition to this, the Pd1-C11 bond distance is also much shorter than Pd-C bonds in Pd(allyl)Cl dimer, indicating stronger σ donation from the carbene center to Pd(II) center. In the same way of **5.5**, all of three carbons of allyl group were coordinated to the Pd center as shown in **Figure 5.4**. Moreover, as seen in **Table 5.4**, the metal geometry is similar to **5.5**, having 91.98(15)º, 100.26(19)º, 67.3(3)º, and 100.5(2)º around Pd center as C11-Pd1-C1, Cl-Pd1-C24, C22-Pd1-C24, and C22-Pd1-C11, indicating distorted square planar. The sum of these four angles is 360.04 º indicating that C11, Pd1, C22, and C24 are in the same plane. Considering the bond lengths between Pd and C of allyl group gave an evidence that allyl group is coordinated to the Pd(II) center in a slightly unsymmetrical mode. Specifically, C22-C23 and C23-C24 were 1.429(15) Å and 1.249(13) Å. Therefore, C22-C23 has more single bond, coordinated directly to the Pd center, and C23-C24

has more double bond characters. Although, three carbons of allyl group are coordinated to the Pd(II) center. Another result that supports this argument is the bond lengths between Pd and C of allyl group. The bond length of C22-Pd1(2.122(6) Å) was shorter than C24-Pd1 (2.188(6) Å), which is indicative of C22 is more donating to the Pd center as expected.

The successful isolations and characterizations of Pd(II)-carbene complexes attracted our interests to explore different methods to synthesize new Pd(II) complexes with our carbene system. Regarding this, one of most challenging tasks to prepare Pd(II)-carbene complexes is to isolate the free carbene and keep it without decompostion. One reason for this can be the short life-time of the free carbene. As a result, the discovery of a new approach without an isolation of the free carbene to synthesize Pd complexes would be attractive and promising. Related to this method, we decided to attempt an *in situ* synthetic method reported in the Pd-NHC literature.[23] These authors used K_2CO_3 as base and combined the base and carbene precursor with $PdCl_2$ in a single step. Interestingly, 3-chloropyridine was used as solvent since it was found to help the catalytic reaction as 3-chloropyridine seems to be labile ligand in the process. Indeed, it has been demonstrated that 3-bromopyridine ligated to the NHC-Ru complexes have three times more reactivity that the simple pyridine analogues. In addition, 3-chloropyridine can donate a pair of electrons so that Pd center can be more stablized as well.

Scheme 5.3

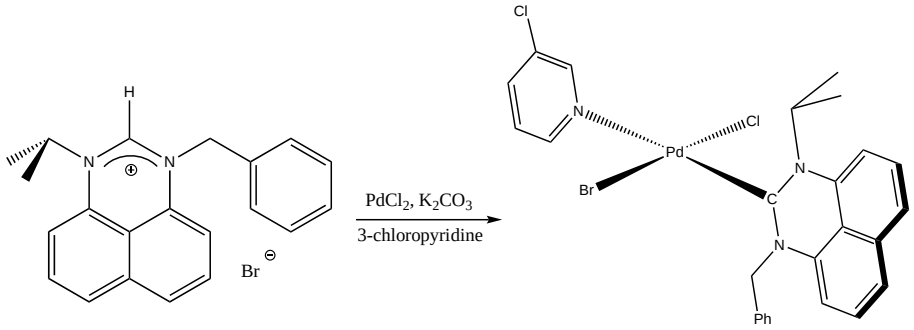

5.7 **5.8**

Therefore, reaction of **5.7** (Bn)(^{i}Pr)-PERI^{+}Br^{-} and $PdCl_2$ was attempted using this procedure. Fortunately, under these conditions K_2CO_3 was capable to deprotonate carbene precursor **5.7** (Bn)(^{i}Pr)-PERI^{+}Br^{-}, leading the new complex **5.8** [(Bn)(^{i}Pr)-carbene]PdClBr(3-chloropyridine). The origin of the Pd-Br is likely the result of an anion exchange between the two starting materials. One of the most interesting features of this reaction is that it does not require a glove box for handling or characterization. In fact, a Schlenk flask was charged with the reagents, the flask was flushed with nitrogen and heated to reflux overnight, followed by filtration in the air. Additionally, crystals were isolated from the solution outside of the glove box by a slow evaporation method.

Interestingly, the ^{1}H NMR spectra showed three sets of septet peaks for the isopropyl proton. An explanation for this observation might be provided by hindered rotation about the Pd-py and or the Pd-carbene. In addition, it is possible that the Br/Cl ion exchange was not complete and would lead to additional NMR signals.

The X-ray structure provided the definitive structural features of **5.8** and gave us an opportunity to compare **5.8** [(Bn)(^{i}Pr)-carbene]PdClBr(3-chloropyridine) with a well-known compound from the literature, PEPPSI-IPent (**Chart 5.3**).[24]

Chart 5.3 PEPPSI-IPent

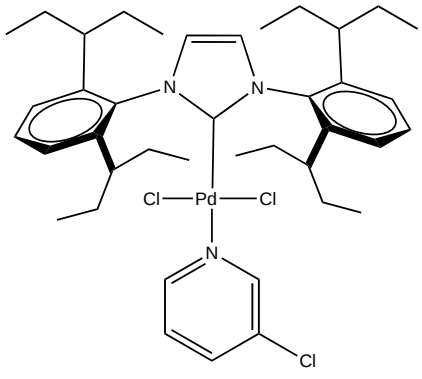

C

In the X-ray structure of the PEPPSI-IPent compound (**C**) the Pd-ligand bond distances were 2.097(3)Å, 1.974(3)Å, 2.2869(9)Å, and 2.3033(9)Å for the Pd-N(3-chloropyridine), Pd-$C_{carbene}$, Pd-Cl(1), and Pd-Cl(2) bonds respectively. The comparable bond distances in the X-ray structure of **5.8** [(Bn)(^{i}Pr)-carbene]PdClBr(3-chloropyridine) (**Table 5.6**) were found to be 2.099(3)Å, 1.975(4)Å, 2.032(2)Å, and 2.423(3)Å as Pd1-N3 (3-chloropyridine), Pd1-$C_{carbene}$ (C1), Pd1-Cl1, and Pd1-Br2. Especially, when we compare the bond distances between Pd and $C_{carbene}$ in these two compounds they are almost identical, indicating similar electronic properties of the carbene center of PEPPSI-IPent and **5.8** [(Bn)(^{i}Pr)-carbene]PdClBr(3-chloropyridine). Therefore, strong σ donation properties of **5.2** (Bn)(^{i}Pr)-carbene was found by a comparison with well known carbene possessing the strong σ donation.

III. Conclusion

Successful synthesis and characterization of perimidine-based carbene with Pd(II) complexes proved that perimidine-based carbenes are capable to form stable complexes Pd that possess a variety of different other ligands. Specifically, comparison of bond distances of Pd-$C_{carbene}$ with the well-known compound, PEEPPSI-IPent, enables us to propose similar electronic properties of the perimidine-carbene and the IPent ligand. Regarding this, further studies on catalytic reactivity of these complexes will be prepared in the future. Based on the extensive literature on the catalytic reaction by using Pd(II)-NHCs, we anticipate a promising potential with our Pd carbene complexes.

Experimental section

General: Unless otherwise noted, all manipulations are carried out in either a nitrogen filled glovebox or under nitrogen using standard Schlenk techniques. Reaction solvents were sparged with nitrogen then dried by passage through column of activated alumina using an apparatus purchased from Anhydrous Engineering. Deuterated benzene and chloroform, were purchased from Aldrich Chemical Company. Acetone, Toluene, 3-chloropyridine, Anhydrous hexane, Anhydrous pentane, Anhydrous tetrahydrofuran, K_2CO_3, Pd(allyl)Cl dimer, $PdCl_2$, and $Pd(OAc)_2$ were purchased from Aldrich Chemical Company and used without further purification. ^1H and spectra were run on either a Bruker 300 MHz, a Bruker 400 MHz, or a Bruker 600MHz spectrometer, and $^{13}C\{^1H\}$ NMR was on a Bruker 75 MHz, a Bruker 100 MHz or a Bruker 150

MHz using the residual protons of the deuterated solvent for reference. Elemental analyses were performed by Midwest micro lab in Indianapolis, IN, USA.

The crystal of **5.3**-**5.6**, and **5.8** were mounted on thin glass fibers using paratone oil. Prior to data collection, the crystals were cooled to 201(2) K. The data were collected on a Bruker AXS single-crystal diffractometer equipped with a sealed Mo tube (wavelength 0.71073 Å) and APEX II CCD detector. The raw data collection and reduction were done with the Bruker APEXII software package. 1 Semi-empirical absorption corrections based on equivalent reflections were applied using SADABS and TWINABS. Systematic absences in the diffraction dataset and unit-cell parameter were consistent with triclinic (**5.3**, **5.4**), orthorhombic (**5.5**, **5.8**), monoclinic (**5.6**) space groups. The structures were solved by direct methods and refined with full-matrix least-squares procedures based on F^2, using SHELXL and WinGX. All non-H atoms were refined anisotropically. All hydrogen atoms were placed in idealized positions. Displacement ellipsoid plots were produced using ORTEP.

Preparation of $\{C_{10}H_6(^iPrN)_2C\}_2Pd(OAc)_2$ (5.3):

In a nitrogen-filled glovebox a vial was charged with $Pd(OAc)_2$ (0.090g, 0.4 mmol), 10 mL of THF, and a stir bar. To this solution carbene **5.1** (0.099g, 0.4mmol), predissolved in 10 mL of toluene was added dropwise. The reaction solution turned a brown color. The reaction was stirred for overnight, then the volume of solvent was reduced under vacuum to small volume and crystallized at -25°C to give colorless crystals. (0.140 g, 48% yield).

^{1}H NMR (C_6D_6, 300MHz): δ 8.34 (sept, 4H, $CHMe_2$, J=7.2Hz), 7.27 (t, 4H, CH, J=8.31Hz) 6.50 (d, 4H, CH, J=7.66Hz), 6.4(d, 4H, CH, J=8.12Hz), 1.96 (s, 6H, CH_3), 1.91(d, 24H, CH_3, J=7.19Hz)

^{13}C{^{1}H} NMR (C_6D_6, 75 MHz): δ 197.0(C-Pd), 175.8 (C=O), 135.2, 134.7, 131.5, 130.7, 121.4, 128.5, 128.4, 127.2, 121.0, 106.9(C_{arom}), 65.5($CHMe_2$), 23.2(CH_3CO), 19.0(CH_3)

Preparation of {$C_{10}H_6$(^{i}PrN)(BnN)C}$_2$Pd(OAc)$_2$(5.4):

In a nitrogen-filled glovebox a vial was charged with $Pd(OAc)_2$ (0.056g, 0.25 mmol), 10 mL of THF, and a stir bar. To this solution, carbene **5.2** (0.076g, 0.25mmol), predissolved in 10 mL of toluene was added dropwise. The solution turned a dark brown color. The reaction was stirred for overnight, then the solvent was removed under vacuum to a small volume and crystallized at -25°C to give colorless crystals. (0.129 g, 68% yield).

^{1}H NMR (C_6D_6, 300MHz): δ 7.82 (sept, 2H, $CHMe_2$, J=6.9Hz), 7.45 (d, 4H, CH_2, J=7.32Hz), 6.73-7.07 (M, 18H, CH), 6,60 (t, 2H, CH, J=8.25Hz), 6.28 (d, 2H, CH, J=7.98Hz), 1.89(s, 6H, CH_3), 1.64(d, 12H, CH_3, J=7.02Hz)

^{13}C{^{1}H} NMR (C_6D_6, 75 MHz): δ 199.0(C-Pd), 174.9(C=O), 136.2, 135.1, 133.5, 132.2, 129.5, 128.5, 128.4, 127.2, 126.9, 126.6, 126.5, 126.1, 122.1, 120.8, 128.0, 106.9(C_{arom}), 61.3(CH_2), 59.5($CHMe_2$), 22.1(CH_3CO), 18.4(CH_3)

Preparation of {$C_{10}H_6$(^{i}PrN)$_2$C}Pd(Allyl)Cl(5.5):

In a nitrogen-filled glovebox a vial was charged with {Pd(allyl)Cl}$_2$ (0.074g, 0.2 mmol), 10 mL of Toluene, and a stir bar. To this solution, carbene **5.1** (0.099g, 0.4mmol), predissolved in 10

mL of toluene was added dropwise. The solution turned a reddish-brown color. The reaction was stirred for overnight, then the solvent was removed under vacuum to a small volume and crystallized at -25°C to give colorless crystals. (0.045 g, 60% yield).

^{1}H NMR (C_6D_6, 300MHz): δ 7.55 (dd, 2H, CH, J=8.28, 1.05 Hz), 7.28 (t, 2H, CH, J=8.00Hz), 7.05-7.13 (m, 4H, CH), 6.90-6.96 (m, 4H, CH), 6.60-6.70(m, 3H, allyl), 6.50 (dd, 2H, allyl, J=7.37, 1.01 Hz), 6.45 (d, 2H, allyl, J=7.87 Hz), 6.22 (sept, 1H, $CHMe_2$, J=8.1 Hz), 5.50 (d, 1H, allyl, J=7.82 Hz), 4.90 (sept, 1H, $CHMe_2$, J=6.8 Hz), 4.51(sept, 1H, $CHMe_2$, J=6.67 Hz), 4.20 (dd, 1H, allyl, J=7.5, 2.5 Hz), 3.42 (sept, 1H, $CHMe_2$, J=6.2 Hz), 3.19(d, 1H, allyl, 13.37 Hz), 1.70(d, 3H, CH_3, J= 7.55 Hz), 1.52 (d, 3H, CH_3, J= 7.31 Hz), 1.24 (d, 3H, CH_3, J= 6.1 Hz), 1.22 (d, 3H, CH_3, J= 7.01 Hz), 1.151.24 (d, 3H, CH_3, J= 7.01 Hz), 1.10 (d, 6H, CH_3, J= 6.52 Hz), 0.71 (d, 3H, CH_3, J= 5.71 Hz)

^{13}C{^{1}H} NMR (C_6D_6, 75 MHz): δ 209.4 (C-Pd), 162.5, 143.7, 137.2, 135.6, 134.2, 133.8, 131.8, 130.1, 129.5, 128.9, 128.4, 126.7, 126.2, 124.3 123.1, 120.7, 116.4, 113.25, 109.9, 107.6(C_{arom}), 69.7, 62.6(C_{allyl}), 61.4($CHMe_2$), 47.9(C_{allyl}), 47.1($CHMe_2$), 43.4, 30.9, 29.8 (C_{allyl}), 22.7, 22.1, 22.0, 21.1, 20.7, 18.2, 17.7, 13.9 (CH_3)

Preparation of {$C_{10}H_6$(^{i}PrN)(BnN)C}Pd(Allyl)Cl(5.6):

In a nitrogen-filled glovebox a vial was charged with $[Pd(allyl)Cl]_2$ (0.055g, 0.15 mmol), 5 mL of Toluene, and a stir bar. To this solution, carbene **5.2** (0.194g, 0.6mmol), pre-dissolved in 5 mL of Toluene was added dropwise. The solution turned a yellow color. The reaction was stirred for 1 hour, and all volatiles were removed with vacuum. The crude product was washed with ether and re-crystallized with benzene /ether, affording colorless crystals. (0.051 g, 68% yield).

^{1}H NMR (C_6D_6, 300MHz): δ 6.95-7.07(m, 16H, CH), 6.62-6.75(m, 6H, CH), 6.10(d, 1H, CH_2, J= 7.7 Hz) 6.01 (d, 1H, CH_2, J= 7.23 Hz), 5.10 (d, 1H, CH_2, J= 16.3 Hz) 4.91 (d, 1H, CH_2, J= 17.2 Hz), 4.80 (sept, 1H, $CHMe_2$, J=6.3 Hz), 4.35 (sept, 1H, $CHMe_2$, J=7.0 Hz), 4.11 (d, 1H, allyl, J= 7.5 Hz), 4.05 (d, 1H, allyl, J=7.4 Hz), 3.1 (d, 2H, allyl, J=12.0 Hz), 2.9 (d, 2H, allyl, J=12.2 Hz) 2.03 (d, 2H, allyl, J=12.3 Hz), 1.77(d, 3H, CH3 J=7.82 Hz), 1.68 (d, 2H, CH3 J=7.82 Hz), 1.50 (d, 2H, allyl, J=12.3 Hz), 1.29 (d, 3H, CH_3, J=7.11 Hz), 1.20 (d, 3H, CH_3 J=8.5 Hz).

^{13}C{^{1}H} NMR (C_6D_6, 75 MHz): δ 212.4, 211.9 (C-Pd), 135.9, 135.8, 135.5, 134.3, 134.3, 132.4, 132.3, 128.9, 128.8, 128.5, 128.4, 127.6, 127.5, 127.4, 127.2, 126.6, 126.4, 123.4, 122.3, 122.2, 121.4, 121.3, 121.2, 121.1, 114.2, 114.1, 108.3, 108.2, 106.8, 106.5 (C_{arom}), 71.7, 70.9 (CH_2), 68.8, 63.8($CHMe_2$) 60.1, 59.0, 49.3, 38.6, 31.9, 30.2 (C_{allyl}), 23.1, 23.0, 18.5, 18.4, (CH_3)

Preparation of {$C_{10}H_6$(^{i}PrN)(BnN)C}$_2$$PdCl_2C_5H_4ClN$(5.8):

In a nitrogen-filled glovebox Schlenk flask was charged with $PdCl_2$, (0.064g, 0.36mmol), (Bn)(^{i}Pr)-PERI^{+}Br^{-}(0.33mmol, 0.127g), and a stir bar. The sealed flask was removed from the glovebox and K_2CO_3 (1.78mmol, 0.246g) was added under flow of nitrogen gas followed by 3ml of 3-chloro-pyridine which was added via syringe. This solution was heated overnight at 80°C. The solution turned a reddish-brown color, then was filtered through a pad of celite. Dichloromethane was added to get a yellow crude product completely. Dichloromethane solvent was slowly evaporated and yellow crystals were formed (0.129 g, 68% yield).

^{1}H NMR ($CDCl_3$, 600MHz): δ 8.98-9.02 (m, 2H, CH), 8.93-8.89 (m, 2H, CH), 8.58 (d, 1H, CH, J= 2.64Hz), 8.48 (dd, 1H, CH, J= 4.86, 1.2Hz), 7.84 (sept, 0.5H, $CHMe_2$, J= 6.84Hz), 7.74 (sept, 0.5H, $CHMe_2$, J= 7.62Hz) 7.71-7.75 (m, 2.5H), 7.65-7.67(m, 1H), 7.62(sept, 1H, $CHMe_2$, J=

7.2Hz), 7.53-7.57(m, 4H), 7.31-7.37(m, 8H), 7.23-7.28(m, 6.5H), 7.12 (d, 2H, CH_2, J=7.14Hz), 7.07-7.11(m, 2H), 6.66-6.89(m, 4H), 6.45-6.49(m, 2H, CH_2) 1.93(d, 3H, CH_3, J=6.72Hz), 1.91(d, 3H, CH_3, J=6.96Hz), 1.90(d, 6H, CH_3, J=7.5Hz).

$^{13}C\{^1H\}$ NMR ($CDCl_3$, 150 MHz): δ 195.7(C-Pd), 195.6(C-Pd), 179.3, 178.9, 151.9, 151.1, 150.8, 150.3, 150.1, 149.3, 148.9, 147.5, 138.1, 138.0, 137.9, 135.8, 134.8, 133.7, 133.5, 133.4, 133.2, 132.7, 132.6, 132.2, 131.9, 131.8, 131,7, 128.8, 128.7, 128.6, 127.7, 127.6, 127.3, 127.1, 127.0, 126.9, 126.8, 124.9, 124.3, 122.9, 122.1 122.0, 121.9, 121.8, 121.7, 121.6, 108.9, 107.8, 107.7(C_{arom}), 62.9($CHMe_2$), 62.8($CHMe_2$), 60.7(CH_2), 60.6(CH_2), 18.4(CH_3), 18.3(CH_3), 18.1(CH_3), 18.0 (CH_3)

Analysis Calcd $C_{57}H_{52}Br_{2.33}Cl_{4.67}N_7Pd_2$ C, 49.43; H, 3.78; N,7.08; Found C, 49.54; H, 3.87; N, 6.88.

Structural determinations

Table 5.1 Crystal data and structure refinement for **5.3** and **5.4**

	5.3	**5.4**
Empirical formula	$C_{45.67}$ $H_{61.50}$ $Br_{0.17}$ N_4 $O_{5.67}$ Pd	C_{54} H_{62} N_4 O_6 Pd
Formula weight	877.23	969.47
Temperature (K)	200(2)	201(2)
Wavelength (Å)	0.71073	0.71073
Crystal system	Triclinic	Triclinic
Space group	P -1	P -1

a (Å)	9.462(2)	10.1099(8)
b (Å)	9.621(2)	11.1360(9)
c (Å)	12.482(3)	11.9833(10)
α (deg)	79.538(3)	101.7370(10)
β (deg)	73.910(2)	94.2250(10)
γ (deg)	76.979(2)	113.4340(10)
Volume ($Å^3$)	1055.0(4)	1193.89(17)
Z	1	1
Density (calculated) (Mg/m^3)	1.381	1.348
Absorption coefficient (mm^{-1})	0.653	0.443
F(000)	461	508
Crystal size (mm^3)	0.346 x 0.212 x 0.070	0.417 x 0.347 x 0.172
Theta range for data collection	1.712 to 28.299	1.762 to 28.291
Index ranges	-12<=h<=12, -12<=k<=12, -16<=l<=16	-13<=h<=13, -14<=k<=14, -15<=l<=15
Reflections collected	12952	11694
Independent reflections	5086 [R(int) = 0.0353]	5635 [R(int) = 0.0366]
Completeness to theta = 25.242	99.8 %	99.5 %
Refinement method	Full-matrix least-squares on F^2	Full-matrix least-squares on F^2
Data / restraints / parameters	5086 / 94 / 320	5635 / 0 / 298
Goodness-of-fit on F^2	1.036	1.015
Final R indices [I>2sigma(I)]	R1 = 0.0420, wR2 = 0.1005	R1 = 0.0467,wR2 = 0.0913
R indices (all data)	R1 = 0.0502, wR2 = 0.1055	R1 = 0.0559,wR2 = 0.0964
Extinction coefficient	n/a	n/a
Largest diff. peak and hole	0.613 and -0.570 e^{-3}	0.614 and -0.609 e^{-3}

Figure 5.1 X-ray structure of **5.3** (Thermal ellipsoids are shown for only selected atoms and hydrogen atoms have been omitted for clarity & The second part of the molecule (with primes') is symmetrically dependent by inversion center (1-x,1-y,2-z))

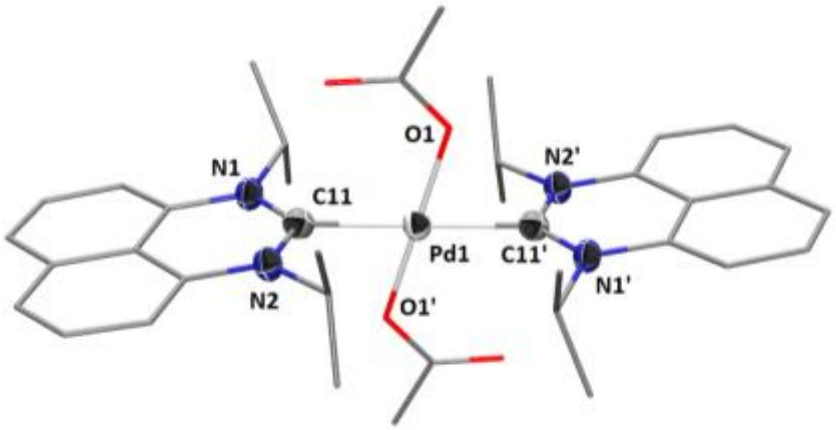

Figure 5.2 – X-ray structure of **5.4** (Thermal ellipsoids are shown for only selected atoms and hydrogen atoms and a crystallized THF molecule have been omitted for clarity & The second part of the molecule (with primes') is symmetrically dependent by inversion center (1-x,1-y,1-z))

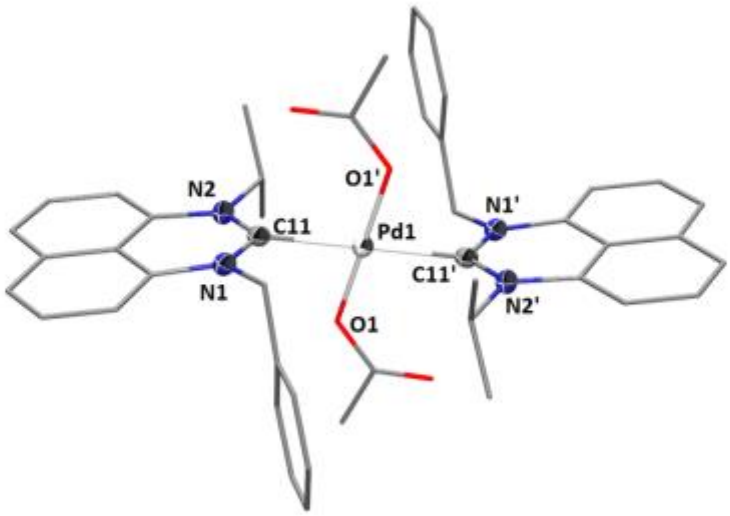

Table 5.2 Selected Bond Lengths [Å] and Angles [°] for **5.3** and **5.4**

5.3		**5.4**	
Bond lengths (Å)			
C11-Pd1	2.064(2)	C11-Pd1	2.061(2)
C11'-Pd1	2.064(2)	C11'-Pd1	2.061(2)
O1-Pd1	2.016(7)	O1-Pd1	2.0337(18)
O1'-Pd1	2.016(7)	O1'-Pd1	2.0337(18)
N1-C11	1.350(3)	N1-C11	1.343(3)
N2-C11	1.350(3)	N2-C11	1.345(3)
Bond Angle (°)			
N1-C11-N2	119.2(2)	N1-C11-N2	118.6(2)
C11-Pd1-C11'	180.0	C11-Pd1-C11'	180.0
C11-Pd1-O1	98.47(16)	C11-Pd1-O1	82.63(8)
C11-Pd1-O1'	81.53(16)	C11-Pd1-O1'	97.37(8)
C11'-Pd1-O1	81.53(16)	C11'-Pd1-O1	97.37(8)
C11'-Pd1-O1'	98.47(16)	C11'-Pd1-O1'	82.63(8)
N2-C11-Pd1	120.14(17)	N1-C11-Pd1	118.77(18)
N1-C11-Pd1	119.95(16)	N2-C11-Pd1	121.63(18)
O1-Pd1-O1'	180.0	O1-Pd1-O1'	180.0

Table 5.3 Crystal data and structure refinement for **5.5** and **5.6**

	5.5	**5.6**
Empirical formula	$C_{20}H_{24}ClN_2Pd$	$C_{24}H_{24}ClN_2Pd$
Formula weight	434.26	482.30
Temperature (K)	200(2)	200(2)
Wavelength (Å)	0.71073	0.71073
Crystal system	Orthorhombic	Monoclinic
Space group	P 2_1 2_1 2_1	P 2_1/n
a (Å)	9.0546(10)	12.5652(6)

b (Å)	18.090(2)	10.6921(6)
c (Å)	23.343(2)	15.9655(7)
α (deg)	90	90
β (deg)	90	100.962(4)
γ (deg)	90	90
Volume ($Å^3$)	3823.5(7)	2105.80(18)
Z	8	4
Density (calculated) (Mg/m^3)	1.509	1.521
Absorption coefficient (mm^{-1})	1.114	1.020
F(000)	1768	980
Crystal size (mm^3)	0.213 x 0.164 x 0.021	0.185 x 0.067 x 0.018
Theta range for data collection	1.745 to 25.248.	2.599 to 28.007.
Index ranges	-10<=h<=7, -21<=k<=19, -25<=l<=28	-15<=h<=16, -13<=k<=14, -20<=l<=20
Reflections collected	17007	9111
Independent reflections	6860 [R(int) = 0.0952]	4970 [R(int) = 0.0449]
Completeness to theta = 25.242	99.9 %	99.1 %
Refinement method	Full-matrix least-squares on F^2	Full-matrix least-squares on F^2
Data / restraints / parameters	6860 / 21 / 452	4970 / 0 / 265
Goodness-of-fit on F^2	1.024	0.983
Final R indices [I>2sigma(I)]	R1 = 0.0607, wR2 = 0.1373	R1 = 0.0538, wR2 = 0.1239
R indices (all data)	R1 = 0.1417, wR2 = 0.1779	R1 = 0.1137, wR2 = 0.1546
Absolute structure parameter	-0.01(4)	
Extinction coefficient	n/a	n/a
Largest diff. peak and hole	1.186 and -0.960 e^{-3}	1.329 and -1.550 e^{-3}

Figure 5.3 X-ray structure of **5.5 (**Only one molecule of the asymmetric unit is shown and thermal ellipsoids are shown for only selected atoms & Hydrogen atoms have been omitted for clarity)

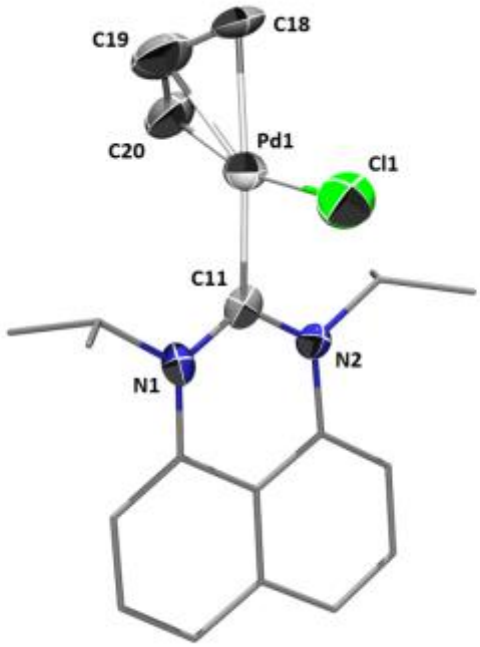

Figure 5.4 X-ray structure of **5.6 (**Thermal ellipsoids are shown for only selected atoms and hydrogen atoms have been omitted for clarity)

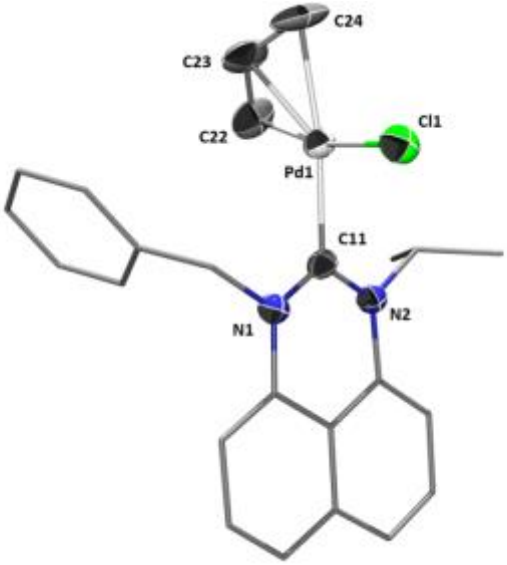

Table 5.4 Selected Bond Lengths [Å] and Angles [°] for **5.5** and **5.6**

5.5		**5.6**	
Bond lengths (Å)			
C11-Pd1	2.071(15)	C11-Pd1	2.065(5)
C11-N1	1.363(18)	C11-N1	1.351(7)
C11-N2	1.361(18)	C11-N2	1.339(7)
C20-Pd1	2.111(19)	C24-Pd1	2.188(6)
C19-Pd1	2.151(18)	C23-Pd1	2.117(10)
C18-Pd1	2.181(15)	C22-Pd1	2.122(6)
Cl-Pd1	2.369(5)	Cl-Pd1	2.3824(14)
C20-C19	1.42(3)	C22-C23	1.429(15)
C19-C18	1.33(3)	C23-C24	1.249(13)
Bond Angle (°)			
N1-C11-N2	118.3(13)	N1-C11-N2	119.3(5)
C11-Pd1-C18	168.9(7)	C11-Pd1-C22	100.5(2)
C11-Pd1-C19	136.2(8)	C11-Pd1-C23	134.9(3)
C11-Pd1-C20	102.9(7)	C11-Pd1-C24	167.7(2)
C11-Pd1-Cl1	90.6(4)	C11-Pd1-Cl1	91.98(15)
N1-C11-Pd1	121.5(10)	N1-C11-Pd1	118.1(4)
N2-C11-Pd1	119.6(11)	N2-C11-Pd1	122.5(4)
Cl1-Pd1-C18	99.8(6)	Cl1-Pd1-C22	167.51(19)
Cl1-Pd1-C19	129.7(7)	Cl1-Pd1-C23	128.7(3)
Cl1-Pd1-C20	166.2(5)	Cl1-Pd1-C24	100.26(19)
C20-Pd1-C19	38.8(8)	C24-Pd1-C23	33.7(4)
C20-Pd1-C18	66.5(8)	C24-Pd1-C22	67.3(3)
C18-Pd1-C19	35.9(7)	C22-Pd1-C23	39.4(4)
C18-C19-C20	118(2)	C22-C23-C24	126.0(16)

Table 5.5 Crystal data and structure refinement for **5.8**

Empirical formula	$C_{57}H_{52}Br_{2.33}Cl_{4.67}N_7Pd_2$
Formula weight	1399.59
Temperature (K)	201(2)
Wavelength (Å)	0.71073
Crystal system	Orthorhombic
Space group	P c c n
a (Å)	30.381(4)
b (Å)	11.1057(13)
c (Å)	16.556(2)
α (deg)	90
β (deg)	90
γ (deg)	90
Volume ($Å^3$)	5586.1(11)
Z	4
Density (calculated) (Mg/m^3)	1.664
Absorption coefficient (mm^{-1})	2.579
F(000)	2784
Crystal size (mm^3)	0.544 x 0.433 x 0.108
Theta range for data collection	2.308 to 28.360
Index ranges	-39<=h<=40, -14<=k<=14, -21<=l<=21
Reflections collected	54514
Independent reflections	6828 [R(int) = 0.0695]
Completeness to theta = 25.242	99.9 %
Refinement method	Full-matrix least-squares on F^2
Data / restraints / parameters	6828 / 72 / 371
Goodness-of-fit on F^2	1.045
Final R indices [I>2sigma(I)]	R1 = 0.0481, wR2 = 0.0897
R indices (all data)	R1 = 0.0917, wR2 = 0.1040
Extinction coefficient	n/a
Largest diff. peak and hole	1.070 and -0.961 e^{-3}

Figure 5.5 X-ray structure of **5.8 (**Thermal ellipsoids are shown for only selected atoms and hydrogen atoms have been omitted for clarity & The 3-chloropyridine solvate, Cl2 and Br1 have been omitted, only Br2 and Cl1 are shown (0.688(3) and 0.525(3) occupancies)

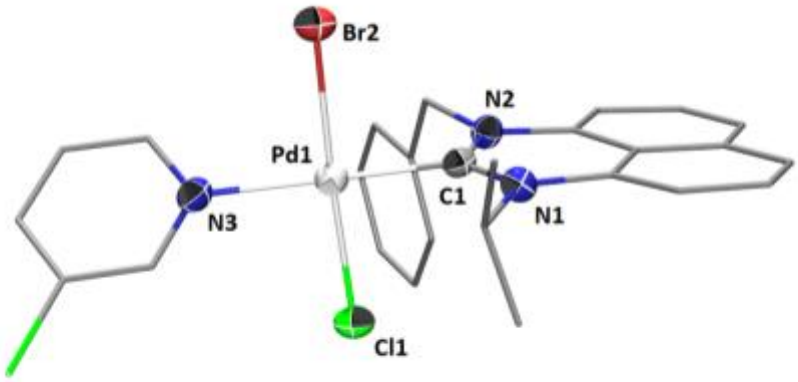

Table 5.6 Selected Bond Lengths [Å] and Angles [°] for **5.8**

Bond lengths (Å)		**Bond Angle (°)**	
C1-Pd1	1.975(4)	N2-C1-N1	119.4(3)
C1-N1	1.335(4)	C1-Pd1-N3	174.13(13)
C1-N2	1.358(4)	C1-Pd1-Cl1	87.3(6)
Br2-Pd1	2.423(3)	C1-Pd1-Cl2	171.7(7)
Cl1-Pd1	2.30(2)	Br1-Pd1-Br2	174.2(2)
N3-Pd1	2.099(3)	Cl1-Pd1-N3	91.8(6)
		Br2-Pd1-N3	91.03(12)
		Pd1-C1-N1	123.0(2)
		Pd1-C1-N2	117.6(2)

IV. References

[1] W. A. Herrmann, *Angew. Chem. Int. Ed.*, 2002, **41**, 1290.

[2] L. Jafarpour, S. P. Nolan, *J. Organomet. Chem.*, 2001, **617**, 17.

[3] K. Denk, P. Sirsch, W. A. Herrmann, *J. Organomet. Chem.*, 2002, **649**, 219.

[4] T. Weskamp, F. J. Kohl, W. Hieringer, D. Gleich, W. A. Herrmann, *Angew. Chem., Int. Ed.*, 1999, **38**, 2416.

[5] J. Huang, L. Jafarpour, A. C. Hillier, E. D. Stevens, S. P. Nolan, *Organometallics*, 2001, **20**, 2878.

[6] R. W. Alder, M. E. Blake, C. Bortolotti, S. Bufali, C. P. Butts, E. Linehan, J. M. Oliva, A. G. Orpen, M. J. Quayle, *Chem. Commun.*, 1999, **241**.

[7] Y. Liu, P. E. Lindner, D. M. Lemal, *J. Am. Chem. Soc.*, 1999, **121**, 10626.

[8] J. Yun, E. R. Marinez, R. H. Grubbs, *Organometallics*, 2004, **23**, 4172.

[9] P. Bazinet, G. P. A. Yap, D. S. Richeson, *J. Am. Chem. Soc.*, 2003, **125**, 13314.

[10] A. Comas-Vives and J. N. Harvey, *Eur. J. Inorg. Chem.*, 2011, **2011**, 5025.

[11] D. M. Khramov, V. M. Lynch and C. W. Bielawski, *Organometallics*, 2007, **26**, 6042.

[12] S. L. Buchwald, L. Jiang in Metal-catalyzed cross-coupling reactions, 2nd ed. (Eds.: A. de Meijere, F. Diederich), Wiley-VCH, Weinheim, 2004, vol. 2, pp. 699 – 760.

[13] W. A. Herrmann, K. Öfele, D. von Preysing, K. S. Schneider, *J. Organomet. Chem.*, 2003, **687**, 229.

[14] E. A. Kantchev, C. J. O Brien, M. G. Organ, *Angew. Chem. Int. Ed.*, 2007, **46**, 2768.

[15] L.-C. Campeau, P. Thansandote, K. Fagnou, *Org. Lett.*, 2005, **7**, 1857.

[16] R. B. Bedford, C. S. J. Cazin, D. Holder, *Coord. Chem. Rev.*, 2004, **248**, 2283.

[17] D. J. Cμrdenas, *Angew. Chem. Int. Ed.*, 2003, **42**, 384.

[18] T.-Y. Luh, M.-K. Leung, K.-T. Wong, *Chem. Rev.*, 2000, **100**, 3187.

[19] D. A. Culkin, J. F. Hartwig, *Organometallics*, 2004, **23**, 3398.

[20] L. Yang, Y. Li, Q, Chen, *Transition Met Chem*, 2013, **38**. 367.

[21] M. F. Lappert, *J. Organomet. Chem.*, 1988, **358**, 185.

[22] A. E. Smith, *Acta Cryst*., 1965, **18**, 331

[23] M. G. Organ, G. A. Chass, D-C. Fang. A. C. Hopkinson, C. Valente, *Synthesis*, 2008, **17**, 2776.

[24] M. G. Organ, S. Calimsiz, M. Sayah, K.H. Hoi, A. J. Lough, *Angew. Chem. Int. Ed.*, 2009, **48**, 2383.